Leslie William Pineda

Germanium-, Tin-, Lead-, and Bismuth-Containing *β*-Diketiminato Complexes for the Synthesis and Structural Characterization of Hydroxide, Carboxylic Acid, Heterobimetallic Oxide, Transition Metal-Main Group, Hydride and Halide Compounds

---

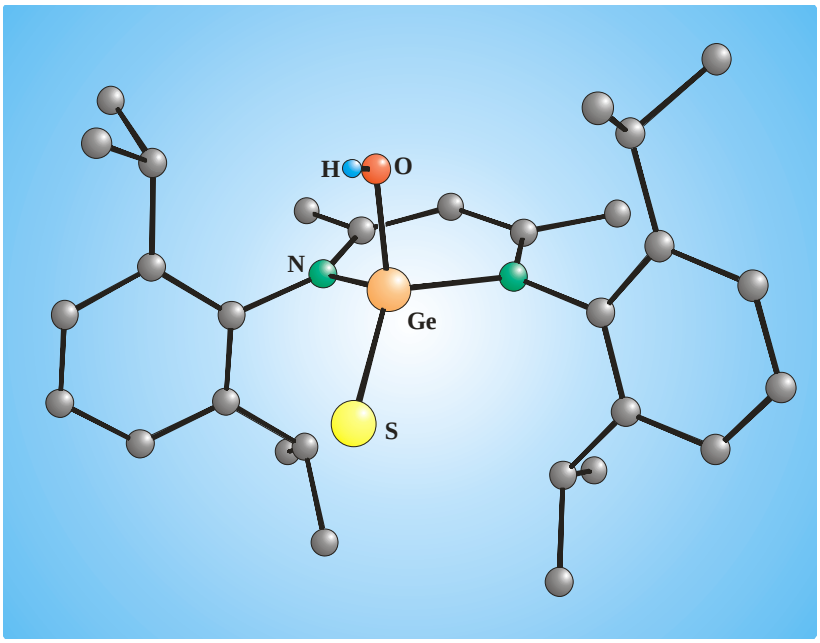

Germanium-, Tin-, Lead-, and Bismuth-Containing β-Diketiminato Complexes for the Synthesis and Structural Characterization of Hydroxide, Carboxylic Acid, Heterobimetallic Oxide, Transition Metal-Main Group, Hydride and Halide Compounds

Dissertation

zur Erlangung des Doktorgrades

der Mathematisch-Naturwissenschaftlichen Fakultäten

der Georg-August-Universität zu Göttingen

vorgelegt von

Leslie William Pineda Cedeño

aus David

(Panamá)

Göttingen 2006

D 7

Referent: Prof. Dr. Dr. h.c. mult. H. W. Roesky

Korreferent: Prof. Dr. D. Stalke

Tag der mündlichen Prüfung: 03.05.2006

The work described in this thesis has been carried out under the supervision of Professor Dr. Dr. h.c. mult. Herbert W. Roesky at the Institute of Inorganic Chemistry of the Georg-August-Universität Göttingen between April 2003 and April 2006.

My sincere thanks and gratitude are due to

Prof. Dr. Dr. h.c. mult. Herbert W. Roesky

for his constant guidance, motivation, suggestions, and discussions throughout this work.

I would like to thank Dr. Vojtech Jancik for numerous fruitful discussions and his help in the X-ray crystal structural investigations. I thank Prof. Dr. Jörg Magull, Dr. Dante Neculai, Dr. Ana Mirela Neculai and Dipl.-Chem. Anja Hofmeister for their help in the X-ray crystal structural investigations. I thank Dr. Rainer B. Oswald and Dipl.-Chem. Kerstin Starke (DFT calculations), Mr. Wolfgang Zolke, Mr. Ralf Schöne and Dr. Gernot Elter (NMR spectra), Mrs. Anke Rehbein, Mr. Thomas Schuchardt and Mr. Jörg Schöne (mass spectra), Mr. Mathias Hesse (IR spectra), Mr. Jürgen Schimkowiak, Mr. Martin Schlote and the staff of the Analytical Laboratories and Workshop for their readiness and timely support during this research work.

The financial support from the Deutscher Akademischer Austauschdienst (DAAD) is gratefully acknowledged.

I thank all colleagues in our research group for the good and motivating working atmosphere. I would like to express my special thanks to Dr. Vojtech Jancik, Dr. Ying Peng, Mr. Gurubasavaraj P. M., Mr. Sharanappa Nembenna, Mr. Z. Yang, Dr. S. Shravan Kumar, Mr. Sanjay Singh, Dr. Umesh Nehete, Dr. Jiangfan Chai, Dr. Hongping Zhu, for their friendliness.

Contents

1. Introduction

For the stabilization of highly reactive species, there are two conceivable approaches, thermodynamic and kinetic stabilization. The former is defined as stabilization of the ground state by the mesomeric effect of neighboring heteroatoms, attachment of an electron-donating or -withdrawing substituent or complexation with transition metal. The latter stabilization is resulting from raising the transition state by taking advantage of steric protection with bulky groups, which prevents oligomerization or reactions with others reagents such as oxygen and water. Kinetic stabilization obviously is superior to thermodynamic stabilization since the latter perturbs the intrinsic nature to a greater extent than the former.[1]

The use of the two approaches together with proper synthetic routes has then produced striking and outstanding results covering a variety of elements. For instance, [(tBu$_3$SiGe)$_3^+$BPh$_4^-$], which incorporates a free germyl cation, was obtained by treating tetrakis(tri-*tert*-butylsilyl)cyclotrigermene with triphenylmetyl tetraphenylborate.[2,3] More recently, the same methodology was employed to generate a cyclotrisilenylium ion by elimination of one tBu$_2$MeSi substituent from a cyclotrisilene (tBu$_2$MeSi)$_2$SiSi$_2$(SitBu$_3$)$_2$ in the presence of Ph$_3$C$^+$·TSFPB$^-$ (TSFPB$^-$ = tetrakis[4-*tert*-butyldimethylsilyl)-2,3,5,6-tetrafluorophenyl]borate.[4] The synthesis of a stable dibismuthene, TbtBi=BiTbt, was accomplished by an efficient steric protection group (Tbt = 2,4,6-tris(bis(trimethylsilyl)methyl)phenyl). It was noted that the sterically demanding Tbt groups effectively surround the reactive Bi–Bi double bond moiety suppressing oligomerization.[5] Interestingly, a stable bicyclic compound with two Si=Si double bonds, a silicon analogue of spiropentadiene, resulted from the reaction of R$_3$SiSiBr$_2$Cl (R = tBuMe$_2$Si) and potassium graphite at low temperature.[6] In contrast, the parent spiropentadiene decomposes within a few minutes in solution and its composition has only been confirmed by NMR spectroscopy and by analyses of a few chemical-trapping reactions.[7,8] The long-sought and quite reactive

species such as the three-coordinate silicon cations, R_3Si^+ (R = alkyl, aryl group)[9] and the (Cp∗)Si^+ (Cp∗ = η^5-pentamethylcyclopentadienyl)[10,11] cation have been recently structurally characterized. In the case of the free silylium ion the isolation could be possible by the stoichiometric reaction of trimesityllylsilane and $Et_3Si(H\text{-}CB_{11}Me_5Br_6)$ to lead to the formation of $[Mes_3Si][H\text{-}CB_{11}Me_5Br_6]$ (Mes = 2,4,6-trimethylphenyl). For the derivate of HSi^+ the corresponding reaction of $(Cp*)_2Si$ with the proton-transfer reagent $Me_5C_5H_2{}^+B(C_6F_5)_4{}^-$ afforded the salt (Cp∗)$Si^+B(C_6F_5)_4{}^-$. By reduction of a tetrabrominated precursor a stable disilyne and its molecular structure was obtained. The Si–Si triple bond is kinetically and thermodynamically stabilized by two large silyl substituents, each bearing one isopropyl and two bis(trimethylsilyl)methyl groups.[12–14]

In addition, the isolation of low-valent and low-coordinate compounds has gained considerable importance due to the possibility of new bonding sytems and new reaction modes. Particularly, the formation of homonuclear M–M and heteronuclear M–M´ multiple bonds between heavier main group elements has gained great interest.[15–18] Most importantly, this provides the chance to revise some concepts of bonding. In the case of ArPbPbAr (Ar = 2,6-$Trip_2C_6H_3$; Trip = 2,4,6-*i*$Pr_3C_6H_2$) a diplumbyne, was claimed as an alkyne analogue compound regarded to have an electron sextet in the valence shell which exists in a *trans*-bent form.[19] However, a revision of this statement by using DFT calculations revealed that the sterically demanding group forces a *trans*-bent equilibrium structure as the lowest lying energy minimum.[20] It is worth emphasizing that the reactivity of heavier Group 14 alkyne analogues (Ge, Sn) was investigated with conjugated dienes or small molecules. It was postulated in the case of ArGeGeAr (Ar = 2,6-$Trip_2C_6H_3$; Trip = 2,4,6-*i*$Pr_3C_6H_2$) which did not give the expected cycloadduct when reacted with 2,3-dimethyl-1,3-butadiene due to its biradical character, a feature which also accounts for the products obtained between digermyne and small molecules (e.g. H_2, N_2O, O_2, N_3SiMe_3, PhCCPh, P_4, S_8 and others).[21,22]

However, it is notable that the digermyne BbtGeGeBbt (Bbt = 2,6-$Me(SiMe_3)_2$-4-$Me(SiMe_3)_3$-C_6H_2) even in the presence of H_20, 2,3-dimethyl-1,3-butadiene, and Et_3SiH, the latter compound known to be very reactive toward radical, showed no biradical character, but rather addition product formation with the former reagents and no reaction at all with Et_3SiH.[23] As for distannyne, formation of $\{Sn(Ar)(\mu–OH)\}_2$ is observed by reacting either N_2O or TEMPO (tetramethylpiperidineoxide) with ArSnSnAr (Ar = 2,6-$Dip_2C_6H_3$; Dip = 2,6-$i Pr_2C_6H_3$).[24]

Of direct relevance in the present context are the contribution of other bulky monodentate alkoxide, aryloxide, diorganoamide ($–NR_2$) and alkyl ($–CH(SiMe_3)_2$) ligands in the stabilization of low-coordinate germanium, tin, and lead compounds. And of particular interest are the Lappert´s amides $M\{N(SiMe_3)_2\}_2$ (M = Ge, Sn, Pb), which remain two coordinate in the solid and behave in solution as a two electron donor analogous to carbenes.[25–28]

The chemistry of the β-diketiminato ligand since its initial recognition as an ancillary ligand and the effective stabilization of lower oxidation states and lower coordination numbers has experienced a burgeoning due to the steric and electronic properties and a variety of coordination modes.[29] The ligand can be regarded as a bidentate and monoanionic ligand and can be prepared by direct condensation of 2,4-pentanedion, 2,6-diisopropylaniline, and HCl in boiling ethanol and subsequent neutralization of the generated ligand hydrochloride with Na_2CO_3 to obtain free **LH** (Scheme 1).[30,31]

Remarkable progress in the stabilization of compounds supported by β-diketiminato ligands has been recently reviewed.[29] It encompasses main-group elements, early and late transition elements to lanthanide and actinide elements. Recently, a great deal of unique and fascinating results reflects the β-diketiminato ligand stabilizing properties. Thus the isolation and structural characterization of a monomeric aluminum(I) compound [{$HC(CMeNAr)_2$}Al]

(Ar = 2,6-*i*$Pr_2C_6H_3$) was reported. It was obtained by the reduction of [{HC(CMeNAr)$_2$}AlI_2] with potassium.[32]

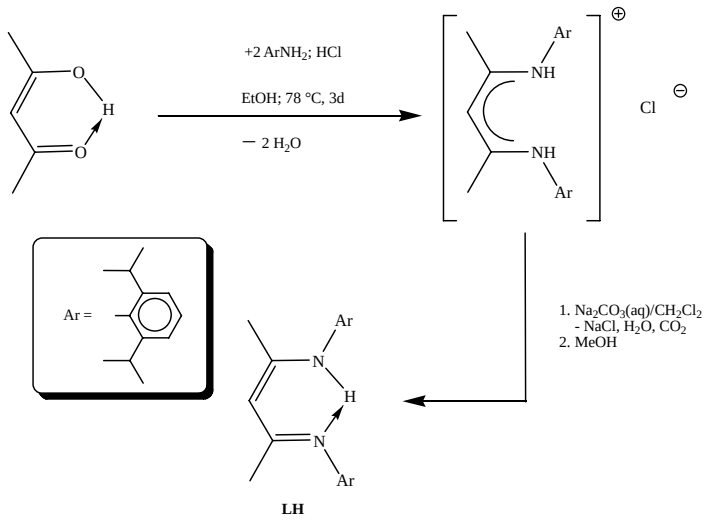

Scheme 1: Synthesis of the *β*-diketiminate ligand [HC(CMeNAr)$_2$] (**LH**).

The *β*-diketiminatoaluminum(I) compound resembles carbenoid-type compounds and possesses according to DFT calculations dual Lewis acid and Lewis base character and stereochemically an active lone pair of electrons at the aluminum atom. Interesting is the reaction of the aluminum(I) compound in the presence of white phosphorous (P_4) and elemental sulfur (S_8) which results in the successful isolation of P_4^{4-} and S_6^{4-} containing aluminum phosphide [{HC(CMeNAr)$_2$}Al]$_2P_4$[33] and sulfide [{HC(CMeNAr)$_2$}Al]$_2S_6$,[34] respectively. Furthermore, the reaction of [{HC(CMeNAr)$_2$}Al] with $B(C_6F_5)_3$ leads to [{HC(CMeNAr)$_2$}$AlB(C_6F_5)_3$], a compound where the aluminum atom exhibits Lewis acid and Lewis base behavior.[35] Recently, an excellent review covering the chemistry of aluminum(I) has been published, which highlights the preparation of aluminum containing heterocyclic compounds, main group-main group and transition metal-main group compounds having donor-acceptor bonds by carrying out reactions with unsaturated compounds and Lewis acids.[36] The synthesis and structure of a boronic acid analogue based on aluminum

[{HC(CMeNAr)$_2$}Al(OH)$_2$] was prepared by hydrolysis of [{HC(CMeNAr)$_2$}AlI$_2$] with KOH, H_2O and KH in liquid ammonia/toluene two-phase system.[37] In a parallel development the use of N-heterocyclic carbene as HCl acceptor was successfully introduced for the ammonolysis and hydrolysis of β-diketiminatoaluminum and β-diketiminatogallium chlorides to render [{HC(CMeNAr)$_2$}Al(NH$_2$)$_2$][38] [{HC(CMeNAr)$_2$}Ga(OH)$_2$] and [{HC(CMeNAr)$_2$}Ga(NH$_2$)$_2$].[39] The use of unconventional synthetic protocols enabled the isolation and molecular characterization of aluminum dithiol [{HC(CMeNAr)$_2$}Al(SH)$_2$][40] and aluminium diselenols [{HC(CMeNAr)$_2$}Al(SeH)$_2$] and [{HC(CMeNAr)$_2$Al(SeH)$_2$}(μ–Se)].[41] In an elegant trapping reaction the first monoalumoxane exhibiting an Al–O double bond was synthesized. As shown in Scheme 2, the two pendant donor arms of the β-diketiminate ligand give enough steric protection and lead to the formation of [HC{(Et$_2$NCH$_2$CH$_2$NCMe)$_2$}AlO·B(C$_6$F$_5$)$_3$] when [HC{(Et$_2$NCH$_2$CH$_2$NCMe)$_2$}AlMe$_2$] reacts with H_2O·B(C$_6$F$_5$)$_3$.[42]

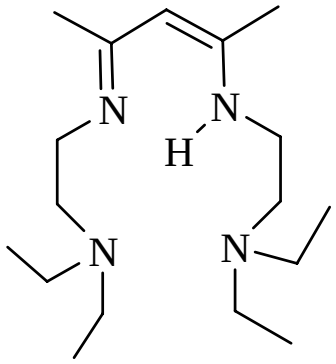

Scheme 2

At this stage some representative examples have been outlined with different ligands whose steric and electronic properties have led to the isolation of striking compounds. Herein the utilization of two different types of β-diketiminate ligands (Schemes 1 and 2) are employed for the synthesis of novel compounds based on germanium, tin, lead and bismuth. In general the new compounds contain the following functionalities and linkages: hydroxides, carboxylic acids, heterobimetalic oxides, hydrides, transition metal-main group bonds and

halides. The sections 2.1.–2.7. will in detail point out the importance, the state of the experimental results and discussion, and conclusion and remark of the chemistry of heavier Group 14 and Group 15 elements. Based on these delineations, the objectives of the present work are:

1. to develope a synthetic methodology for the preparation of a stable and terminal germanium(II) hydroxide by kinetic stabilization.
2. to investigate the reactivity of the lone pair of electrons on the germanium(II) hydroxide compound for the generation of new functionalities.
3. to explore the reactivity of the OH functionality on the germanium(II) hydroxide compound for the isolation of heterobimetallic oxides.
4. to develop methodologies for the synthesis of germanium(II) and tin(II) hydrides.
5. to explore the reactivity of β-diketiminate ligands for the preparation of lead and bismuth organohalides in low oxidation states.
6. to investigate by DFT methods the electronic properties of some of the new compounds.

2. Results and Discussion

2.1. Preparation and Structure of the First Germanium(II) Hydroxide: The Congener of an Unknown Low-Valent Carbon Analogue

In 1984 it was noted that the picture of the structural chemistry of hydroxides is far from complete,[43–45] and since then this is still the case. Roesky et al. reported the preparation and structural characterization of unusual compounds such as [{HC(CMeNAr)$_2$}Al(OH)$_2$][37] (Ar = 2,6-*i*Pr$_2$C$_6$H$_3$), [(Me$_3$Si)$_3$CSnO(OH)]$_3$,[46] [(Cp*Zr)$_6$(μ_4–O)(μ–O)$_4$(μ–OH)$_8$],[47] and a series of experiments concerning the so-called water effect in organometallic chemistry.[48] Interestingly, only a few examples of well-characterized germanium(IV) hydroxides are known: Ph$_3$GeOH, (C$_{10}$H$_7$)$_3$GeOH, (C$_6$H$_{11}$)$_3$GeOH,[49] 2*t*Bu$_2$Ge(OH)$_2$·(*t*Bu$_2$GeOH)$_2$O·H$_2$O,[50] and [Fc(*t*Bu)(OH)Ge]$_2$O (Fc = CpFe(η^5-C$_5$H$_4$),[51] and no such compounds based on germanium(II) have been reported. The most common route to organogermanium hydroxides is through the hydrolysis of organohalogermanes, but they can be only isolated when the supporting ligand is bulky enough.[52]

Here we describe the hydrolysis of the β-diketiminatogermanium(II) chloride [{HC(CMeNAr)$_2$}GeCl] (**1**),[53] with a slight excess of water and one equivalent of 1,3-dimesitylimidazol-2-ylidene[54] (**2**; Mes = 2,4,6-Me$_3$C$_6$H$_2$) in toluene at room temperature, which led to the formation of [{HC(CMeNAr)$_2$}GeOH] (**3**) in good yield (Scheme 3). In contrast, conventional hydrolysis of **1** in the presence of an amine or in liquid ammonia was unsuccessful due to the formation of several side products. Moreover, the separation of **3** from the amine·HCl was not possible. Addition of HCl to the N-heterocyclic carbene **2** is clearly a key step in this reaction. The easy formation of **4** and its low solubility allow the separation of **3** from **4**.

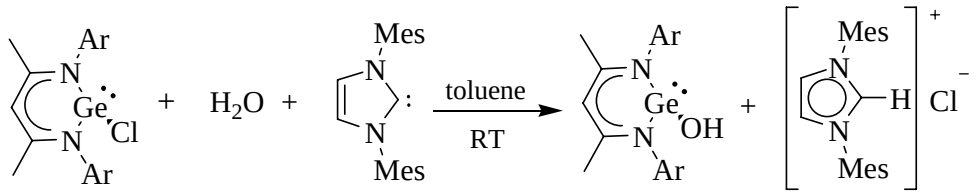

1 **2** **3** **4**

Scheme 3. Ar = 2,6-*i*Pr$_2$C$_6$H$_3$, Mes = 2,4,6-Me$_3$C$_6$H$_2$.

Compound **3** is a yellow solid that is soluble in pentane, THF, dichloromethane, benzene and diethyl ether, but insoluble in hexane. In the IR spectrum a sharp absorption was observed around 3571 cm^{-1}, which can be attributed to the O–H stretching frequency. Theoretical calculations on Ge(OH)$_2$ showed that two vibrational frequencies could be expected at 3675 cm^{-1} and 3735 cm^{-1}.[55] These values are in good agreement with those of **3** when it is taking into account that some symmetry constrains are involved. In addition, the monoanionic ligand in **3** might affect the vibrational frequency by means of its steric demand and bonding mode. The ^{1}H NMR spectrum shows the expected pattern for the β-diketiminato ligand[53] and a resonance for the hydroxide proton at high field (δ 1.54 ppm), which is in accordance with the chemical shift observed for the OH group in *t*Bu$_2$Ge(OH)$_2$ (δ 1.49 ppm).[56] Surprisingly, the resonance for the corresponding group of (FcN)$_3$GeOH [FcN = CpFe{η^5-C$_5$H$_3$(CH$_2$NMe$_2$)-2}] was found at δ 8.98 ppm.[57] The most intense peak in the EI mass spectrum appeared at *m*/*z* 403 [*M* – Me–Ge–OH]$^+$, and the signal at *m*/*z* 508 (25%) was assigned to the molecular ion [*M*]$^+$.

Single crystals of **3** suitable for X-ray structural analysis were grown by maintaining the reaction mixture in toluene/hexane (2.5:1) at –20 °C for three weeks. Complex **3** crystallizes in the monoclinic space group $C1_2/c$ with two half dimers in the asymmetric unit. In **3** a germanium atom is attached to two nitrogen atoms from the backbone of the chelating

ligand, one hydroxyl group and a lone pair presumably occupies the fourth coordination site, an assumption that is supported by the presence of an intermolecular interaction between the H atom of the OH group, which was located and refined, and another germanium atom (*d*(O–H···Ge): 3.064(26) Å). The coordination geometry about germanium is derived from a distorted tetrahedron (Figure 1).

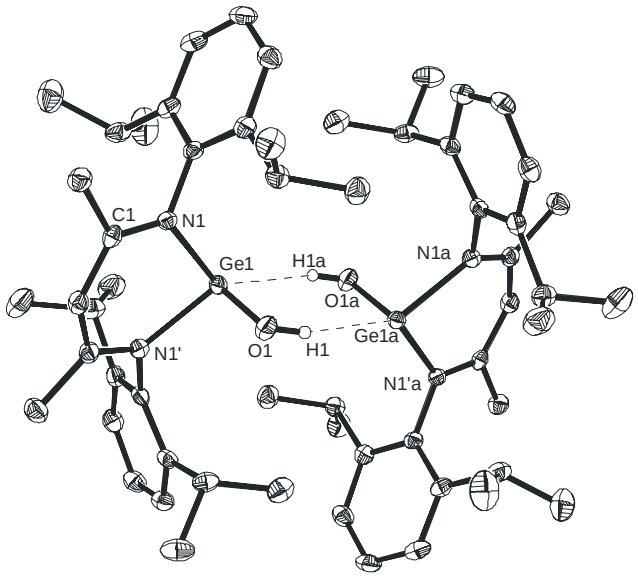

Figure 1. Thermal-ellipsoid plot of **3** at the 50 % probability level. H atoms, except for the OH group, are omitted for clarity. Selected bond lengths [Å] and angles [°]: Ge(1)–O 1.828(1), Ge(1)–N(1) 2.008(1), Ge(1)–N(1′) 2.008(1); O(1)–Ge(1)–N(1) 93.9(6), O(1)–Ge(1)–N(1′) 94.8(6), N(1)–Ge(1)–N(1′) 89.5(1).

The Ge–N bond lengths and N–Ge–N angle are 2.008(1) Å and 89.5(1)°, respectively. These data can be compared with the slightly shorter Ge–N bond distances in **1** (1.988(2) and 1.997(3) Å) and [{HC(CMeNAr)$_2$}GeF] (1.977(19) and 1.978(18) Å); Ar = 2,6-*i*Pr$_2$C$_6$H$_3$).[58–60] Conversely, the Ge–N bond lengths are slightly longer in [HB(3,5-Me$_2$pz)$_3$Ge]I[61] (av 2.03(2) Å); pz = pyrazole ring) and [{HC(CMeNAr)$_2$}GeMe] (2.008(2) and 2.038(2) Å).[58] A

noteworthy feature of compound **3** is the GeOH moiety (Ge–O 1.828(1), O–H 0.795(7) Å); the Ge–O bond length is in good agreement with those predicted for $Ge(OH)_2$ (av 1.804 Å).[55] Moreover, the O–H distance of **3** is somewhat shorter than that of water (0.96 Å). Interestingly, and as might be expected, shorter Ge–OH bond lengths are found in germanium(IV) compounds due to the smaller radius of Ge(IV) relative to Ge(II) (e.g. Ge–O 1.781(4) and 1.779(2) Å in $tBu_2Ge(OH)_2$,[56] and 1.779(5) Å in $(FcN)_3GeOH$).[57]

In summary, compound **3** is the first example of the hitherto unknown germanium(II) hydroxides. A low-coordinate carbon analogue of composition RC(OH) has so far not been reported. An RC(OH) species should be extremely unstable and rearrange to the corresponding aldehyde.

2.2. Germacarboxylic Acid: An Organic-Acid Analogue Based on a Heavier Group 14 Element

Carbon multiple-bonded species, especially those containing carbonyl groups (aldehydes, amide esters, ketones) are widely known and useful systems in organic chemistry.[62] As far as the heavier congeners of Group 14 are concerned, a steady and remarkable development has been experienced, leading to unsaturated species. Additionally a myriad of mixed unsaturated compounds has been prepared containing elements of Groups 14–16.[15] However, owing to the high reactivity and tendency to polymerize these species have to be thermodynamically and kinetically stabilized.

In the case of germanium-chalcogen double-bonded species, a few thio-, seleno- and telluroketones were prepared.[1,63,64] Roesky and co-workers have already reported the synthesis and structure of [{HC(CMeNAr)$_2$}Ge(S)X][59] (X = Cl, F) with Group 14 and 16 elements bearing a halide. Furthermore, the synthesis and structures of the selenium analogue [{HC(CMeNAr)$_2$}Ge(Se)X] (X = Cl, F), as well as the functionalized derivative [{HC(CMeNAr)$_2$}Ge(E)R] (E = S, Se; R = Me, *n*Bu) were reported.[65]

As a stable precursor compound **3** is quite intriguing for the generation of new functional groups. To our knowledge the co-existence and fast tautomeric equilibrium for thiolocarboxylic acid **5** and thionocarboxylic acid **6** is known, but the latter group does not exist in the free state (Scheme 4).[66,67] Herein we describe the isolation and characterization of a germanium thionoacid [{HC(CMeNAr)$_2$}Ge(S)OH] (**7**), which has no isolated precedent in the carbon system (Scheme 5).

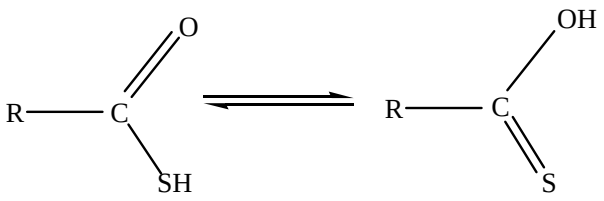

5 **6**

Scheme 4. Tautomeric equilibrium for the thiolo- and thionocarboxylic acid.

The reaction of **3** in the presence of equivalent amounts of elemental sulfur at room temperature in toluene leads after three days to white compound **7** in good yield (Scheme 5).

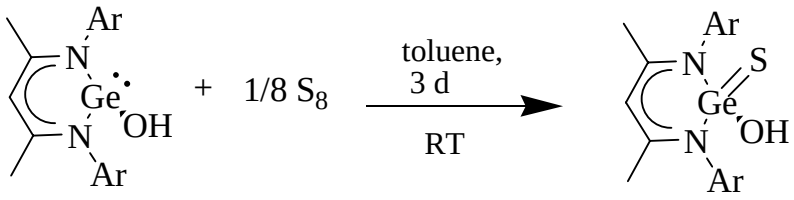

3 **7**

Scheme 5. Ar = 2,6-*i*Pr$_2$C$_6$H$_3$.

Compound **7** is soluble in benzene, THF, and hexane, but insoluble in pentane and shows no decomposition on exposure to air. By comparison of the IR spectrum of **3**, which exhibits a sharp OH stretching vibration at 3571 cm^{-1} with the corresponding frequency of **7** (3238 cm^{-1}) a significant shift to lower wave numbers is observed. Such behavior may be due to the formation of hydrogen bonds. Interestingly, the ^{1}H NMR spectrum of **7** exhibits a resonance signal at δ 2.30 ppm for the hydroxy hydrogen, which by comparison with that of **3** (δ 1.54 ppm) clearly shows a downfield shift. Again intermolecular hydrogen interaction and a change of the oxidation state of the germanium atom are plausible explanations for the observed shift. Thus, this resonance shift indicates a fairly acid nature of the terminal OH proton. Furthermore no evidence was found for any tautomeric equilibrium of **7**. The most

abundant ion peak in the EI mass spectrum appeared at *m/z* 525 $[M - Me]^+$, and the signal at *m/z* 540 (40 %) was assigned to the molecular ion $[M]^+$ (correct isotopic pattern).

Maintaining a toluene solution of **7** for two weeks at –20 °C, resulted in colorless single crystals suitable for X-ray structural analysis. Compound **7** crystallizes in the monoclinic space group *C*2/*c* with one monomer and one molecule of toluene in the asymmetric unit. Intermolecular interaction of the hydroxyl group with the sulfur atom results in the formation of the hydrogen-bonding array (O–H···S) leading to dimers (Figure 2).

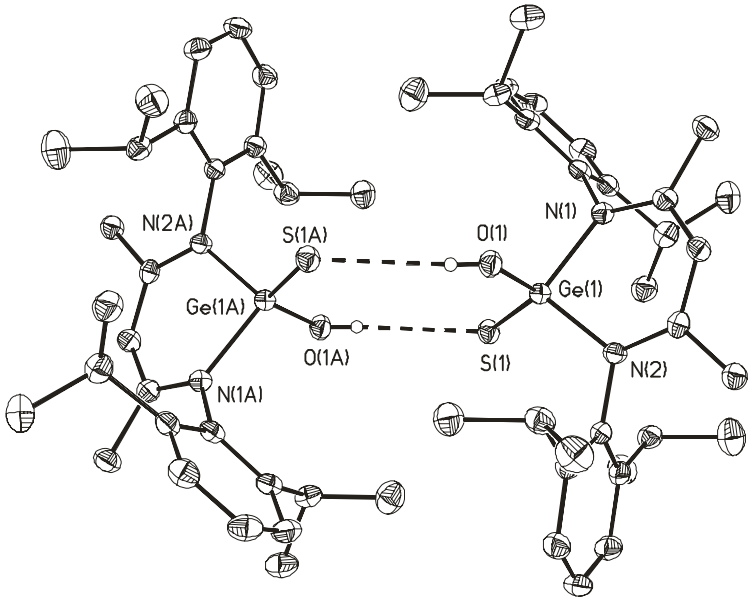

Figure 2. Thermal ellipsoid plot of **7** (thermal ellipsoids set at the 50 % probability). H atoms, except for the OH group, and interstitial toluene molecules, are omitted for clarity. Selected bond lengths [Å] and angles [°]: Ge(1)–O(1) 1.751(2), Ge(1)–N(2) 1.911(2), Ge(1)–N(1) 1.916(2), Ge(1)–S(1) 2.077(1); O(1)–Ge(1)–N(2) 99.6(1), O(1)–Ge(1)–N(1) 102.2(1), N(2)–Ge(1)–N(1) 95.6(1) O(1)–Ge(1)–S(1) 121.4(1), N(2)–Ge(1)–S(1) 118.8(1), N(1)–Ge(1)–S(1) 114.9(1).

The hydrogen bonded donor-acceptor separations (*d*(H···S): 2.537 Å; *d*(O···S): 3.234 Å) follow the same trend as those reported in literature.[43,45] The coordination environment

around the germanium atom comprises two nitrogen atoms from the supporting ligand, one hydroxyl group, and one sulfur atom, and has distorted tetrahedral geometry. The Ge–O bond length (1.751(2) Å) in **7** is significantly shorter than that in **3** (1.828(1) Å), as a result of the smaller atomic radius of Ge(IV) compared with that of Ge(II). Indeed, similar Ge–O bond lengths of Ge(IV) species have been described, (tBu$_2$Ge(OH)$_2$ (1.781(4) and 1.779(2) Å)[56] and 1.779(5) Å in [(FcN)$_3$GeOH] (Fc = CpFe(η^5-C$_5$H$_4$)).[68] A shorter Ge–N bond length and wider N–Ge–N angle are expected (av 1.914(2) Å and 95.6(1)°) than in **3**. A comparison of the Ge–S bond length in [{η^3-[(μ-tBuN)$_2$(SiMeNtBu)$_2$]}]GeS][69–72] (2.063(3) Å), and in [{HC(CMeNAr)$_2$}Ge(S)X][59] (X = Cl, F), (2.053(6) and 2.050(9) Å), with that in **7** (2.077(1) Å) shows a good agreement. Likewise, the Ge–O bond length in [(dppe)Pd(μ–S)(μ–CH$_2$O)Ge{N(SiMe$_3$)$_2$}$_2$] (dppe = bis(diphenylphosphino)ethene)[73] (1.785(6) Å), a compound which has almost the same coordination environment and geometry at the germanium center as **7**, correlates well with that in **7**.

In summary, the reaction of **3** and elemental sulfur resulted in the formation of compound **7** which represents a new class of “carbon-free” carbonic acid analogues based on germanium.

2.3. Preparation of [{HC(CMeNAr)$_2$}Ge(Se)OH]: A Germanium Analogue of a Selenocarboxylic Acid (Ar = 2,6-*i*Pr$_2$C$_6$H$_3$)

The chemical reactivity of heavier congeners of carbenes either as dicoordinate species or with higher coordination numbers, is well documented.[1,63,74–87] Again, steric and electronic stabilization are fundamental factors in avoiding self-condensation and polymerization. For instance, the N-heterocyclic silylene 1,3-di-*tert*-butyl-2,3-dihydro-1H-1,2,3-diazasilol-2-ylidene in the presence of water leads to a transient silanol, which further self-condenses to the disiloxane.[88]

The organic chemistry of selenium has received less attention than that of oxygen and sulfur.[89,90] However, studies of the chemistry of selenocarbonyl compounds are steadily increasing, leading to new synthetic approaches in a wide range of applications.[91–97] Although the existence of selenocarboxylic acids (RCSeOH) (R = alkyl, aryl) has been confirmed at low temperatures, structural evidence of such species has been elusive.[98,99] Furthermore, [{HC(CMeNAr)$_2$}Ge(Se)Cl] (Ar = 2,6-*i*Pr$_2$C$_6$H$_3$) was used as a precursor to prepare [{HC(CMeNAr)$_2$}Ge(Se)F] and [{HC(CMeNAr)$_2$}Ge(Se)(X)] (X = Me, *n*Bu).[65] Herein, we describe the preparation of [{HC(CMeNAr)$_2$}Ge(Se)OH] (**8**) by the reaction of **3** with elemental selenium.

Treatment of **3** in the presence of selenium in toluene at ambient temperature resulted in the oxidative addition of selenium to the germanium center affording a germanium analogue of a selenocarboxylic acid in good yield (Scheme 6). Compound **8** is thermally stable, decomposing above 200 ^{o}C. Its mass spectrum shows its molecular ion peak $[M]^+$ with calculated isotopic pattern (*m*/*z* 586). The vibrational spectrum of **8** shows a broad absorption at 3299 cm^{-1} that is tentatively assigned to the OH group. [{HC(CMeNAr)$_2$}Ge(S)OH] showed the OH stretching frequency at lower wave number in comparison to **8** (3238 cm^{-1}).

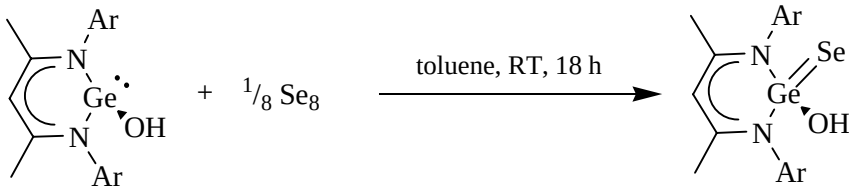

3 **8**

Scheme 6. Ar = 2,6-*i*Pr$_2$C$_6$H$_3$.

In the ^{1}H NMR spectrum of **8** the OH proton resonance was observed at δ 2.19 ppm, which is downfield compared to that of **3** (δ 1.54 ppm). However, it is shifted to high field compared to that of [{HC(CMeNAr)$_2$}Ge(S)OH] (δ 2.30 ppm). The ^{77}Se NMR resonance of **8** (δ –439 ppm) falls within the range of compounds exhibiting ylide-type and multiple bond character at the germanium-selenium bond: [{HC(CMeNAr)$_2$}Ge(Se)Cl] (δ –287 ppm; Ar = 2,6-*i*Pr$_2$C$_6$H$_3$); [{HC(CMeNAr)$_2$}Ge(Se)F] (δ –465 ppm); [{HC(CMeNAr)$_2$}Ge(Se)(X)] (δ –349 ppm, δ –297 ppm; X = Me, *n*Bu;).[65]

Light green crystals of **8** were grown from a toluene/hexane solution (10:2 mL) at –20 ^{o}C for one week. Compound **8** crystallizes in the monoclinic space group *C*2/*c* with one monomer and one molecule of toluene in the asymmetric unit. In **8**, a four coordinate germanium atom occupies the center position of a distorted tetrahedron, which derives from the nitrogen atoms of the β-diketiminato ligand, a hydroxyl group and a selenium atom. Compound **8** prefers a selenoxo tautomeric form of hydrogen bonded dimers, which derives from weak intermolecular hydrogen interactions (O–H···Se, *d*(O···Se): 3.336(2) Å; *d*(H···Se): 2.61(2) Å; O–H–Se 163(2)°). The structure of **8** is shown in Figure 3. The Ge–Se bond length (2.206(1) Å) in **8** is comparable with that reported for [{HC(CMeNAr)$_2$}Ge(Se)Cl][65,74] (2.197(6) Å, 2.210(1) Å), [{HC(CMeNAr)$_2$}Ge(Se)F] (av 2.174(7) Å), [{HC(CMeNAr)$_2$}Ge(Se)(*n*Bu)] (2.219(6) Å) and [{HC(CMeNAr)$_2$}Ge(Se)Me] (2.199(1) Å).[65] This is very much in line with resonance structure contributions between a Ge–Se

ylide-type bond and multiple bond character rather than a germanium-selenium single bond, whose bond distances range from 2.24 Å to 2.77 Å.[59,64,100–103] In **8** the Ge–O bond length (1.756(1) Å) remains nearly unchanged when compared with that of [{HC(CMeNAr)$_2$}Ge(S)OH] (1.751(2) Å). A similar finding was also observed for **8** having a Ge–N bond length (av 1.914(1) Å), in good agreement with that of [{HC(CMeNAr)$_2$}Ge(S)OH] (av 1.914(2) Å), as well as for that of [{HC(CMeNAr)$_2$}Ge(Se)Cl] (av 1.901(2) Å) and [{HC(CMeNAr)$_2$}Ge(Se)F] (av 1.887(3) Å).[65]

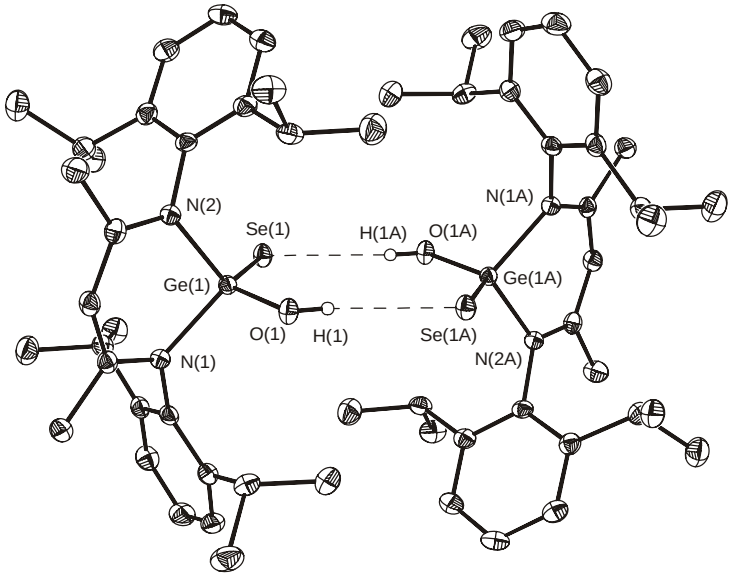

Figure 3. Thermal ellipsoid plot of **8** showing the 50% probability level. H atoms, except for the OH group and interstitial toluene molecule are omitted for clarity. Selected bond lengths [Å] and angles [deg]: Ge(1)–O(1) 1.756(1), Ge(1)–Se(1) 2.206(1), O(1)–H(1) 0.76(2), Ge(1)–N(1) 1.915(1), Ge(1)–N(2) 1.912(1); N(2)–Ge(1)–N(1) 95.7(1), N(1)–Ge(1)–Se(1) 115.0(1), N(2)–Ge(1)–Se(1) 119.2(1), O(1)–Ge(1)–N(1) 102.0(1), O(1)–Ge(1)–N(2) 99.3(1), O(1)–Ge(1)–Se(1) 121.4(1), H(1)–O(1)–Ge(1) 112.5(2).

The acid strength of compounds **8** and [{HC(CMeNAr)$_2$}Ge(S)OH] were investigated by DFT and making use of the depicted thermodynamic cycle (Scheme 7).

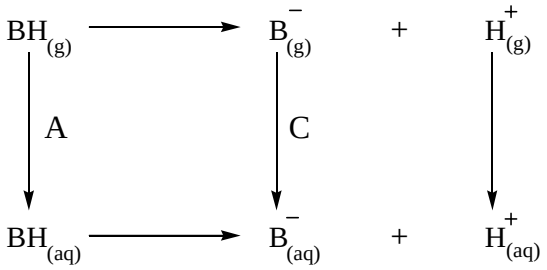

Scheme 7. Born-Haber thermodynamic cycle.

For all calculations the well established DFT variant B3LYP method was used.[104,105] The computations were carried out with the Gaussian G03[106] program package employing a modified 6-31G basis set extended with additional double-diffuse functions.[107,108] In the first step all molecules were fully optimized to their equilibrium structures. The resulting structures were in good agreement with the crystallographic data. To avoid the recourse to experimental data as much as possible only, the values for the proton have been taken from references.[109,110] The ab initio values for the energy of solvation (A,C) have been calculated with a modification of the polarizable continuum model (PCM) termed IEFPCM.[111] The pKa value can be calculated by the following formula

$$\Delta G^0_{aq} = G^0(B^-_{gas}) + \Delta G_{solv}(B^-) + G^0(H^+_{gas}) + G^0_{solv}(H^+) - G^0(BH_{gas}) - \Delta G^0_{solv}(BH)$$

and

$$pK_a = \frac{\Delta G^0_{aq}}{2.303 * R * T}$$

The resulting acid strengths of **8** (pK_a 38.3) and [{HC(CMeNAr)$_2$}Ge(S)OH] (pK_a 37.2) are weak. The pK_a values are in the range of aromatic (pK_a ~33) and aliphatic (pK_a ~48)

compounds. However, when compared with oxygen containing organic Brønsted acids (pK_a ~15), they have weaker acid strength.[112] Likewise, these pK_a values correlate well when compared with the ^1H NMR resonances of the hydroxyl moiety of both compounds. Thus, compound [{HC(CMeNAr)$_2$}Ge(S)OH] can be regarded to be more acidic by virtue of its chemical shift and acid strength (δ 2.30 ppm; pK_a 37.2) when compared to those of **8** (δ 2.19 ppm pK_a 38.3).

Table 1. Results of the bonding analysis for compounds **7** and **8**.

	Bond	Occ.[a]	MO 1	Contr.[b] [%]	Type (contr. [%])	MO 2	Contr. [%]	Type (contr. [%])
7								
	S–Ge	1.912	S	61.4	s(16.0)p$^{5.2}$(83.7)	Ge	38.6	s(34.2)p$^{1.9}$(65.3)
	Ge–O	1.965	Ge	16.2	s(23.5)p$^{3.2}$(76.1)	O	83.8	s(26.5)p$^{2.7}$(73.5)
	Ge–N(5)	1.932	Ge	15.6	s(21.3)p$^{3.7}$(78.5)	N(5)	84.4	s(27.8)p$^{2.6}$(72.2)
	Ge–N(6)	1.932	Ge	15.6	s(21.3)p$^{3.7}$(78.5)	N(6)	84.4	s(27.8)p$^{2.6}$(72.2)
	O–H	1.985	O	75.6	s(22.8)p$^{3.4}$(77.1)	H	24.4	s(99.7)
8								
	Se–Ge	1.903	Se	58.1	s(14.0)p$^{6.2}$(86.0)	Ge	42.0	s(34.0)p$^{1.9}$(65.4)
	Ge–O	1.966	Ge	16.2	s(23.4)p$^{3.3}$(76.3)	O	83.8	s(27.0)p$^{2.7}$(73)
	Ge–N(5)	1.933	Ge	15.8	s(21.4)p$^{3.7}$(78.3)	N(5)	84.2	s(28.2)p$^{2.6}$(71.8)
	Ge–N(6)	1.933	Ge	15.8	s(21.4)p$^{3.7}$(78.3)	N(6)	84.2	s(28.2)p$^{2.6}$(71.8)
	O–H	1.985	O	75.6	s(22.6)p$^{3.4}$(77.4)	H	24.4	s(99.7)

[a] Occupancy. [b] Contribution.

To further investigate the bonding around the germanium atom in **8** and [{HC(CMeNAr)$_2$}Ge(S)OH] compounds, an NBO[113–116] procedure was carried out. The results of this analysis were also interpreted in terms of the donor–acceptor interaction.[117] As can be seen from the values given in Table 1, the Ge–S bond can be described in terms of the overlap between a p rich sp hybrid at the sulfur atom with a sp^2 hybrid of the germanium atom. The Ge–O bond also involves the overlap of two p rich hybrids, but in this case the contribution of the germanium atom is far smaller. The Ge–N bonds show the same distribution. In addition, the Ge–S bond is further stabilized by 26 kcal/mol through the interaction of antibonding orbitals of the Ge–O and Ge–N bonds. The Ge–N bond forms part of a delocalized system with the germanium acting as bridging atom. In the case of compound **8** the analysis mostly differs at the Ge–Se bond which shows a higher contribution of the germanium atom to the molecular orbital. The direct consequence of this electron drain is visible in the hydroxyl group, which now shows a positive interaction with the Ge–O bond which was not visible in the sulfur system.

In summary, oxidative addition of selenium at the germanium center led to [{HC(CMeNAr)$_2$}Ge(Se)OH]. Also, the first assessment of the acid strength of this new class of “carbon-free” carbonic acids based on germanium was carried out by DFT calculations.

2.4. OH Functionality of Germanium(II) Compounds for the Formation of Heterobimetallic Oxides

The interest in metal and organometallic oxides stems from the application of these compounds in industry as catalysts, cocatalysts and as a model for the fixation of catalysts on oxide surfaces.[118] Moreover, steady and increasingly attention has been focused on the synthesis and characterization of heterobimetallic oxides, which are used as polyfunctional catalysts and precursors for the preparation of bi- and polymetallic heterogeneous catalysts.[119–124] Regarding the chemistry of the germanium(II) compounds bearing a Ge–O linkages was limited to alkoxy- and arylalkoxygermylenes,[125–127] and the isolation of μ-oxo linkages with two different metals was elusive so far. Herein we describe the reactions of **3** with methylated metallocene derivatives of Group 4 (M = Zr, Hf) that lead to the isolation and characterization of discrete new μ-oxo heterobimetallic oxide systems.

By taking advantage of the oxophilicity of Group 4 elements, we accomplished the isolation of compounds **9** and **10** by treatment of equivalent amounts of **3** and Cp_2MMe_2 (M = Zr, Hf)[128] in diethyl ether at –4 °C under methane evolution (Scheme 8).

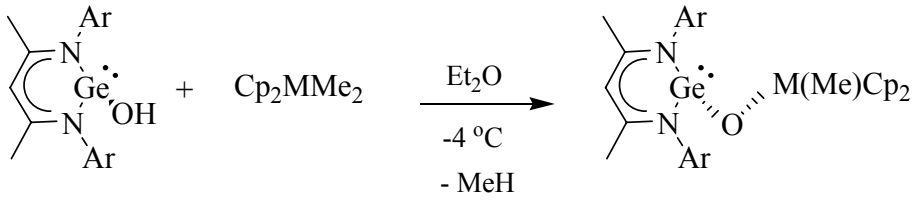

3

9, M = Zr
10, M = Hf

Scheme 8. Ar = 2,6-*i*$Pr_2C_6H_3$, Cp = C_5H_5.

The low solubility of **9** in the ethereal solution facilitates its separation as air-sensitive yellow-orange microcrystalline solid. Conversely, **10** after removal of the solvent and

recrystallization from a toluene/hexane mixture resulted in air-sensitive yellow-orange microcrystalline product. The IR spectra of **9** and **10** are devoid of any OH absorption in the range 3000-3500 cm^{-1}. ^1H NMR spectra of **9** and **10** exhibit the characteristic Cp resonances as singlets (δ 5.39 ppm and δ 5.33 ppm, respectively). In addition, a set of resonances assignable to the isopropyl and methyl protons associated with the β-diketiminato ligand in the range between δ 1.54 and 1.12 ppm and the absence of the hydroxyl proton resonance features both **9** and **10**. At higher field appears the resonance of the methyl protons coordinated to the metal (δ 0.14 ppm in **9** and δ 0.02 ppm in **10**). Electron impact (EI) spectrometry shows the parent ion $[M]^+$ with the isotopic pattern for **8** and **9** (m/z = 742 and m/z = 830). Particularly interesting is the same fragmentation pattern of both compounds featuring the cleavage of $[M - OM(Me)Cp_2]^+$ (m/z = 491).

The composition of **9** and **10** was unambiguously assigned by X-ray analysis. Yellow-orange crystals of **8** and **9** were obtained from a toluene/hexane mixture at –32 °C. Compounds **9** and **10** crystallize in the triclinic space group $P\bar{1}$ with one molecule in the asymmetric unit. Compounds **9** and **10** exhibit a germanium atom bounded through a bridging oxygen atom to a zirconium and hafnium atom, respectively. The coordination environment about the germanium atom is completed by a β-diketiminato ligand. Two Cp ligands and one methyl group complete the coordination sphere at the zirconium and hafnium atom, respectively. The geometry around the zirconium, as well as at the hafnium, is tetrahedral. The same geometry can be assigned for the germanium assuming that a lone pair of electrons occupies the fourth vacant site. The structures of **9** and **10** are shown in Figures 4 and 5. For **9** the Ge(1) and C(3) (γ-CH) deviate from the C_2N_2 ligand plane by 1.020 and 0.152 Å, respectively, resulting in a boat conformation. The Ge–N bond lengths (2.030 and 2.061 Å) and N–Ge–N angle (87.0°) are comparable to those reported in **3** and further examples.[57,58,129] A bent Ge–O–Zr (143.8°) linkage with Ge–O (1.797 Å) and a Zr–O bond

length (1.951 Å) show the characteristic features of compound **8**. The Zr–O bond length in $[(Cp)_2ZrCl]_2O$ (1.94 Å)[130] is in good agreement with **9**; nevertheless, a slightly shorter Zr–O bond length is observed in $Cp(CO)_3WOZr(Cl)Cp_2$ (1.871 Å)[131] and a longer distance in $[Cp_2Zr(Me)OAl(Me)_2]_2$ (2.044 Å).[122] The Zr–C(Cp) bond lengths range from 2.517 to 2.568 Å. The X_{Cp1}–Zr–X_{Cp2} centroid distances are 2.240 and 2.259 Å with an angle of 129.2°. Both Cp ligands are twisted to each other by 21° from the eclipsed conformation.

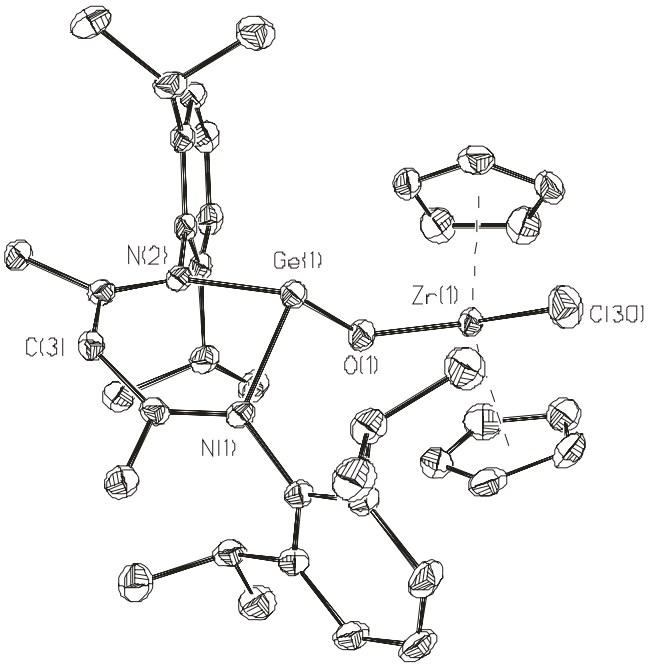

Figure 4. Thermal ellipsoid plot of **9** (thermal ellipsoids set at the 50 % probability). H atoms are omitted for clarity. Selected bond lengths [Å] and angles [°]: Zr(1)–O(1) 1.951(2), Zr(1)–C(30) 2.285(3), Ge(1)–O(1) 1.797(2), Ge(1)–N(1) 2.030(2), Ge(1)–N(2) 2.061(2); O(1)–Ge(1)–N(1) 99.0(1), O(1)–Ge(1)–N(2) 99.3(1), N(1)–Ge(1)–N(2) 87.0(1), O(1)–Zr(1)–C(30) 98.5(1), Ge(1)–O(1)–Zr(1) 143.8(1), X_{Cp1}–Zr(1) 2.240, X_{Cp2}–Zr(1) 2.259; X_{Cp1}–Zr(1)–X_{Cp2} 129.2 ($^*X_{Cp}$ = centroid distance of the Cp rings).

Compound **10** shows similar structural parameters compared with that of **9** but with different orientation of the Cp and C(30) groups (torsion angle for C(30)–Zr(1)–O(1)–Ge(1) of –41.7°, and C(30)–Hf(1)–O(1)–Ge(1) of –12.3°). A boat-like conformation is also observed due to the nonplanar Ge(1) and C(3) (γ-CH) atoms (1.038 and 0.154 Å) within the C_2N_2 framework.

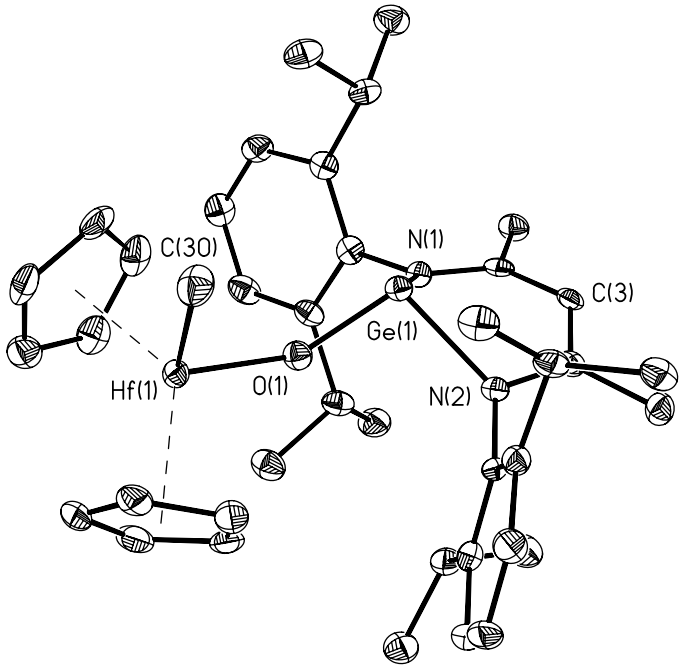

Figure 5. Thermal ellipsoid plot of **10** (thermal ellipsoids set at the 50 % probability). H atoms are omitted for clarity. Selected bond lengths [Å] and angles [°]: Hf(1)–O(1) 1.940(3), Hf(1)–C(30) 2.276(6), Ge(1)–O(1) 1.799(3), Ge(1)–N(1) 2.038(4), Ge(1)–N(2) 2.052(4); O(1)–Ge(1)–N(1) 97.5(2), O(1)–Ge(1)–N(2) 100.7(2), N(1)–Ge(1)–N(2) 86.8(1), O(1)–Hf(1)–C(30) 96.3(2), Ge(1)–O(1)–Hf(1) 141.9(2), X_{Cp1}–Hf(1) 2.222, X_{Cp2}–Hf(1) 2.236; X_{Cp1}–Hf(1)–X_{Cp2} 128.0 ($^{*}X_{Cp}$ = centroid distance of the Cp rings).

The Ge–N bond length and N–Ge–N angle is 2.045(av) Å and 86.8°, respectively. Aside from the Ge–O bond distance (1.799 Å) and the Hf–O bond length (1.940 Å) a bent Ge–O–Hf angle (141.9°) features the structure of **10**.The X_{Cp1}–Hf–X_{Cp2} centroid distances are 2.222 and 2.236 Å with an angle of 128.0°. A deviation (23°) from an ideally eclipsed Cp group is also observed in **10**. A comparison with earlier examples, even though they are based on Ge(IV) as in $Ph_3SiOGePh_3$ and $Ph_3GeOSnPh_3$,[132] shows that M–O–M´ angles (142.5° and 134.9°, respectively) are quite similar to those in compounds **9** and **10**. The slight shortening of the Ge–O bond length observed for both **9** and **10** compared with that in **3** (1.828 Å) is due to the tendency of both transition metals to form a strong bond toward hard donors with the consequence that the electron density shifts from the donor atom to the transition metal center and enhances the interaction between the germanium atom and the donor.

In summary, it has been shown the synthesis and structural characterization of two novel heterobimetallic complexes based on germanium(II) and an oxygen bridge. Compounds **9** and **10** contain two metal centers in high and low oxidation states.

2.5. Lewis Base Character of Hydroxygermylenes for the Preparation of Heterobimetallic [{HC(CMeNAr)$_2$}Ge(OH)M] Systems (Ar = 2,6-*i*Pr$_2$C$_6$H$_3$; M = Fe, Mn)

The preparation of compounds with bonds between a transition metal and either silicon, germanium, tin or lead has provided a rich chemistry including synthetic and structural aspects as well as catalytic applications.[133–147] Furthermore, the investigation of the reactivity of divalent heavier Group 14 elements has prompted a constant interest due to the wide range of reaction possibilities.[78,79,81,83,86,87] The presence of bulky ligands and the complexation with transition metals greatly increase the stability of otherwise unstable species. In this regard, a compound of composition ArGeOH·W(CO)$_5$ was obtained by hydrolysis of ArGeNR$_2$·W(CO)$_5$ (Ar = 2,6-bis((diethylamino)methyl)phenyl; R = *i*Pr).[148] In some cases such low-valent Group 14 compounds, by virtue of the electron lone pair, function as Lewis bases toward coordinatively unsaturated transition metals.[149–151] Compound **3** is therefore interesting because it may act either as a donor or react at the OH functionality with transition metals. The latter mode of reaction is reminiscent of a water gas shift reaction.[152] Herein, we describe the reaction of **3** with iron- and manganese-carbonyl complexes.

Compounds **11** and **12** were obtained by reaction of **3** with the respective transition metal fragments. Compound **11** was isolated after separation of Fe(CO)$_5$, also a product of the reaction of **3** and diiron nonacarbonyl, as a light brown powder (Scheme 9).

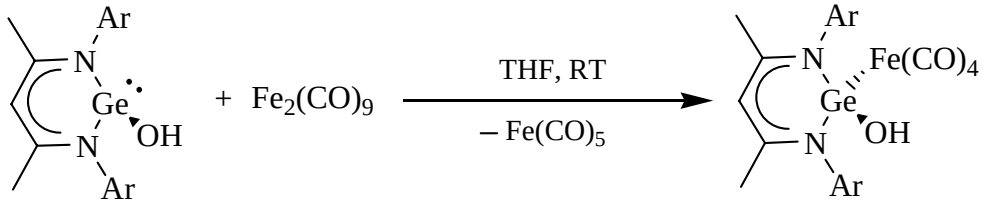

3 **11**

Scheme 9. Ar = 2,6-*i*Pr$_2$C$_6$H$_3$.

Compound **12** was prepared by the reaction of **3** with cyclopentadienylmanganese tricarbonyl with concomitant CO elimination during 3 h of UV-irradiation in THF at ambient temperature (Scheme 10). Compounds **11** and **12** are air- and moisture-sensitive. Compound **11** is soluble in THF, sparingly soluble in toluene and insoluble in common organic solvents, whereas compound **12** is insoluble in the aforementioned solvents and in DMSO as well. Compounds **11** and **12** are thermally quite stable and their mass spectra show the molecular ion peaks $[M]^+$ with proper isotopic patterns (*m*/*z* 676 and *m*/*z* 684, respectively), followed by stepwise elimination of CO. Compound **12** displays a very sharp OH band in the IR spectrum ($\tilde{\nu}$ 3642 cm^{-1}). The corresponding absorption for **11** was found at lower wave number ($\tilde{\nu}$ 3599 (OH) cm^{-1}). These values are in agreement with the OH frequency reported for $ArGeOH{\cdot}W(CO)_5$ ($\tilde{\nu}$ 3645 cm^{-1}).[148] Moreover carbonyl absorptions for **11** and **12** were found at $\tilde{\nu}$ 2039, 1956, 1942 cm^{-1} and 1864, 1846 cm^{-1}, respectively, in the expected range for terminal carbonyl groups.[153]

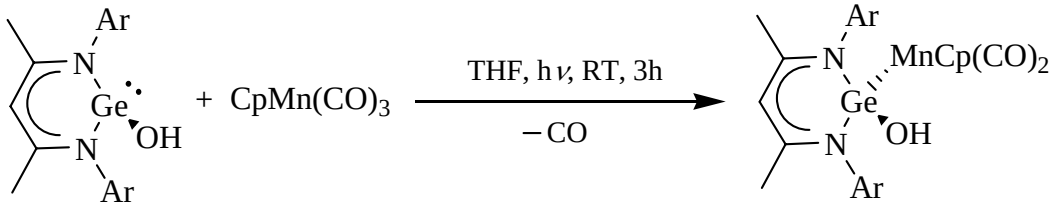

3 **12**

Scheme 10. Ar = 2,6-*i*$Pr_2C_6H_3$, Cp = C_5H_5.

The ^1H NMR spectrum of **11** in D_8-THF revealed a downfield (δ 4.24 ppm) resonance of the hydroxyl proton. The CO resonance in the ^{13}C NMR spectrum was found at δ 214.8 ppm, a value comparable to that of $[\{HC(CMeNAr)_2\}Ge(Cl)Fe(CO)_4]$ (δ 213.1 ppm; Ar = Ph).[154] Due to the poor solubility of **12** analogous measurements could not be carried out.

The molecular structures of **11** and **12** were determined by single-crystal X-ray analyses. Compounds **11** and **12**, respectively, were dissolved in hot toluene and after cooling

the solution to ambient temperature single crystals were obtained. **11** formed light brown, **12** light orange-yellow crystals.

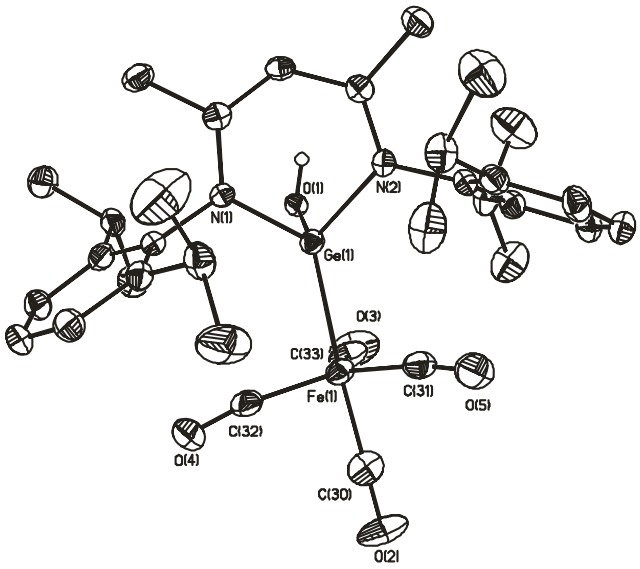

Figure 6. Thermal ellipsoid plot of **11** showing the 50% probability level. H atoms, except for the OH group, are omitted for clarity. Selected bond lengths [Å] and angles [°]: Ge(1)–O(1) 1.840(2), Ge(1)–N(1) 1.945(2), Ge(1)–N(2) 1.948(2), Fe(1)–Ge(1) 2.330(1), Fe(1)–C(30) 1.772(3), Fe(1)–C(31) 1.796(3), Fe(1)–C(32) 1.795(4), Fe(1)–C(33) 1.782(3); O(1)–Ge(1)–N(1) 98.3(1), O(1)–Ge(1)–N(2) 98.8(1), N(1)–Ge(1)–N(2) 93.2(1), O(1)–Ge(1)–Fe(1) 113.5(1), N(2)–Ge(1)–Fe(1) 123.3(1), N(1)–Ge(1)–Fe(1) 124.3(1), C(30)–Fe(1)–C(33) 91.6(1), C(30)–Fe(1)–C(32) 88.6(1), C(33)–Fe(1)–C(32) 116.9(2), C(30)–Fe(1)–C(31) 86.8(1), C(33)–Fe(1)–C(31) 124.7(2), C(32)–Fe(1)–C(31) 118.3(1), C(30)–Fe(1)–Ge(1) 175.8(1), C(33)–Fe(1)–Ge(1) 85.1(1), C(32)–Fe(1)–Ge(1) 95.2(1), C(31)–Fe(1)–Ge(1) 93.0(1).

Both compounds crystallize in the monoclinic space group $P2_1/n$. In **11**, a germanium atom binds to a monoanionic β-diketiminato ligand, a hydroxyl group and to an iron-carbonyl

fragment generating a four coordinate germanium center, which adopts a distorted tetrahedral geometry.

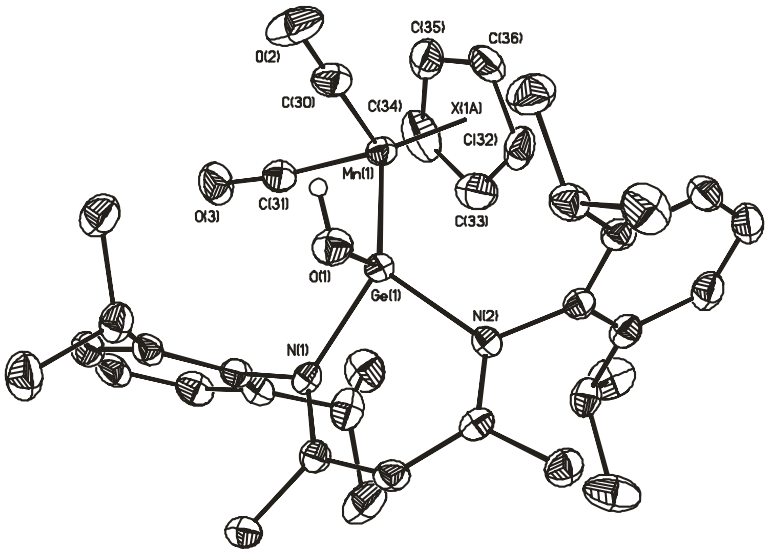

Figure 7. Thermal ellipsoid plot of **12** showing the 50% probability level. H atoms, except for the OH group, are omitted for clarity. Selected bond lengths [Å] and angles [°]: Ge(1)–O(1) 1.816(2), Ge(1)–N(2) 1.970(2), Ge(1)–N(1) 1.963(2), Mn(1)–Ge(1) 2.345(1), O(2)–C(30) 1.187(3), O(3)–C(31) 1.165(4), Mn(1)–C(30) 1.744(3), Mn(1)–C(31) 1.772(3); O(1)–Ge(1)–N(2) 93.7(1), O(1)–Ge(1)–N(1) 93.4(1), N(1)–Ge(1)–N(2) 91.1(1), O(1)–Ge(1)–Mn(1) 119.0(1), N(1)–Ge(1)–Mn(1) 123.5(1), N(2)–Ge(1)–Mn(1) 127.4(1), C(30)–Mn(1)–Ge(1) 87.6(1), C(31)–Mn(1)–Ge(1) 95.0(1), $X_{(1A)}$–Mn(1)* 1.779(3), $X_{(1A)}$–Mn(1)–Ge(1) 128.9(3), $X_{(1A)}$–Mn(1)–C(30) 123.8(3), $X_{(1A)}$–Mn(1)–C(31) 120.7(3) ($^{*}X_{(1A)}$ = centroid of the Cp ring).

Also one can argue that germanium takes up the axial position of a distorted trigonal bipyramidal geometry at the $Fe(CO)_4$ fragment (Figure 6). The Ge–Fe bond length in **11** (2.330(1) Å) is comparable to that (2.348(1) Å) in [{η^3-[(μ-*t*BuN)$_2$(SiMeN*t*Bu)$_2$]}GeFe(CO)$_4$],[155] but slightly longer when compared with that in

[{HC(CMeNAr)$_2$}Ge(Cl)Fe(CO)$_4$] (2.298(2) Å),[154] (Ar = Ph) and is clearly shortened (2.240(2) Å) in [Fe(CO)$_4${Ge(OC$_6$H$_2$*t*Bu$_2$-2,6-Me-4)$_2$}].[156] Moreover, a longer Ge–O bond length in **11** (1.840(2) Å) is observed compared with that in [{HC(CMeNAr)$_2$}GeOH] (1.828(1) Å). This is in contrast with the shortened Ge–O bond length found in [{HC(CMeNAr)$_2$}Ge(S)OH] (1.751(2) Å). In **12** both the germanium and the manganese atom reside in the center of a distorted tetrahedral environment, where germanium is bonded to a β-diketiminato ligand, a hydroxyl group and to a manganese atom, while the coordination sphere around the manganese atom comprises two carbonyl groups and a cyclopentadienyl ligand (Figure 7). Previously reported germanium-manganese complexes such as [(η^5-MeC$_5$H$_4$)Mn(CO)$_2$]$_3$Ge and [(η^5-MeC$_5$H$_4$)Mn(CO)$_2$]$_3$Ge, have Ge–Mn bond lengths between 2.236(1) Å and 2.573(1) Å, and are in the range with that found in **12** (2.345(1) Å).[157–160] Further structural analysis of **12** shows that the Ge–O bond length (1.816(2) Å) is unchanged with respect to that in **11** and displays an OH orientation pointing to the transition-metal center, by contrast to **11** where it is pointing to the C_3N_2Ge backbone.

In summary, the reactivity of the [{HC(CMeNAr)$_2$}GeOH] compound with an electron lone pair and an OH moiety was demonstrated by the reaction with transition metal fragments of manganese and iron, respectively.

2.6. Stable Monomeric Germanium(II) and Tin(II) Compounds with Terminal Hydrides

Metal hydrides and their complexes are considered valuable synthons in chemistry. It was demonstrated that main-group and transition-metal hydrides are important intermediates in some industrial processes and also function as catalysts.[161–169] Furthermore, in the quest for alternative energy sources metal hydrides have been considered as potential feedstock for hydrogen storage.[170–173] Group 14 hydrides such as R_3SiH, R_3GeH, and R_3SnH are important reagents for some key reactions in organic synthesis. The preparation of these species is commonly carried out by reduction of the corresponding chloride compounds with lithium aluminum hydride.[49,52,174–180] However, the isolation and structural characterization of monomeric, terminal low valent Group 14 hydrides seem to be difficult as a result of the potential reactivity and instability of these species. So far, only [{2,6-$Trip_2C_6H_3Sn(\mu$–H)}$_2$] (Trip = 2,4,6-*i*$Pr_3C_6H_2$) has been structurally characterized and exhibits a dimeric structure with tin(II) atoms connected by bridging hydrides ligands,[181] although the existence of MH_2 (M = Si to Pb) has been anticipated by theoretical calculations.[182] Previously, Roesky and co-workers reported the preparation of the germanium(II) [{HC(CMeNAr)$_2$}GeCl] (**1**; Ar = 2,6-*i*$Pr_2C_6H_3$) and tin(II) [{HC(CMeNAr)$_2$}SnCl] (**13**).[53,58] Treatment of **1** with $LiAlH_4$ or $NaBH_4$ did not afford the terminal germanium(II) hydride, but rather, the four-coordinate adduct [{HC(CMeNAr)$_2$}Ge(H)BH_3] was formed. Moreover, attempts to prepare terminal tin(II) hydride from **13** in reactions with reducing reagents such as $NaBH_4$, KBH_4, and KH were unsuccessful. In contrast, the reaction of **1** and **13** with AlH_3·NMe_3[183–185] in toluene at –4 ^oC yield the first monomeric and terminal germanium(II) and tin(II) hydrides [{HC(CMeNAr)$_2$}GeH] (**14**, Scheme 11)[186] and [{HC(CMeNAr)$_2$}SnH] (**15**). Elimination of

trimethylamine as a volatile by-product was observed during the course of the reaction of **14** and **15** with $AlH_3{\cdot}NMe_3$. The color of the reaction mixture changed from yellow to orange-red in the synthesis of **14**, and from pale yellow to green in the synthesis of **15**. No further color change was observed for either reaction mixture upon warming to ambient temperature.

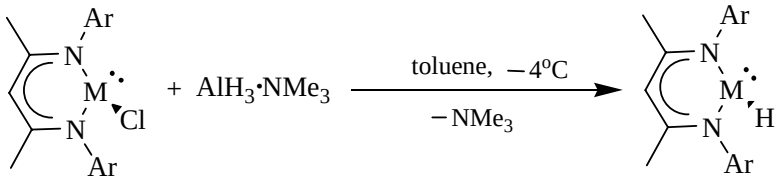

M = Ge (**1**)
Sn (**13**)
Ar = 2,6-*i*$Pr_2C_6H_3$

M = Ge (**14**)
Sn (**15**)

Scheme 11. Ar = 2,6-*i*$Pr_2C_6H_3$.

Compound **14** is thermally stable over a long period of time when stored in an inert atmosphere in a glove box, whereas **15** decomposes slowly under the same conditions to form an insoluble gray solid within 4 days. However, **15** is stable at –32 °C over a longer period of time. Both **14** and **15** are air- and moisture-sensitive. In the IR spectrum of **14**, a strong absorption was observed 1733 cm^{-1}, which can be attributed to the Ge–H stretching mode and compares well with that reported for Ar(H)GeGe(H)Ar[187] (1785 cm^{-1}; Ar = 2,6-$Dipp_2C_6H_3$; Dipp = 2,6-*i*$Pr_2C_6H_3$), but is found at a lower frequency than that for [{$HC(CMeNAr)_2$}Ge(H)BH_3] (1928 cm^{-1}).[53] Hydrides complexes of germanium(IV) show Ge–H absorptions in the range from 1953 to 2175 cm^{-1}.[174,188–190] The Sn–H stretching mode of **15** (1849 cm^{-1}) is comparable to those in the hydrogen-bridged tin compound [{2,6-$Trip_2C_6H_3Sn(\mu$–H)$\}_2$] (1828 and 1771 cm^{-1}).[181] In the ^{1}H NMR spectrum of **14**, the Ge–H hydrogen atom resonates at lower field (δ 8.08 ppm) than those in Ar(H)GeGe(H)Ar (δ 3.48 ppm) and $Ar(H)_2GeGeAr{\cdot}PMe_3$ (δ 3.81 ppm; Ar = 2,6-$Dipp_2C_6H_3$; Dipp = 2,6-*i*$Pr_2C_6H_3$).[187] Interestingly, the Ge–H proton resonance of **14** is in the range of germanium(IV) hydrides.[191]

The Sn–H proton resonance of **15** is found at a surprisingly lowfield shift (δ 13.83 ppm) relative to that in [{2,6-Trip$_2$C$_6$H$_3$Sn(μ–H)}$_2$] (δ 7.87 ppm),[181] and is flanked by Sn satellites ($^1J(^{119}\text{Sn}, ^1\text{H})$ = 64 Hz) (Figure 8). The Sn–H resonance of **15** is the lowest-field chemical shift observed for tin hydride.[174,192–194] The ^{119}Sn NMR resonance of **15** (δ –224.7 ppm) is in accordance with a three-coordinate tin(II) enviroment ([{HC(CMeNAr)$_2$}SnCl]: δ –224 ppm;[53] [H$_2$B(pz)$_2$]SnCl: δ –305 ppm; [(Ph)$_2$B(pz)$_2$]SnCl: δ –353 ppm; [H$_2$B(pz´)$_2$]SnCl: δ –271 ppm; pz = pyrazole; pz´ = 3-methylpyrazole).[195]

Orange-red single crystals of **14** and green crystals of **15** suitable for X-ray structural analysis were grown from saturated hexane solutions at –32 °C within two days (**14**) or after one week (**15**). Compound **14** crystallizes in the monoclinic space group $P2_1/n$ with two independent isostructural monomers in the asymmetric unit. Although the Ge–H hydrogen atom in **14** could not be localized in the difference-electron density map, the Ge–H linkage was unequivocally confirmed by IR and ^{1}H NMR spectroscopy (see above).

Figure 8. Section of the ^{1}H NMR spectrum (500 MHz, C_6D_6) of **15** showing the Sn–H proton resonance flanked by tin satellites.

In **14**, the germanium atom is tetrahedrally coordinated by the *β*-diketiminato ligand, a hydrogen atom, and, we assume, a lone pair of electrons at the fourth coordination site (Figure 9). Compound **14** exhibits Ge–N bond lengths of 1.989(2) Å (molecule 1) as well as 1.994(2) and 1.988(2) Å (molecule 2), and these lengths are very similar to those of **1** (1.988(2), 1.997(2) Å).[58]

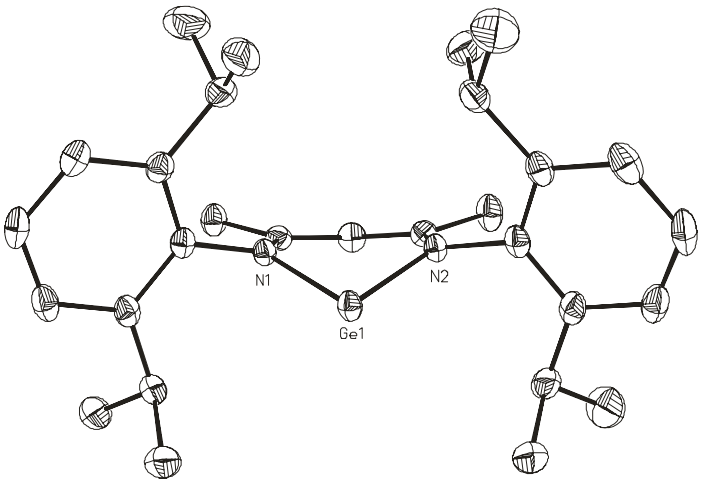

Figure 9. Thermal ellipsoids plot of one molecule of **14** showing the atoms at the 50 % probability level. Hydrogen atoms are omitted for clarity. The Ge–H hydrogen atom could not be localized. Only the numbering scheme of molecule 1 is depicted. Selected bond lengths [Å] and angles [°]: molecule 1: Ge(1)–N(1) 1.989(2), Ge(1)–N(2) 1.989(2); N(1)–Ge(1)–N(2) 90.3(1); molecule 2: Ge(2)–N(1A) 1.994(2), Ge(2)–N(2A) 1.988(2); N(1A)–Ge(2)–N(2A) 90.5(1).

Further structural analysis of **14** reveals a weak intermolecular interaction between the lone pair of electrons at the germanium atom in one molecule and the *γ*-C–H hydrogen atom from the C_3N_2Ge backbone of another molecule (*d*(Ge(1)···H(3AA): 2.98 Å; *d*(Ge(2)···H(3A): 3.19 Å) (Figure 10). Complex **15** crystallizes in the monoclinic space group *C*2/*c* with one monomer in the asymmetric unit. Weak intermolecular contacts between the lone pair of

electrons on the tin and the Sn–H the hydrogen atom from another molecule generate hydrogen bridges formation of a dimer (*d*(Sn(1)···H(1A): 4.01(3) Å; *d*(Sn···Sn): 3.71 Å).

Compound **15** comprises a distorted tetrahedral geometry at the tin atom, which coordinates to a monoanionic β-diketiminato ligand, a hydrogen atom, and, we assume, a lone pair of electrons at the fourth coordination site (Figure 11). The Sn–H hydrogen atom was localized from the residual electron density. The most prominent structural feature of **15** is the Sn–H bond length of 1.74(3) Å, which is in good agreement with Sn–H bond lengths predicted by theoretical calculations (1.77 Å).[182,196] However, this length is shorter than those of [{2,6-Trip$_2$C$_6$H$_3$Sn(μ–H)}$_2$], which exhibits two different μ-hydrogen bonds (*d*(Sn–H): 1.89(3), 1.95(3) Å).[181]

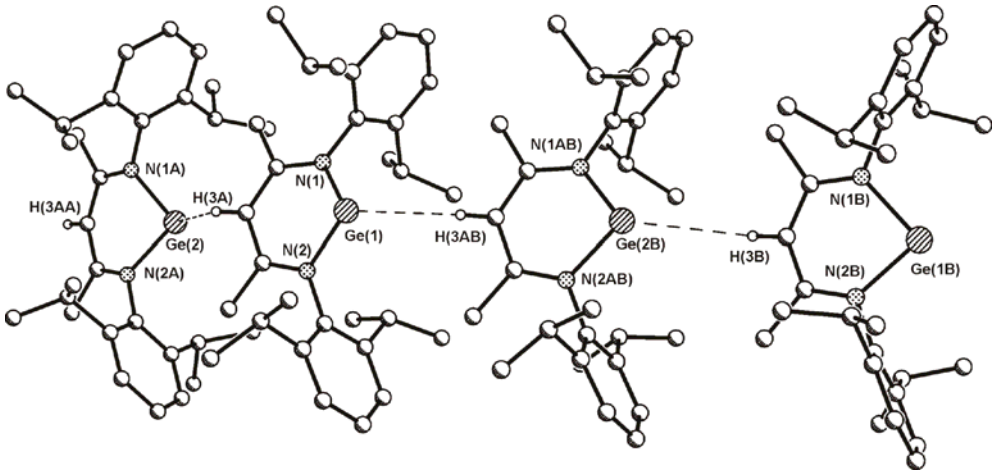

Figure 10. Packing diagram of **14** in the solid state showing the formation of chains through intermolecular contacts between a lone pair of electrons at the germanium atom to the γ-C–H hydrogen atom of another molecule.

To investigate the electronic properties in **14** and **15**, ab initio calculations were carried out by using the Gaussian program package[106] with the well-established DFT-variant B3LYP.[104,105,197] Two different basis sets were employed to achieve a suitable description of the electronic structure. The LANL2DZ[198–200] basis set (for Ge and Sn) and the 6-31G[107,108]

basis set (for the remaining atoms) with additional double-diffuse functions were used. The structures of both complexes were determined by full geometry optimization. The obtained equilibrium geometries were in good agreement with the X-ray data. Since the structural parameters are the result of the calculated molecular orbitals, an analysis of the electronic structure was perfomed with the NBO[113–116] procedure, which makes it possible to describe and quantify the contribution of the atomic orbitals to the molecular orbitals. The calculations showed that the electronic density the lone pair on the central atom in each of **14** and **15** contributes to the bonding in the complex. The NBO analysis of the M–H bond shows that the contribution of the lone pair of electrons on germanium can best be described as an $sp^{0.32}$ hybrid, while the hybrid for tin is of type $sp^{0.25}$ (Figures S1–S3; Supporting Materials). The larger p character at the Ge center in compound **14** (20 % greater than that at the Sn center in **15**) leads to an enhanced delocalization of π electrons over the neighboring p orbitals of the nitrogen atoms. Remarkably, in the case of **15** there is no participation of the hydrogen s orbital in the lone pair of electrons. Analysis of the metal–hydrogen bond by using the natural localized molecular orbitals (NLMO) reveals significant differences between **14** and **15**. For the Ge–H bond in **14**, the hydrogen atom contributes 65 %, and the corresponding hydrogen atom in the Sn–H bond contributes 70 %. Analysis of the molecular orbitals of **15** also shows that there is no participation of the hydrogen s orbital to the wave function describing the lone pair of electrons. Another factor that influences the electron density at the hydrogen atom is the amount of donor-acceptor interaction with the nitrogen atoms of the ring system. This interaction occurs mainly through two-electron stabilization in a donor-acceptor situation[117] involving the bonding Ge–H orbital and nonbonding orbitals of the ring system, which transfers electron density from the nitrogen atoms into the Ge–H bond. This effect is 50% larger for **14** than for **15**. Taking these findings into account, the low-field chemical shift of the hydrogen atom in **15** might be deduced. The lack of further stabilization from

delocalization causes the tin atom to pull out electron density strongly from the hydride to compensate for its electron-deficient character. Hence the "naked" nature of the hydrogen atom in the Sn–H bond is a reflection of extreme deshielding and leads to such a low-field chemical shift.

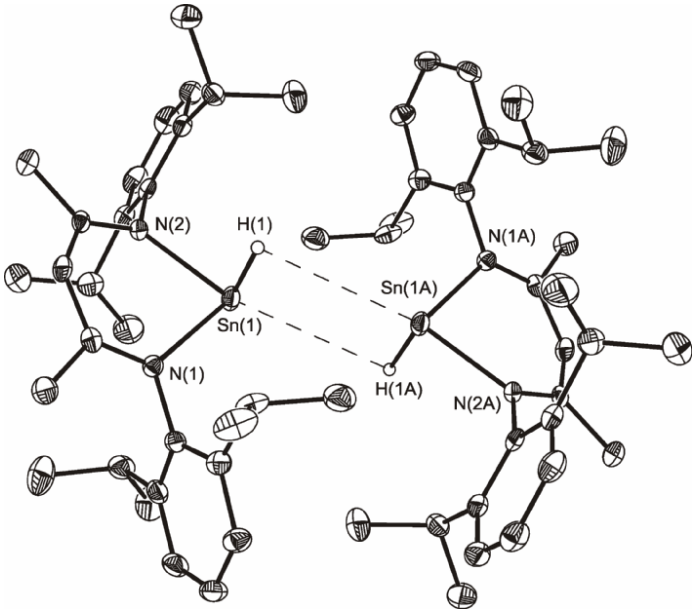

Figure 11. Thermal ellipsoids plot of **15** showing the atoms at the 50 % probability level. H atoms, except for Sn–H are omitted for clarity. Selected bond lengths [Å] and angles [^{o}]: Sn(1)–H(1) 1.74(3), Sn(1)–N(1) 2.194(2), Sn(1)–N(2) 2.198(2), Sn(1)···H(1A) 4.01(3); H(1)–Sn(1)–N(1) 93.4(8), H(1)–Sn(1)–N(2) 92.6(8), N(1)–Sn(1)–N(2) 85.1(1).

In summary, we were able to isolate and structurally characterize compounds of composition [{HC(CMeNAr)$_2$}GeH] and [{HC(CMeNAr)$_2$}SnH] by the reaction of AlH_3·NMe_3 with appropiate chloride precursor. These compounds represent the first examples of terminal, monomeric hydrides of germanium(II) and tin(II).

2.7. Low-Valent Lead and Bismuth Organohalides Bearing a β-Diketiminato Ligand

Of the heavier Group 14 and Group 15 elements lead and bismuth can exhibit nonhybridization effect which derives from relativistic considerations and therefore favors lower oxidation states for both elements.[201–204]

Although the organochemistry of low-valent lead(II) is known, its access is rather limited due to the poor stability and facile disproportionation of lead(II) to elemental lead.[205,206] In this context the use of a bulky ligand has facilitated the isolation and structural characterization of several low-valent species. The compounds $[Pb(\mu\text{–}Cl)\{C(SiMe_2Ph)_3\}]_2$[207] and $[Pb(\mu\text{–}Cl)\{C(SiMe_3)_3\}]_3$[208] were reported and structurally investigated. The diffraction studies of both compounds show that they are bridged by chlorine atoms, and the latter compound exhibits a six-membered ring. Moreover, the preparation of $[Pb(\mu\text{–}Cl)\{C(SiMe_3)_2(SiMe_2OMe)\}]_2$, stabilized by intramolecular coordination between a methoxy group and the metal center, shows the importance of electronic stabilization.[208] Organolead(II) compounds can display four- and three-coordination at the metal center (e.g. $[Pb\{N(SiMe_3)C(Ph)C(SiMe_3)(C_5H_4\text{-}2)\}_2]$ and $[Pb\{N(SiMe_3)C(Ph)C(SiMe_3)(C_5H_4\text{-}2)\}Cl]$). In each case, it was shown that additional donor sites of the nitrogen atom of a pyridyl enamino ligand greatly stabilized the structures.[209] Again, the use of an encumbering ligand precludes the lead atom from decomposition, and led to the isolation of $[ArPb\cdot\eta^2\text{-}PhMe][MeB(C_6F_5)_3]$, which further reacts with pyridine to give $[ArPb(py)_2][MeB(C_6F_5)_3]$ (Ar = 2,6-$Trip_2C_6H_3$; Trip = 2,4,6-i-$Pr_3C_6H_2$).[210]

In addition, the formation of homonuclear lead multiple bonds and heteronuclear lead transition metal multiple bonds has also gained attention due to the multiple bonding formation such as: diplumbyne ArPbPbAr (Ar = 2,6-$Trip_2C_6H_3$; Trip = 2,4,6-i-$Pr_3C_6H_2$)[19]

lead triple bonds to molybdenum [$Br(PMe_3)_4MoPbAr$],[137] and lead triple bonds to tungsten [$BX(PMe_3)_4WPbAr$] (Ar = 2,6-$Trip_2C_6H_3$; Trip = 2,4,6-*i*$Pr_3C_6H_2$; X = Br, I).[211]

Low-valent organobismuth chemistry is structurally diverse and has been widely explored. Ligands with nitrogen-base pendant arms give additional intramolecular coordination in [{2-$(Me_2NCH_2)C_6H_4$}$_3$Bi],[212] and in addition show bismuth compounds with high coordination numbers at the metal center [Ar_2BiCl; (Ar = 2-$(Me_2NCH_2)C_6H_4(C_9H_{12}N)$; Ar = 8-$(Me_2N)C_{10}H_6(C_{12}H_{12}N)$)].[213] An interesting recent development results from the reaction of an organobismuth halide and a reducing agent to generate a terminal bismuth hydride Ar_2BiH (Ar = 2,6-$C_6H_3Mes_2$; Mes = 2,4,6-$Me_3C_6H_2$).[214] Several structural motifs and fashion bonding, among them dibismuthane, dibismuthene, and monocyclo, bismuthines and polycyclic bismuthines compounds show the versatility of bismuth to the formation of unsaturated species.[215,216]

Essential for the access of novel low-valent lead and bismuth compounds are appropriate ligands. Here we describe the synthesis and characterization of low-valent organolead and organobismuth halides [{$HC(CMeNAr)_2$}PbBr] (**17**; Ar = 2,6-*i*$Pr_2C_6H_3$) and [{$HC(Et_2NCH_2CH_2NCMe)_2$}$BiCl_2$] (**19**). Compounds **17** and **19** were prepared by salt elimination reaction of the corresponding lithium salt [{$HC(CMeNAr)_2$}Li(Et_2O)][217] (**16**; Scheme 12) and [{$HC(Et_2NCH_2CH_2NCMe)_2$}Li][218] (**18**; Scheme 13) with lead and bismuth halides, respectively.

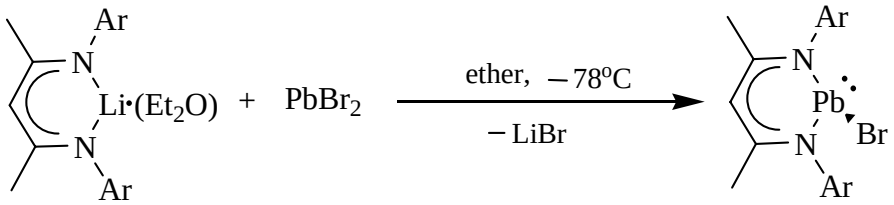

16 **17**

Scheme 12. Ar = 2,6-*i*$Pr_2C_6H_3$.

Compounds **17** and **19** were recrystallized from saturated toluene and a toluene/pentane solution at –32 °C. Compound **17** as pale green crystals and yellow crystals of compound **19**.

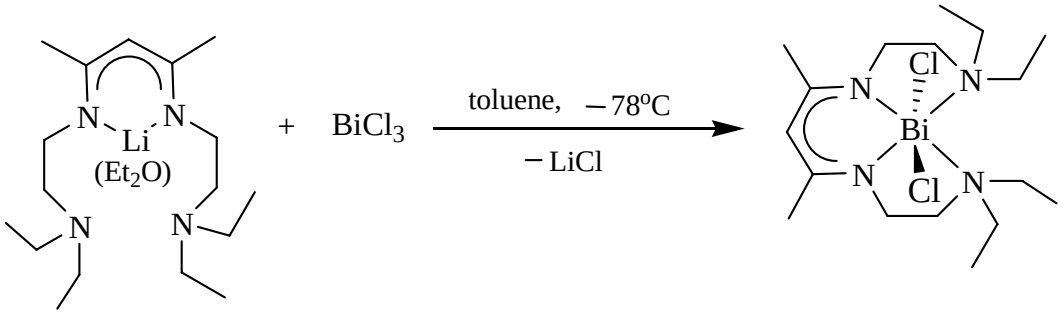

18 **19**

Scheme 13. Preparation of **19**.

In the ^{1}H NMR spectrum of **17** the γ-C–H proton resonates at δ 4.89 ppm, while the corresponding resonance for **19** resonates at δ 4.47 ppm. However, no ^{207}Pb resonance could be observed for **17**. It has been noted that difficulties in detecting this signal might be due to the large anisotropy effects expected for the three components of the chemical shift tensor since large chemical shift anisotropies result in short T_1 and T_2 relaxation times, very broad and difficult to detect isotopic signals are often the outcome.[219] Furthermore, the presence of large 2,6-*i*Pr$_2$C$_6$H$_3$ substituents could slow the molecular tumbling rates required to average the three anisotropic shift components. Another factor that might account for the lack of a resonance is the presence of the quadrupolar moment of ^{79}Br or ^{81}Br bound to the lead atom which leads to the broadening of the ^{207}Pb NMR signal.[220] Similar behavior was also found in other organolead halide compounds (e.g. [Pb(μ–Cl){C(SiMe$_2$Ph)$_3$}]$_2$,[207] [Pb(μ–Cl){C(SiMe$_3$)$_3$}]$_3$,[208] [ArPb(py)$_2$][MeB(C$_6$F$_5$)$_3$],[210] and [Pb(μ–Br)Ar´*i*Pr$_2$]$_2$ and [Pb(μ–Br)Ar**i*Pr$_2$*t*Bu]$_2$ (Ar´ = 2,6-*i*Pr$_2$(C$_6$H$_3$)$_2$-2,6-C$_6$H$_3$; Ar* = 2,6-*i*Pr-4-*t*Bu(C$_6$H$_2$)$_2$-2,6-C$_6$H$_3$).[221] Compounds **17** and **19** show molecular ion peaks $[M]^+$ with correct isotopic patterns at *m*/*z* 704 and *m*/*z* 574, respectively. In **17**, ion peaks at *m*/*z* 625 and *m*/*z* 417 were assigned to [*M* –

$Br]^+$ and to $[M - PbBr]^+$, respectively; whereas **19** exhibits an ion at *m*/*z* 539 ascribed to $[M - Cl]^+$.

Pale green and yellow single crystals of compounds **17** and **19**, respectively, were subjected to X-ray diffraction studies to determine their molecular composition in the solid state. Compound **17** crystallizes in the triclinic space group $P\bar{1}$ with two molecules per unit cell. In **17**, the lead atom is tetrahedrally coordinated by two nitrogen atoms of the monoanionic *β*-diketiminato ligand, a terminal bromine atom, and, we assume, a lone pair of electrons at the fourth coordination site (Figure 12). The Pb–Br bond length (2.716(6) (Å) in **17** is comparable with that of [py·Pb(Br)Ar] (Ar = 2,6-$Trip_2C_6H_3$; Trip = 2,4,6-$i Pr_3C_6H_2$; 2.706(6) (Å)),[222] but significantly shorter than that those observed in [Pb(μ–Br)Ar]$_2$ (Ar = 2,6-$Trip_2C_6H_3$; Trip = 2,4,6-$i Pr_3C_6H_2$; 2.789(16) and 2.784(16) (Å)),[222] [Pb(μ–Br)Ar´$i Pr_2$]$_2$ (2.813(5) and (3.035(5) (Å)), and [Pb(μ–Br)Ar*$i Pr_2 t$Bu]$_2$ (2.920(7) and (2.919(7) (Å)),[221] and in [$ArPbBr(NH_3)$] (Ar = 2,6-$Trip_2C_6H_3$; Trip = 2,4,6-$i Pr_3C_6H_2$; 2.804(5) (Å)).[223] The Pb–N bond length observed for [Pb{N($SiMe_3$)C(Ph)C($SiMe_3$)(C_5H_4-2)}$_2$] (2.274(7) to 2.626(8) (Å)), [Pb{N($SiMe_3$)C(Ph)C($SiMe_3$)(C_5H_4-2)}Cl] (2.279(7) (Å) and 2.320(6) (Å)) and in [Pb{Ph_2PC(H)Py}{N($SiMe_3$)$_2$}][224] (2.233(18) and 2.362(19) (Å)) are within the range of those found for **17** (2.283(2) and 2.293(2) (Å)).

Compound **19** crystallizes in the monoclinic space group $P2_1/c$ with four molecules per unit cell. In **19**, the bismuth atom occupies the center of a distorted octahedron and coordinates to two nitrogen atoms from the *β*-diketiminato ligand, to two nitrogen atoms from the pendant arms of the same ligand, and to two chlorine atoms in *trans* position (Figure 13). By comparing the Bi–Cl bond lengths (2.675(8) and 2.736(9) Å) in **19** they were found shorter than similar Bi–Cl linkages observed in Ar_2BiCl (2.483(9) Å),[214] [{($Me_3Si)_2CH$}$_2$]$_2$BiCl (2.530(2) Å),[225] and in $ArBiCl_2$ (2.539(1) and 2.501(1) Å) and [$ArBiCl_2$]$_2$ (2.496(6) to 2.544(5) Å) (Ar = 2,6-$Mes_2C_6H_3$; Mes = 2,4,6-$Me_3C_6H_2$),[226]

however, they show good agreement with that found for Ar_2BiCl (Ar = 2-$(Me_2NCH_2)C_6H_4(C_9H_{12}N)$ (2.667(2) Å).[213]

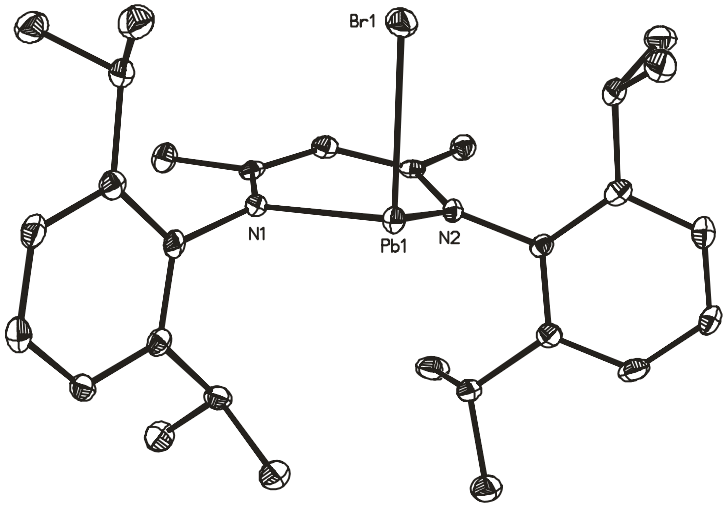

Figure 12. Thermal ellipsoids plot of **17** showing the atoms at the 50 % probability level. H atoms are omitted for clarity. Selected bond lengths [Å] and angles [°]: Pb(1)–Br(1) 2.716(6), Pb(1)–N(1) 2.293(2), Pb(1)–N(2) 2.283(2); N(2)–Pb(1)–N(1) 82.9(9), N(2)–Pb(1)–Br(1) 93.2(6), N(1)–Pb(1)–Br(1) 90.7(6).

Compound **19**, displays shorter and longer Bi–N bond lengths in the range from 2.232(2) to 2.736(9) Å. Although the bismuth–nitrogen distance (av 2.736(9) Å) is shorter than the sum of the van der Waals radii for bismuth and nitrogen (4.0 Å), it is longer than a typical Bi–N covalent bond length (2.25 Å).[43,227] In fact, the weak amine nitrogen interactions in **19** are even shorter than that of compounds with intermolecular interaction as was observed for [{2-$(Me_2NCH_2)C_6H_4\}_3Bi$] (av 3.07(3) Å).[212] The Bi–N bond lengths of $[(RNH)Bi(\mu\text{–}NR)]_2$ (R = 2,6-iPr$_2$C$_6$H$_3$; range from 2.158(4) to 2.174(5) Å),[228] or those reported for $[Bi(NMe_2)_3]$ (2.189(18) and 2.180(21) Å),[229] can be compared with that of **19**. Nonetheless, the Bi–N

bond lengths in **19** differ significantly when compared with Ar_2BiCl (Ar = 2-$(Me_2NCH_2)C_6H_4(C_9H_{12}N)$ (2.570(5) Å).[213]

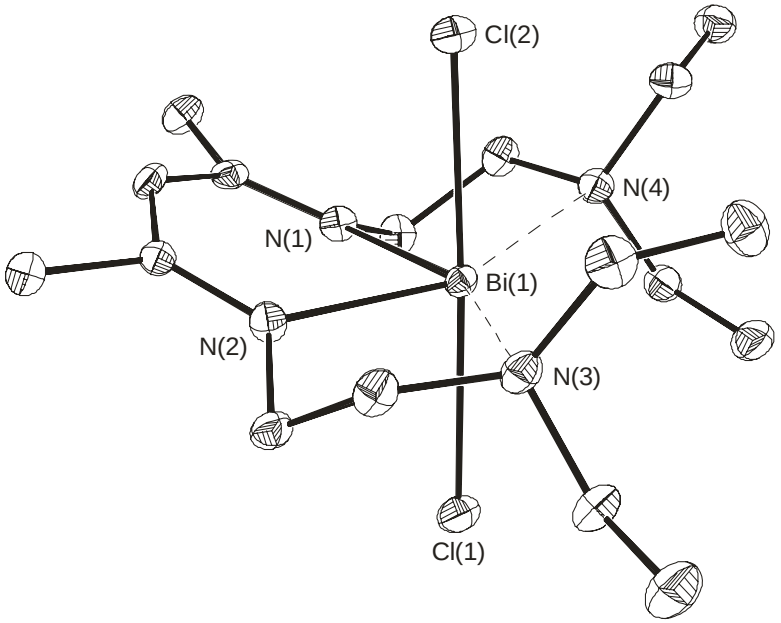

Figure 13. Thermal ellipsoids plot of **19** showing the atoms at the 50 % probability level. H atoms are omitted for clarity. Selected bond lengths [Å] and angles [°]: Bi(1)–Cl(1) 2.736(9), Bi(1)–Cl(2) 2.675(8), Bi(1)–N(1) 2.232(2), Bi(1)–N(2) 2.246(2), Bi(1)–N(3) 2.747(2); N(1)–Bi(1)–N(2) 82.9(9), N(1)–Bi(1)–Cl(2) 89.0(7), N(2)–Bi(1)–Cl(2) 88.6(7), N(1)–Bi(1)–Cl(1) 89.8(7), N(2)–Bi(1)–Cl(1) 89.5(7), Cl(2)–Bi(1)–Cl(1) 177.8(2), N(1)–Bi(1)–N(3) 153.9(8), N(2)–Bi(1)–N(3) 71.2(8), Cl(2)–Bi(1)–N(3) 87.8(6), Cl(1)–Bi(1)–N(3) 92.6(6).

In summary we prepared and structurally characterized compounds of composition [{$HC(CMeNAr)_2$}PbBr] (**17**) and [{$HC(Et_2NCH_2CH_2NCMe)_2$}$BiCl_2$] (**19**). To our knowledge compound **17** represents the first report of a lead(II) bearing a *β*-diketiminato ligand of the type ($HC(CMeNAr)_2$), furthermore the isolation of **19** is also intriguing because of the high coordination number at the bismuth atom.

3. Summary

A germanium(II) hydroxide [{HC(CMeNAr)$_2$}GeOH] (**3**) was trapped by using an Arduengo-type carbene as HCl acceptor prior to hydrolysis of the corresponding *β*-diketiminatogermanium(II) chloride. The crystal structure of compound **3** has been determined by X-ray diffraction analysis and showed a monomer, which exhibits a terminal hydroxyl group attached to the germanium atom, and displays weak intermolecular interactions to another molecule that leads to a weakly coordinated dimer.

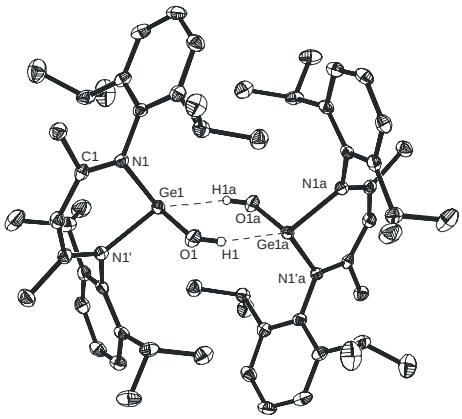

Molecular Structure of 3

The chemical feature of **3** was first tested by using the lone pair of electrons at germanium as reaction site with chalcogens (Ch = S, Se) and resulted in the oxidative adducts [{HC(CMeNAr)$_2$}Ge(S)OH] (**7**) and [{HC(CMeNAr)$_2$}Ge(Se)OH] (**8**). Single crystal X-ray structural determinations were carried out for compounds **7** and **8**. The molecular structures of **7** and **8** in the crystal show that there is preference for the thiono- and selenoxo-form, respectively, and formation of hydrogen bond arrays. Likewise, compounds **7** and **8** were subjected to DFT calculations to shed light on their acid strengths. The preparation of **7** and **8** shows how heavier congeners of Group 14 can mimic well know organic functional groups. Second, hydrogen abstraction of the OH functionality led to the synthesis of transition metal-main group heterobimetallic oxides of composition [{HC(CMeNAr)$_2$}GeZr(Me)Cp$_2$] (**9**) and [{HC(CMeNAr)$_2$}GeHf(Me)Cp$_2$] (**10**) by reaction of **3** in the presence of Cp$_2$MMe$_2$ (M = Zr,

Hf), respectevily. The crystal structures of compounds **9** and **10** were determined by X-ray single-crystal structure analysis. From the metrical parameters it was shown that both compounds exhibit boatlike conformations.

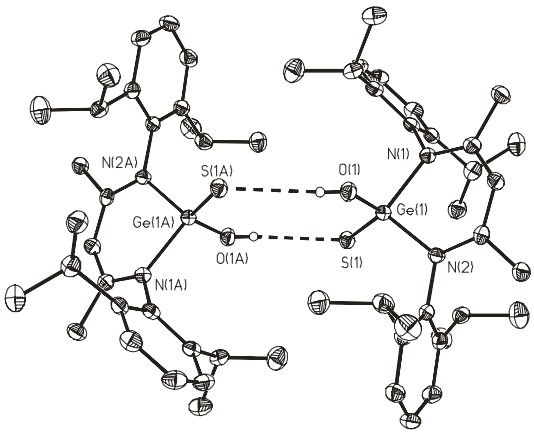

Molecular Structure of 7

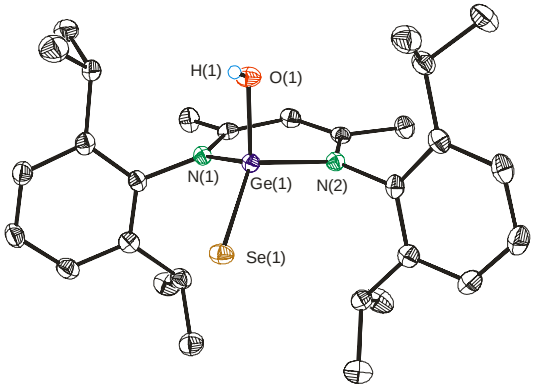

Molecular Structure of 8

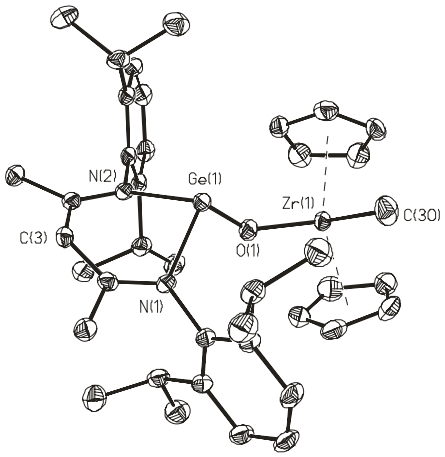

Molecular Structure of 9

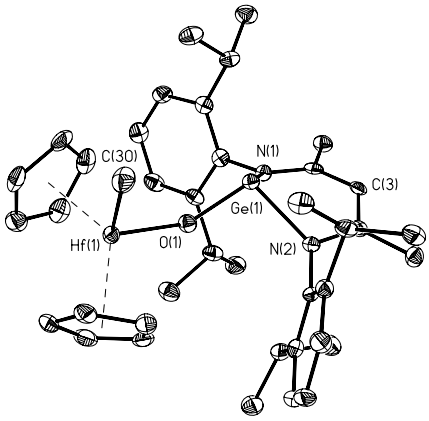

Molecular Structure of 10

A third type of reaction of **3** involves Lewis acid behavior (two electron donor) toward transition metal fragments to afford compounds [{HC(CMeNAr)$_2$}Ge(OH)Fe(CO)$_4$] (**11**) and [{HC(CMeNAr)$_2$}Ge(OH)Mn(Cp)(CO)$_2$] (**12**). The molecular composition of compounds **11** and **12** was investigated by X-ray crystallography.

The preparation of low-valent stable germanium(II) [{HC(CMeNAr)$_2$}GeH] (**14**) and tin(II) [{HC(CMeNAr)$_2$}SnH] (**15**) terminal hydrides was accomplished when the

corresponding *β*-diketiminatogermanium(II) and *β*-diketiminatotin(II) chlorides were reacted with $AlH_3 \cdot NMe_3$. The electronic properties of compounds **14** and **15** as well as their crystal structures were studied by DFT calculations and X-ray diffraction analysis.

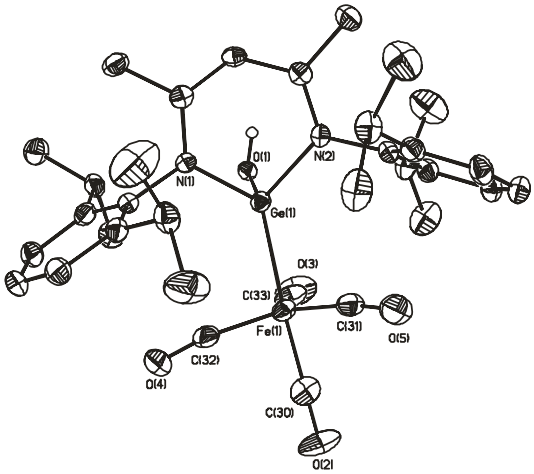

Molecular Structure of 11

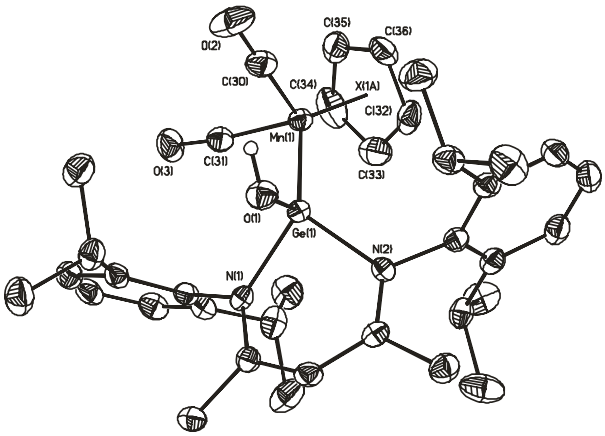

Molecular Structure of 12

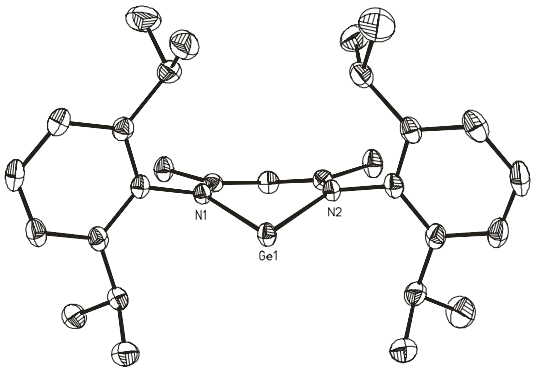

Molecular Structure of 14

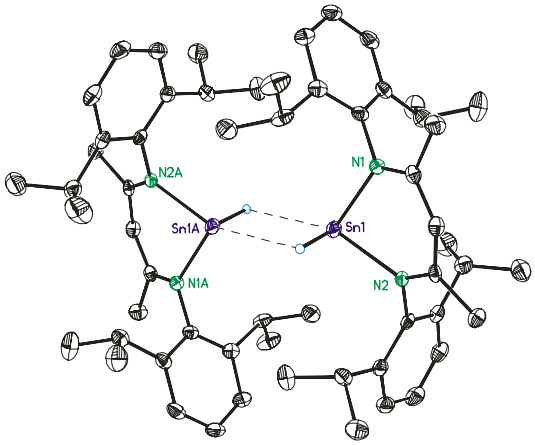

Molecular Structure of 15

Metathetical exchange reactions of the *β*-diketiminatolithium salt and the corresponding lead and bismuth halides led to the isolation of two novel compounds with low-valent lead [{$HC(CMeNAr)_2$}PbBr] (**17**) and bismuth [{$HC(Et_2NCH_2CH_2NCMe)_2$}$BiCl_2$] (**19**).

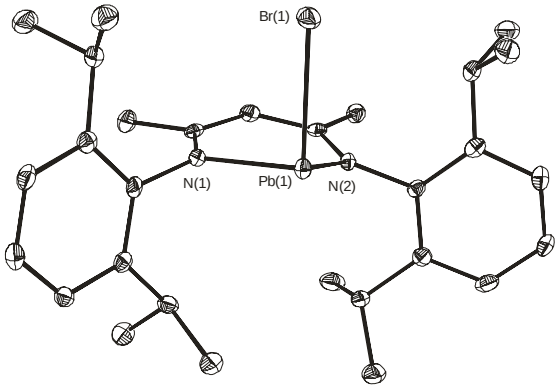

Molecular Structure of 17

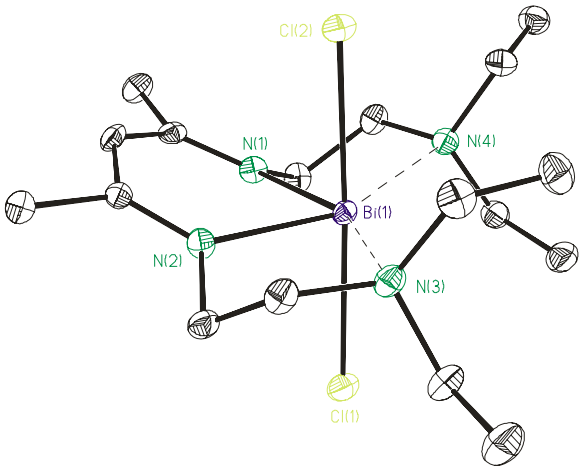

Molecular Structure of 19

4. Experimental Section

4.1. General Procedures

All reactions and handling of reagents were performed under an atmosphere of dry nitrogen or argon using Schlenk techniques[230] or a glovebox where the O_2 and H_2O levels were usually kept bellow 1 ppm. All glassware was oven-dried at 140 °C for at least 24 h, assembled hot and cooled under high vacuum prior to use. Toluene (Na/benzophenone ketyl and diphenylether), benzene (K/benzophenone ketyl and diphenylether), hexane (Na/K/benzophenone ketyl and diphenylether), pentane (Na/K/benzophenone ketyl and diphenylether), tetrahydrofuran (K/benzophenone ketyl), diethylether (Na/benzophenone ketyl), dichloromethane (CaH_2) were dried and distilled prior to use. Ethanol free trichloromethane stabilized with amylene was stirred for three min. with P_4O_{10} and after filtration stored over molecular sieves in a sealed vessel.

4.2. Physical Measurements

Melting points were measured in sealed glass tubes on a Büchi B-540 melting point apparatus.

NMR spectra were recorded on Bruker Avance 200, Bruker Avance 300, and Bruker Avance 500 NMR spectrometers. Chemical shifts are reported in ppm with reference to $SiMe_4$ (external) for ^1H and ^{13}C isotopes, $SeMe_2$ (external) for ^{77}Se nuclei, $SnMe_4$ (external) for ^{119}Sn nuclei. Downfield shifts from the reference are quoted positive; upfield shifts are assigned negative values. The NMR grade deuterated solvents were dried as follows: C_6D_6 – overnight stirring with Na/K alloy followed by vacuum distillation, $CDCl_3$ – 3 min. stirring with P_4O_{10} followed by filtration, THF – storing over freshly activated molecular sieves for one week. Heteroatom NMR spectra were recorded ^1H decoupled.

IR spectra were recorded on a Bio-Rad Digilab FTS7 spectrometer in the range 4000–350 cm^{-1} as KBr pellets. Only the absorption of significant moieties (O–H, CO, Ge–H, Sn–H) are listed except for compounds **17** and **19**, where all the absorptions (weak to very strong) are reported as the only method for their identification.

Mass spectra were obtained with a Finnigan MAT 8230 or a Varian MAT CH5 instrument (70 eV) by EI-MS methods.

Elemental analyses were performed by the Analytisches Labor des Instituts für Anorganische Chemie der Universität Göttingen.

Crystal structure determination: Intensity data for compounds **11** and **12** were collected on an IPDS II Stoe image-plate diffractometer using graphite monochromated Mo-Kα radiation (λ = 0.71073 Å). The diffraction data for the compounds **3**, **7**–**10**, **14**, **15**, **17**, and **19** were measured on a Bruker three-circle diffractometer equipped with a SMART 6000 CCD detector using mirror monochromated Cu-Kα radiation (λ = 1.54178 Å). The data for all compounds were collected at low temperature (for exact values see Tables in Section 6). The structures were solved by direct methods (SHELXS-97)[231] and refined with all data by full-matrix least-squares methods on F^2 using SHELXL-97.[232] The non-hydrogen atoms were refined anisotropically; the hydrogen atoms of C–H bonds except the ones on γ-CH of the ligand were placed in idealized positions, and refined with a riding model, whereas the hydrogen atoms of the O–H, Sn–H and γ-C–H moieties, except the hydrogen atom in the Ge–H moiety, were localized from the difference electron-density maps and refined isotropically. The hydrogen atoms of C–H bonds in **14**, except H(3A) and H(3AA) were included in geometrically idealized positions and refined with the riding model. Localization of H(3A) and H(3AA) hydrogen atoms from the electron-density map proved to be more accurate than fixing the atoms in the idealized positions and led to lower $R1$ and $wR2$ values. The crystal

data for all compounds along with the final residuals and other pertaining details are tabulated in Section 6.

4.3. Starting Materials

Cp_2MCl_2 (M = Zr, Hf) (Aldrich), sulfur (Aldrich), $Fe_2(CO)_9$ (Aldrich), $CpMn(CO)_3$ (Strem Chemicals) were used as received. [{HC(CMeNAr)$_2$}GeCl],[53] [{HC(CMeNAr)$_2$}SnCl],[58] Cp_2MMe_2 (M = Zr, Hf),[128] N,N'-*bis*-mesitylimidazolyl carbene,[54] elemental red selenium,[233] $AlH_3{\cdot}NMe_3$,[183] [{HC(CMeNAr)$_2$}Li(Et$_2$O)],[217] [{HC(Et$_2$NCH$_2$CH$_2$NCMe)$_2$}Li][218] were prepared by literature procedures.

4.4. Syntheses of Compounds **3**, **7–12**, **14**, **15**, **17** and **19**

4.4.1. *Synthesis of [{HC(CMeNAr)$_2$}GeOH] (**3**)*

Compound **1** (1.28 g, 2.43 mmol) and **2** (0.74 g, 2.43 mmol) were dissolved in toluene (20 mL) at ambient temperature, then water (87.5 μL, 2.0 mmol) was slowly added, and the mixture was stirred. A white precipitate was immediately formed. The reaction mixture was stirred for about 15 min, and then the white precipitate was separated by filtration in vacuo. The remaining colorless solution was evaporated, and the resulting yellow solid of **3** was rinsed with hexane (2 x 10 mL) and dried in vacuo. Yield: 1.04 g (84%); m.p. 140 °C; IR (KBr pellet): $\tilde{\nu}$ = 3571 s (OH) cm^{-1}; ^{1}H NMR (200 MHz, C_6D_6, 25 °C, TMS): δ 7.09–7.15 (m, 6H; *m*-, *p*- Ar–*H*), 4.91 (s, 1H; γ-C*H*), 3.60–3.80 (sept, 2H, $^3J_{H–H}$ = 6.8 Hz; C*H*(CH$_3$)$_2$), 3.20–3.40 (sept, 2H, $^3J_{H–H}$ = 6.8 Hz; C*H*(CH$_3$)$_2$), 1.60 (s, 6H; C*H*$_3$), 1.54 (s, 1H; O*H*), 1.33 (d, 6H, $^3J_{H–H}$ = 6.8 Hz; CH(C*H*$_3$)$_2$), 1.29 (d, 6H, $^3J_{H–H}$ = 6.8 Hz; CH(C*H*$_3$)$_2$), 1.21 (d, 6H, $^3J_{H–H}$ = 6.8 Hz; CH(C*H*$_3$)$_2$), 1.12 ppm (d, 6H, $^3J_{H–H}$ = 6.8 Hz; CH(C*H*$_3$)$_2$); ^{13}C NMR (50.327 MHz, D$_8$-THF, 25 °C, TMS): δ 163.3 (*C*N), 146.4 (*C*N), 143.6, 141.0, 124.8, 124.1 (*i*-, *o*-, *m*-, *p*-*Ar*), 97.0 γ-*C*H), 29.2 (*C*H$_3$) 28.0 (*C*H(CH$_3$)$_2$), 26.7 (*C*H(CH$_3$)$_2$), 24.7 (CH(*C*H$_3$)$_2$), 24.6 ppm

($CH(CH_3)_2$), 24.1 ($CH(CH_3)_2$), 23.3 ($CH(CH_3)$); EI-MS (70 eV): *m/z* (%): 508 (25) $[M]^+$, 403 (100) $[M - Me–Ge–OH]^+$. Elemental analysis (%) calcd for $C_{29}H_{42}GeN_2O$ (507.24): C, 68.67; H, 8.35; N, 5.52. Found: C, 69.20; H, 8.48; N, 5.52.

4.4.2. *Synthesis of [{HC(CMeNAr)$_2$}Ge(S)OH] (**7**)*

A solution of **3** (1.56 g, 3.07 mmol) in toluene (30 mL) was slowly added to a suspension of elemental sulfur (0.09 g, 3.07 mmol) in toluene (15 mL) by cannula at ambient temperature. After 3 days under constant stirring at ambient temperature the yellow solution turned slightly green. After removal of all volatiles the remaining crude product was rinsed with pentane (3 x 10 mL) and dried under reduced pressure to yield pure **7**. Yield: 1.10 g (66 %); m.p. 300 °C dec; IR (KBr): $\tilde{\nu}$ = 3238 br (OH) cm^{-1}; ^1H NMR (500.13 MHz, C_6D_6, 25 °C, TMS): δ 7.09–7.16 (m, 6H; *m*-, *p*- Ar–*H*), 4.83 (s, 1H; γ-C*H*), 3.62 (sept, 2H, $^3J_{H–H}$ = 6.8 Hz; C*H*(CH_3)$_2$), 3.35 (sept, 2H, $^3J_{H–H}$ = 6.8 Hz; C*H*(CH_3)$_2$), 2.30 (s, 1H; O*H*), 1.57 (d, 6H, $^3J_{H–H}$ = 6.8 Hz; CH(C*H*$_3$)$_2$), 1.47 (s, 6H; C*H*$_3$), 1.26 (d, 6H, $^3J_{H–H}$ = 6.8 Hz; CH(C*H*$_3$)$_2$), 1.16 (d, 6H, $^3J_{H–H}$ = 6.8 Hz; CH(C*H*$_3$)$_2$), 1.05 ppm (d, 6H, $^3J_{H–H}$ = 6.8 Hz; CH(C*H*$_3$)$_2$); ^{13}C NMR (125.8 MHz, C_6D_6, 25 °C, TMS): δ 169.9 (*C*N), 145.9, 144.9, 137.2, 128.9, 124.8, 124,6 (*i*-, *o*-, *m*-, *p*-, *Ar*), 98.5 (γ-*C*H), 29.5 (*C*H_3), 27.9 (*C*H(CH_3)$_2$), 26.3 (*C*H(CH_3)$_2$), 24.7 ($CH(CH_3)_2$), 24.6 ($CH(CH_3)_2$), 23.8 ($CH(CH_3)_2$), 23.7 ppm ($CH(CH_3)_2$); EI-MS (70 eV): *m*/*z* (%): 540 (40) $[M]^+$, 525 (100) $[M - CH_3]^+$. Elemental analysis (%) calcd for $C_{29}H_{42}GeN_2OS$ (539.32): C, 64.70; H, 7.85; N, 5.20. Found: C, 64.20; H, 7.60; N, 5.12.

4.4.3. *Synthesis of [{HC(CMeNAr)$_2$}Ge(Se)OH] (**8**)*

To a suspension of elemental red selenium (0.29 g, 3. 67 mmol) in toluene (20 mL) was added via cannula a solution of **3** (1.86 g, 3.67 mmol) in toluene (30 mL). A pale green solution appeared after 30 min, that finally remained unchanged after 18 h of stirring. Subsequent

filtration and solvent removal gave a pale green solid, which was washed twice with cold pentane (2 x 10 mL). Yield: 1.66 g (77%); m.p. 220 °C dec; IR (KBr pellet): $\tilde{\nu}$ = 3292 br (OH) cm^{-1}; ^1H NMR (500.13 MHz, C_6D_6, 25 °C, TMS) δ 7.09–7.16 (m, 6H; *m*-, *p*- Ar–*H*), 4.85 (s, 1H; γ-C*H*), 3.65 (sept, 2H, $^3J_{H–H}$ = 6.8 Hz; C*H*$(CH_3)_2$), 3.29 (sept, 2H, $^3J_{H–H}$ = 6.8 Hz; C*H*$(CH_3)_2$), 2.19 (s, 1H; O*H*), 1.56 (d, 6H, $^3J_{H–H}$ = 6.8 Hz; CH(C*H*$_3)_2$), 1.48 (s, 6H; C*H*$_3$), 1.30 (d, 6H, $^3J_{H–H}$ = 6.8 Hz; CH(C*H*$_3)_2$), 1.17 (d, 6H, $^3J_{H–H}$ = 6.8 Hz; CH(C*H*$_3)_2$), 1.04 ppm (d, 6H, $^3J_{H–H}$ = 6.8 Hz; CH(C*H*$_3)_2$); ^{13}C NMR (125.75 MHz, C_6D_6, 25 °C, TMS) δ 169.6 (*C*N), 146.0, 144.7, 137.4, 129.0, 124.9, 124.7 (*i*-, *o*-, *m*-, *p*- *Ar*), 99.0 (γ-*C*H), 29.7 (*C*H_3), 28.0 (*C*H$(CH_3)_2$), 26.4 (*C*H$(CH_3)_2$), 24.7 (CH(*C*$H_3)_2$), 24.6 (CH(*C*$H_3)_2$), 24.0 (CH(*C*$H_3)_2$), 23.8 ppm (CH(*C*$H_3)_2$); ^{77}Se NMR (95.38 MHz, C_6D_6, 25 °C, Me_2Se) δ – 439.8 ppm; EI-MS (70 eV): *m*/*z* (%): 586 (35) $[M]^+$, 571 (15) $[M – Me]^+$, 553 (15) $[M – MeOH]^+$, 507 (15) $[M – Se]^+$. Elemental analysis (%) calcd for $C_{29}H_{42}GeN_2OSe$ (586.22): C, 59.42; H, 7.22; N, 4.78. Found: C, 59.20; H, 7.24; N, 4.70.

4.4.4. *Synthesis of [{HC(CMeNAr)$_2$}Ge(μ–O)Zr(Me)Cp$_2$] (**9**)*

A solution of freshly sublimed Cp_2ZrMe_2 (0.44 g, 1.77 mmol) in ether (10 mL) was added by cannula to a solution of **3** (0.90 g, 1.77 mmol) in diethyl ether (25 mL) at –4°C. The reaction mixture was kept stirring at this temperature for 15 min and then was allowed to warm to ambient temperature under formation of a precipitate. Once the gas evolution ceased, the yellow-orange precipitate was filtered off and dried in vacuo. Yield: 0.65 g (50%); m.p. 292 °C dec; ^1H NMR (500.13 MHz, C_6D_6, 25 °C, TMS) δ 7.13–7.24 (m, 6H; *m*-, *p*- Ar–*H*), 5.39 (s, 10H; C_5H_5), 4.65 (s, 1H; γ-C*H*), 3.54 (sept, 2H, $^3J_{H–H}$ = 6.8 Hz; C*H*$(CH_3)_2$), 3.35 (sept, 2H, $^3J_{H–H}$ = 6.8 Hz; C*H*$(CH_3)_2$), 1.53 (d, 6H, $^3J_{H–H}$ = 6.8 Hz; CH(C*H*$_3)_2$), 1.48 (d, 6H, $^3J_{H–H}$ = 6.8 Hz; CH(C*H*$_3)_2$), 1.44 (s, 6H; C*H*$_3$), 1.16 (d, 6H, $^3J_{H–H}$ = 6.8 Hz; CH(C*H*$_3)_2$), 1.13 ppm (d, 6H, $^3J_{H–H}$ = 6.8 Hz; CH(C*H*$_3)_2$), 0.14 (s, 3H; C*H*$_3$); ^{13}C NMR (125.75 MHz, C_6D_6, 25

^{o}C, TMS) δ 163.5 (*C*N), 144.5, 144.3, 141.0, 126.8, 124.5, 124.2 (*i*-, *o*-, *m*-, *p*- *Ar*), 110.2 (C_5H_5), 95.5 (γ-*C*H), 28.5 (CH_3), 28.5 ($CH(CH_3)_2$), 26.4 ($CH(CH_3)_2$), 24.6 ($CH(CH_3)_2$), 24.3 ($CH(CH_3)_2$), 24.1 ($CH(CH_3)_2$), 22.6 ($CH(CH_3)_2$), 20.8 ppm (CH_3); EI-MS (70 eV): *m*/*z* (%): 742 (15) $[M]^+$, 491 (100) [*M* – OZr(Me)Cp_2]$^+$. Elemental analysis (%) calcd for $C_{40}H_{54}GeN_2OZr$ (742.69): C, 64.69; H, 7.33; N, 3.77. Found: C, 64.51; H, 7.30; N, 3.90.

4.4.5. *Synthesis of [{HC(CMeNAr)$_2$}Ge(μ–O)Hf(Me)Cp$_2$] (**10**)*

Freshly sublimed Cp_2HfMe_2 (0.59 g, 1.77 mmol) dissolved in ether (15 mL) was transferred using a cannula to a flask charged with **3** (0.90 g, 1.77 mmol) in diethyl ether (25 mL) at –4^{o}C. After 25 min the cooling bath was removed and stirring was continued until the methane evolution ceased. Finally, after removal of the solvent the remaining crude product was recrystallized from a toluene/hexane mixture resulting in a yellow-orange microcrystalline solid at –32 ^{o}C that was filtered off and dried in vacuo. Yield: 0.75 g (51%); m.p. 317 ^{o}C dec; ^{1}H NMR (500.13 MHz, C_6D_6, 25 ^{o}C, TMS): δ 7.14-7.23 (m, 6H; *m*-, *p*- Ar-*H*), 5.33 (s, 10H; C_5H_5), 4.65 (s, 1H; γ-C*H*), 3.56 (sept, 2H, $^{3}J_{H–H}$ = 6.8 Hz; C*H*(CH_3)$_2$), 3.35 (sept, 2H, $^{3}J_{H–H}$ = 6.8 Hz; C*H*(CH_3)$_2$), 1.54 (d, 6H, $^{3}J_{H–H}$ = 6.8 Hz; CH(C*H*$_3$)$_2$), 1.48 (d, 6H, $^{3}J_{H–H}$ = 6.8 Hz; CH(C*H*$_3$)$_2$), 1.44 (s, 6H; C*H*$_3$), 1.17 (d, 6H, $^{3}J_{H–H}$ = 6.8 Hz; CH(C*H*$_3$)$_2$), 1.13 (d, 6H, $^{3}J_{H–H}$ = 6.8 Hz; CH(C*H*$_3$)$_2$), 0.02 ppm (s, 3H; C*H*$_3$). ^{13}C NMR (125.75 MHz, C_6D_6, 25 ^{o}C, TMS): δ 164.0 (*C*N), 145.0, 144.5, 141.5, 127.1, 125.0, 124.4 (*i*-, *o*-, *m*-, *p*- *Ar*), 110.0 (C_5H_5), 95.8 (γ-*C*H), 29. (CH_3), 28.8 ($CH(CH_3)_2$), 26.7 ($CH(CH_3)_2$), 25.0 ($CH(CH_3)_2$), 24.6 ($CH(CH_3)_2$), 24.4 ($CH(CH_3)_2$), 24.0 ($CH(CH_3)_2$), 23.0 ppm (CH_3). EI-MS (70 eV): *m*/*z* (%): 830 (15) $[M]^+$, 491 (100) [*M* – OHf(Me)Cp_2]$^+$. Elemental analysis (%) calcd for $C_{40}H_{54}GeHfN_2O$ (829.95): C, 57.89; H, 6.56; N, 3.38. Found: C, 57.71; H, 6.80; N, 3.24.

4.4.6. *Synthesis of [{HC(CMeNAr)$_2$}Ge(OH)Fe(CO)$_4$] (**11**)*

A flask was charged with **3** (1.99 g, 3.93 mmol) and $Fe_2(CO)_9$ (1.42 g, 3.93 mmol) in THF (40 mL). The solution was stirred overnight at ambient temperature. The byproduct was removed by filtration over Celite resulting in a clear pale brown filtrate. From the resulting solution the volatiles were removed giving a pale brown solid. Recrystallization of the crude product was attained by gently heating a solution of toluene and **3** (20 mL) and keeping it at ambient temperature. **11** separates as pale brown crystals. Yield: 2.17 g (72%); m.p. 231 ^{o}C dec; IR (KBr pellet): $\tilde{\nu}$ = 3599 s (OH), 2039 s, 1956 s, 1942 s (CO) cm^{-1}; ^{1}H NMR (500.13 MHz, D$_8$-THF, 25 ^{o}C, TMS) δ 7.19–7.29 (m, 6H; *m*-, *p*- Ar–*H*), 5.69 (s, 1H; γ-C*H*), 4.24 (s, 1H; O*H*), 3.67 (sept, 2H, $^{3}J_{H-H}$ = 6.8 Hz; C*H*(CH$_3$)$_2$), 3.07 (sept, 2H, $^{3}J_{H-H}$ = 6.8 Hz; C*H*(CH$_3$)$_2$), 1.93 (s, 6H; C*H*$_3$), 1.34 (d, 6H, $^{3}J_{H-H}$ = 6.8 Hz; CH(C*H*$_3$)$_2$), 1.31 (d, 6H, $^{3}J_{H-H}$ = 6.8 Hz; CH(C*H*$_3$)$_2$), 1.24 (d, 6H, $^{3}J_{H-H}$ = 6.8 Hz; CH(C*H*$_3$)$_2$), 1.16 ppm (d, 6H, $^{3}J_{H-H}$ = 6.8 Hz; CH(C*H*$_3$)$_2$); ^{13}C NMR (125.75 MHz, D$_8$-THF, 25 ^{o}C, TMS) δ 214.8 (*C*O), 169.0 (*C*N), 147.1, 145.0, 140.0, 129.5, 125.8, 125.4 (*i*-, *o*-, *m*-, *p*- *Ar*), 101.6 (γ-*C*H), 30.0 (*C*H$_3$), 28.8 (*C*H(CH$_3$)$_2$), 25.6 (*C*H(CH$_3$)$_2$), 25.0 (CH(*C*H$_3$)$_2$), 24.8 (CH(*C*H$_3$)$_2$), 24.8 (CH(*C*H$_3$)$_2$), 24.4 ppm (CH(*C*H$_3$)$_2$); EI-MS (70 eV): *m*/*z* (%): 676 (5) [*M*]$^{+}$, 592 (20) [*M* – 3CO]$^{+}$, 564 (70) [*M* – 4CO]$^{+}$, 491 (100) [*M* – 4CO – Fe – OH]$^{+}$. Elemental analysis (%) calcd for $C_{33}H_{42}FeGeN_2O_5$ (675.13): C, 58.71; H, 6.27; N, 4.15. Found: C, 59.0; H, 6.20; N, 4.12.

4.4.7. *Synthesis of [{HC(CMeNAr)$_2$}Ge(OH)MnCp(CO)$_2$] (**12**)*

Compound **3** (0.50 g, 0.98 mmol) and CpMn(CO)$_3$ (0.20 g, 0.98 mmol) were dissolved in THF (30 mL) and irradiated for 3 h by UV light, during which the initial yellow solution became orange. Stirring was continued for 2 h and the solvent was removed in vacuo and the resulting orange-yellow residue was rinsed with pentane (2 x 20 mL). Recrystallization of **12** was accomplished by gently heating a toluene solution. From the solution at ambient

temperature resulted orange-yellow crystals overnight. Yield: 0.51 g (76%); m.p. 265 °C dec; IR (KBr pellet): $\tilde{\nu}$ = 3642 s (OH), 1921 s, 1864 w, 1846 s (CO) cm^{-1}; EI-MS (70 eV): *m*/*z* (%): 684 (5) [M^+], 610 (10) [M – 2CO – OH]$^+$, 491 (100) [M – 2CO – Cp – Mn – OH]$^+$. Elemental analysis (%) calcd for $C_{36}H_{47}GeMnN_2O_3$ (684.22): C, 63.14; H, 6.92; N, 4.10. Found: C, 63.30; H, 7.00; N, 4.20.

4.4.8. *Synthesis of [{HC(CMeNAr)$_2$}GeH] (**14**)*

To a solution of **1** (0.62 g, 1.18 mmol) in toluene (25 mL) at –4 °C a solution of AlH_3·NMe_3 (1.18 mL, 1.0 M solution in toluene) was slowly added and immediately the yellow solution turned to orange-red. The cooling bath was removed after 20 min and stirring was continued until the elimination of NMe_3 had ceased. All volatiles were removed in vacuum and the remaining orange-red residue was extracted with *n*-hexane (15 mL), the solvent was removed in vacuum to yield **14** as an orange-red powder. Yield: 0.32 g (60 %); m.p. 170 °C dec; IR (KBr pellet): $\tilde{\nu}$ = 1733 s (Ge–H) cm^{-1}; ^{1}H NMR (300 MHz, C_6D_6, 25 °C, TMS): δ 8.08 (s, 1H; Ge–*H*), 7.07–7.15 (m, 6H; *m*-, *p*- Ar–*H*), 4.92 (s, 1H; γ-C*H*), 3.58 (sept, 2H, $^3J_{H–H}$ = 6.8 Hz; C*H*(CH$_3$)$_2$), 3.41 (sept, 2H, $^3J_{H–H}$ = 6.8 Hz; C*H*(CH$_3$)$_2$), 1.55 (s, 6H; C*H*$_3$), 1.37 (d, 6H, $^3J_{H–H}$ = 6.8 Hz; CH(C*H*$_3$)$_2$), 1.29 (d, 6H, $^3J_{H–H}$ = 6.8 Hz; CH(C*H*$_3$)$_2$), 1.19 (d, 6H, $^3J_{H–H}$ = 6.8 Hz; CH(C*H*$_3$)$_2$), 1.17 ppm (d, 6H, $^3J_{H–H}$ = 6.8 Hz; CH(C*H*$_3$)$_2$); ^{13}C NMR (125.8 MHz, C_6D_6, 25 °C, TMS): δ 167.5 (*C*N), 146.5, 143.5, 141.6, 127.3, 124.6, 124.3 (*i*-, *o*-, *m*-, *p*-, *Ar*), 97.8 (γ-*C*H), 29.0 (*C*H$_3$), 28.2 (*C*H(CH$_3$)$_2$), 27.0 (*C*H(CH$_3$)$_2$), 24.8 (CH(*C*H$_3$)$_2$), 24.4 (CH(*C*H$_3$)$_2$), 23.7 (CH(*C*H$_3$)$_2$), 22.8 ppm (CH(*C*H$_3$)$_2$); EI-MS (70 eV): *m*/*z* (%): 491 (100) [M – H]$^+$, 449 (40) [M – *i*Pr]$^+$. Elemental analysis (%) calcd for $C_{29}H_{42}GeN_2$ (491.26): C, 70.69; H, 8.60; N, 5.70. Found: C, 70.20; H, 8.53; N, 5.40.

4.4.9. *Synthesis of [{HC(CMeNAr)$_2$}SnH] (**15**)*

Compound **13** (1.85 g, 3.24 mmol) was dissolved in toluene (30 mL) and cooled at –4 ^{o}C and was slowly added to a solution of AlH_3·NMe_3 (3.24 mL, 1.0 M solution in toluene). The cooling bath was removed after 15 min and the solution further stirred until NMe_3 elimination ceased. During the course of the reaction a color change of the solution was observed from pale yellow to green. The solvent was removed in vacuum and the green residue was extracted with *n*-hexane followed by removal of the solvent to afford **15** as a green powder. Yield: 1.58 g (91 %); m.p. 125 °C dec; IR (KBr pellet): $\tilde{\nu}$ = 1849 m (Sn–H) cm^{-1}; ^{1}H NMR (500 MHz, C_6D_6, 25 °C, TMS): δ 13.83 (s, 1H, $^1J^{119}_{Sn,\,^1H}$ = 64 Hz; Sn–*H*), δ 7.06–7.15 (m, 6H; *m*-, *p*- Ar–*H*), 4.89 (s, 1H; γ-C*H*), 3.52 (sept, 2H, $^3J_{H–H}$ = 6.8 Hz; C*H*(CH$_3$)$_2$), 3.46 (sept, 2H, $^3J_{H–H}$ = 6.8 Hz; C*H*(CH$_3$)$_2$), 1.62 (s, 6H; C*H*$_3$), 1.34 (d, 6H, $^3J_{H–H}$ = 6.8 Hz; CH(C*H*$_3$)$_2$), 1.27 (d, 6H, $^3J_{H–H}$ = 6.8 Hz; CH(C*H*$_3$)$_2$), 1.19 (d, 6H, $^3J_{H–H}$ = 6.8 Hz; CH(C*H*$_3$)$_2$), 1.17 ppm (d, 6H, $^3J_{H–H}$ = 6.8 Hz; CH(C*H*$_3$)$_2$); ^{13}C NMR (125.8 MHz, C_6D_6, 25 °C, TMS): δ 167.7 (*C*N), 145.5, 143, 142.8, 126.8, 124.7, 124.3 (*i*-, *o*-, *m*-, *p*-, *Ar*), 98.3 (γ-*C*H), 29 (*C*H$_3$), 27.8 (*C*H(CH$_3$)$_2$), 26.8 (*C*H(CH$_3$)$_2$), 24.8 (CH(*C*H$_3$)$_2$), 24.4 (CH(*C*H$_3$)$_2$), 24.0 (CH(*C*H$_3$)$_2$), 23.4 ppm (CH(*C*H$_3$)$_2$); ^{119}Sn NMR (186.5 MHz, C_6D_6, 25 °C, $SnMe_4$): δ –224.7 ppm; EI-MS (70 eV): *m*/*z* (%): 537 (5) [*M* – H]$^+$. Elemental analysis (%) calcd for $C_{29}H_{42}N_2Sn$ (537.36): C, 64.82; H, 7.88; N, 5.21. Found: C, 64.20; H, 7.45; N, 5.33.

4.4.10. *Synthesis of [{HC(CMeNAr)$_2$}PbBr] (**17**)*

To a suspension of $PbBr_2$ (3.0 g, 8.17 mmol) in ether (25 mL) was added by cannula a solution of **16** (4.08 g, 8.17 mmol) in ether (35 mL) at –78 °C. The cooling bath was removed after 2 h and the green solution further stirred overnight. Removal of all volatiles and subsequent extraction with toluene (30 mL) resulted in a pale green filtrate which was kept at –32 °C for 2 days to give **17** as pale green crystals. Yield: 3.53 g (61.4 %); m.p. 200 °C dec;

IR (KBr pellet): $\tilde{\nu}$ = 2960 s, 2925 m, 2867 m, 1625 m, 1553 s, 1515 m, 1462 m, 1433 m, 1384 m, 1363 m, 1316 m, 1263 m, 1169 m, 1098 m, 1019 m, 935 m, 840 w, 800 s, 790 s, 758 m cm^{-1}; ^{1}H NMR (500 MHz, C_6D_6, 25 °C, TMS): δ 7.04–7.19 (m, 6H; *m*-, *p*- Ar–*H*), 4.89 (s, 1H; γ-C*H*), 3.97 (sept, 2H, $^3J_{H–H}$ = 6.8 Hz; C*H*(CH_3)$_2$), 3.04 (sept, 2H, $^3J_{H–H}$ = 6.8 Hz; C*H*(CH_3)$_2$), 1.65 (s, 6H; C*H*$_3$), 1.48 (d, 6H, $^3J_{H–H}$ = 6.8 Hz; CH(C*H*$_3$)$_2$), 1.24 (d, 6H, $^3J_{H–H}$ = 6.8 Hz; CH(C*H*$_3$)$_2$), 1.16 (d, 6H, $^3J_{H–H}$ = 6.8 Hz; CH(C*H*$_3$)$_2$), 1.06 ppm (d, 6H, $^3J_{H–H}$ = 6.8 Hz; CH(C*H*$_3$)$_2$); ^{13}C NMR (125.8 MHz, C_6D_6, 25 °C, TMS): δ 164.4 (*C*N), 145.8, 142.6, 128.5, 126.9, 125.5, 123.6 (*i*-, *o*-, *m*-, *p*-, *Ar*), 105.0 (γ-*C*H), 28.7 (*C*H$_3$), 28.4 (*C*H(CH_3)$_2$), 27.7 (*C*H(CH_3)$_2$), 25.1 (CH(*C*H$_3$)$_2$), 24.7 (CH(*C*H$_3$)$_2$), 24.0 (CH(*C*H$_3$)$_2$), 24.2 ppm (CH(*C*H$_3$)$_2$); EI-MS (70 eV): *m*/*z* (%): 704 (35) $[M]^+$, 625 (95) $[M – Br]^+$, 417 (100) $[M – PbBr]^+$. Elemental analysis (%) calcd for $C_{29}H_{41}BrPbN_2$ (704.22): C, 49.42; H, 5.82; N, 3.97. Found: C, 49.20; H, 5.53; N, 3.73.

4.4.11. *Synthesis of [{HC(Et$_2$NCH$_2$CH$_2$NCMe)$_2$}BiCl$_2$] (**19**)*

To a suspension of $BiCl_3$ (1.04 g, 3.3 mmol) in toluene (15 mL) was slowly added by cannula a solution of **18** (1.04 g, 3.3 mmol) in toluene (25 mL) at –78 °C. The stirring was continued for 3 h at this temperature. After 12 h of stirring at ambient temperature the yellow solution was filtered to remove the LiCl precipitate. Solvent removal of the filtrate resulted in an oily yellow residue that was dissolved in warm toluene (10 mL) and pentane (10 mL). Overnight storage of this solution at –32 °C resulted in yellow crystals of **19**. Yield: 1.20 g (63.5 %); m.p. 215 °C; ^{1}H NMR (300 MHz, C_6D_6, 25 °C, TMS): δ 4.47 (s, 1H; γ-C*H*), 3.91 (t, 4H, $^3J_{H–H}$ = 6.8 Hz; CH_2C*H*$_2$N), 2.98–3.05 (q, 8H, $^3J_{H–H}$ = 6.8 Hz; CH_3C*H*$_2$N), 2.61 (t, 4H, $^3J_{H–H}$ = 6.8 Hz; C*H*$_2$$CH_2$N), 1.52 (s, 6H; C*H*$_3$), 0.85 ppm (t, 12H, $^3J_{H–H}$ = 6.8 Hz; C*H*$_3$$CH_2$N); ^{13}C NMR (75.46 MHz, C_6D_6, 25 °C, TMS): δ 163.7 (*C*N), 107.2 (γ-*C*H), 55 (CH_2*C*H$_2$N), 49.7 (*C*H$_2$$CH_2$N), 44 ($CH_3$*C*H$_2$N), 23.5 (*C*H$_3$$CH_2$N), 9 (*C*H$_3$); EI-MS (70 eV): *m*/*z* (%): 574 (5)

$[M]^+$, 539 (15) $[M - Cl]^+$, 86 (100) $[C_5H_{12}N]^+$. Elemental analysis (%) calcd for $C_{17}H_{35}BiCl_2N_4$ (575.38): C, 49.42; H, 5.82; N, 3.97. Found: C, 49.20; H, 5.53; N, 3.73.

5. Handling and Disposal of Solvents and Residual Waste

1. The recovered solvents were distilled or condensed into a cold-trap under vacuum and collected in halogen-free or halogen-containing solvent containers, and stored for disposal.
2. Used NMR solvents were classified into halogen-free and halogen-containing solvents and were disposed as selenium and tellurium containing wastes and halogen-containing wastes, respectively.
3. The selenium and tellurium residues were dissolved in nitric acid and after neutralization stored in containers for heavy element wastes.
4. Drying agents such as KOH, $CaCl_2$ and P_4O_{10} were hydrolyzed and disposed as acid or base wastes.
5. Whenever possible, sodium metal used for drying solvents was collected for recycling.[234] The non-reusable sodium metal was carefully hydrolyzed in cold ethanol and poured into the base-bath used for cleaning glassware.
6. Ethanol and acetone used for cold-baths (with solid CO_2 or liquid N_2) were subsequently used for cleaning glassware.
7. The acid-bath used for cleaning glassware was neutralized with Na_2CO_3 and the resulting NaCl solution was washed-off in the water drainage.
8. The residue of the base-bath used for glassware cleaning was poured into container for base wastes.

Amounts of various types of disposable wastes generated during the work:

Heavy elements containing wastes	2 L
Halogen-containing solvent wastes	7 L
Halogen-free solvent wastes	40 L
Acid wastes	10 L
Base wastes	20 L

6. Crystal Data and Refinement Details

Table CD1. Crystal Data and Structure Refinement Details for [{HC(CMeNAr)$_2$}GeOH] (3).

Empirical formula	$C_{29}H_{42}GeN_2O$
Formula weight	507.24
Temperature	100(2) K
Wavelength	1.54178 Å
Crystal system	Monoclinic
Space group	$C1_2/c$
Unit cell dimensions	a = 24.765(3) Å
	b = 15.155(2) Å β = 94.56(2)°
	c = 14.700(2) Å
Volume	5499.6(1) Å^3
Z	8
Density (calculated)	1.225 Mg/m^3
Absorption coefficient	1.669 mm^{-1}
F(000)	2160
Crystal size	0.20 x 0.10 x 0.10 mm^3
θ range for data collection	3.42 to 59.60°.
Index ranges	$-27 \le h \le 27$, $0 \le k \le 16$, $0 \le l \le 16$
Reflections collected	3752
Independent reflections	3635 (R_{int} = 0.0162)
Completeness to θ = 59.60°	98.8%
Refinement method	Full-matrix least-squares on F^2
Data / restraints / parameters	3635 / 0 / 313
Goodness-of-fit on F^2	1.071
Final R indices ($I > 2\sigma(I)$)	R1 = 0.0254, wR2 = 0.0247
R indices (all data)	R1 = 0.0650, wR2 = 0.0644
Largest difference peak and hole	0.318 and –0.338 e·Å^{-3}

Table CD2. Crystal Data and Structure Refinement Details for [{HC(CMeNAr)$_2$}Ge(S)OH]·toluene (7).

Empirical formula	$C_{36}H_{50}GeN_2OS$
Formula weight	631.43
Temperature	100(2) K
Wavelength	1.54178 Å
Crystal system	Monoclinic
Space group	*C*2/*c*
Unit cell dimensions	a = 26.021(1) Å
	b = 16.045(1) Å β = 114.79(1)°
	c = 18.006(1) Å
Volume	6825(1) Å^3
Z	8
Density (calculated)	1.229 Mg/m^3
Absorption coefficient	2.002 mm^{-1}
F(000)	2688
Crystal size	0.20 x 0.10 x 0.10 mm^3
θ range for data collection	3.33 to 59.04°.
Index ranges	$-17 \le h \le 28$, $-17 \le k \le 17$, $-20 \le l \le 18$
Reflections collected	21505
Independent reflections	4748 (R_{int} = 0.0363)
Completeness to θ = 59.61°	96.6%
Refinement method	Full-matrix least-squares on F^2
Data / restraints / parameters	4748 / 0 / 389
Goodness-of-fit on F^2	1.040
Final *R* indices ($I > 2\sigma(I)$)	*R*1 = 0.0283, *wR*2 = 0.0694
R indices (all data)	*R*1 = 0.0356, *wR*2 = 0.0730
Largest difference peak and hole	0.355 and –0.279 e·Å^{-3}

Table CD3. Crystal Data and Structure Refinement Details for [{HC(CMeNAr)$_2$}Ge(Se)OH]·toluene (8).

Empirical formula	$C_{36}H_{50}GeN_2OSe$
Formula weight	678.33
Temperature	100(2) K
Wavelength	1.54178 Å
Crystal system	Monoclinic
Space group	*C*2/*c*
Unit cell dimensions	a = 25.974(4) Å
	b = 16.195(3) Å β = 115.82(3)°
	c = 18.151(3) Å
Volume	6873(2) Å^3
Z	8
Density (calculated)	1.311 Mg/m^3
Absorption coefficient	2.632 mm^{-1}
F(000)	2832
Crystal size	0.15 x 0.10 x 0.08 mm^3
θ range for data collection	3.32 to 58.70°.
Index ranges	$-28 \le h \le 28$, $-17 \le k \le 17$, $-18 \le l \le 20$
Reflections collected	14278
Independent reflections	4734 (R_{int} = 0.0210)
Completeness to θ = 59.61°	96.9%
Refinement method	Full-matrix least-squares on F^2
Data / restraints / parameters	4734 / 0 / 388
Goodness-of-fit on F^2	1.052
Final *R* indices ($I > 2\sigma(I)$)	*R*1 = 0.0225, *wR*2 = 0.0608
R indices (all data)	*R*1 = 0.0238, *wR*2 = 0.0620
Largest difference peak and hole	0.391 and –0.300 e·Å^{-3}

Table CD4. Crystal Data and Structure Refinement Details for [{HC(CMeNAr)$_2$}Ge(μ–O)Zr(Me)Cp$_2$] (9).

Empirical formula	$C_{40}H_{54}GeN_2OZr$	
Formula weight	742.66	
Temperature	100(2) K	
Wavelength	1.54178 Å	
Crystal system	Triclinic	
Space group	$P\bar{1}$	
Unit cell dimensions	a = 9.444(1) Å	α = 88.64(1)°
	b = 10.522(1) Å	β = 89.60(1)°
	c = 19.750(1) Å	γ = 67.44(1)°
Volume	1812(1) Å^3	
Z	2	
Density (calculated)	1.361 Mg/m^3	
Absorption coefficient	3.617 mm^{-1}	
F(000)	776	
Crystal size	0.10 x 0.08 x 0.03 mm^3	
θ range for data collection	2.24 to 58.96°.	
Index ranges	$-10 \le h \le 10$, $-11 \le k \le 11$, $-21 \le l \le 21$	
Reflections collected	14140	
Independent reflections	5044 (R_{int} = 0.0265)	
Completeness to θ = 59.61°	96.6%	
Refinement method	Full-matrix least-squares on F^2	
Data / restraints / parameters	5044 / 0 / 421	
Goodness-of-fit on F^2	1.063	
Final R indices ($I > 2\sigma(I)$)	R1 = 0.0288, wR2 = 0.0728	
R indices (all data)	R1 = 0.0297, wR2 = 0.0735	
Largest difference peak and hole	1.232 and –0.553 e·Å^{-3}	

Table CD5. Crystal Data and Structure Refinement Details for [{HC(CMeNAr)$_2$}Ge(μ–O)Hf(Me)Cp$_2$] (10).

Empirical formula	$C_{40}H_{54}GeHfN_2O$	
Formula weight	829.93	
Temperature	100(2) K	
Wavelength	1.54178 Å	
Crystal system	Triclinic	
Space group	$P\bar{1}$	
Unit cell dimensions	a = 9.323(1) Å	α = 89.13(1)°
	b = 10.474(1) Å	β = 89.87(1)°
	c = 20.200(1) Å	γ = 67.04(1)°
Volume	1816(1) Å^3	
Z	2	
Density (calculated)	1.518 Mg/m^3	
Absorption coefficient	6.440 mm^{-1}	
F(000)	840	
Crystal size	0.10 x 0.08 x 0.04 mm^3	
θ range for data collection	2.19 to 58.94°.	
Index ranges	$-10 \le h \le 9$, $-11 \le k \le 11$, $-21 \le l \le 22$	
Reflections collected	13915	
Independent reflections	5077 (R_{int} = 0.0221)	
Completeness to θ = 59.61°	96.8%	
Refinement method	Full-matrix least-squares on F^2	
Data / restraints / parameters	5077 / 0 / 422	
Goodness-of-fit on F^2	1.265	
Final R indices ($I > 2\sigma(I)$)	R1 = 0.0287, wR2 = 0.0782	
R indices (all data)	R1 = 0.0296, wR2 = 0.0785	
Largest difference peak and hole	1.551 and –0.801 e·Å^{-3}	

Table CD6. Crystal Data and Structure Refinement Details for [{HC(CMeNAr)$_2$}Ge(OH)Fe(CO)$_4$] (11).

Empirical formula	$C_{33}H_{42}FeGeN_2O$
Formula weight	675.13
Temperature	133(2) K
Wavelength	0.71073 Å
Crystal system	Monoclinic
Space group	$P2_1/n$
Unit cell dimensions	a = 16.004(9) Å
	b = 9.874(7) Å β = 96.42(4)°
	c = 20.379(11) Å
Volume	3200.1(3) Å^3
Z	4
Density (calculated)	1.401 Mg/m^3
Absorption coefficient	1.435 mm^{-1}
F(000)	1
Crystal size	0.31 x 0.12 x 0.10 mm^3
θ range for data collection	1.71 to 24.81°.
Index ranges	$-18 \le h \le 18$, $-11 \le k \le 11$, $-23 \le l \le 22$
Reflections collected	19288
Independent reflections	5445 (R_{int} = 0.0614)
Completeness to θ = 59.61°	98.7%
Refinement method	Full-matrix least-squares on F^2
Data / restraints / parameters	5445 / 0 / 391
Goodness-of-fit on F^2	0.999
Final R indices ($I > 2\sigma(I)$)	R1 = 0.0320, wR2 = 0.0614
R indices (all data)	R1 = 0.0501, wR2 = 0.0643
Largest difference peak and hole	0.348 and –0.254 e·Å^{-3}

Table CD7. Crystal Data and Structure Refinement Details for [{HC(CMeNAr)$_2$}Ge(OH)MnCp(CO)$_2$] (12).

Empirical formula	$C_{36}H_{47}GeMnN_2O_3$
Formula weight	683.29
Temperature	133(2) K
Wavelength	0.71073 Å
Crystal system	Monoclinic
Space group	$P2_1/n$
Unit cell dimensions	a = 10.705(7) Å
	b = 20.487(10) Å β = 98.02(5)°
	c = 15.160(10) Å
Volume	3292.4(3) Å^3
Z	4
Density (calculated)	1.378 Mg/m^3
Absorption coefficient	1.334 mm^{-1}
F(000)	1104
Crystal size	0.31 x 0.12 x 0.15 mm^3
θ range for data collection	1.68 to 24.84°.
Index ranges	$-12 \le h \le 12$, $-24 \le k \le 23$, $-17 \le l \le 17$
Reflections collected	31533
Independent reflections	5672 (R_{int} = 0.0791)
Completeness to θ = 59.61°	99.6%
Refinement method	Full-matrix least-squares on F^2
Data / restraints / parameters	5672 / 0 / 400
Goodness-of-fit on F^2	0.806
Final R indices ($I > 2\sigma(I)$)	R1 = 0.0304, wR2 = 0.0587
R indices (all data)	R1 = 0.0610, wR2 = 0.0632
Largest difference peak and hole	0.406 and –0.413 e·Å^{-3}

Table CD8. Crystal Data and Structure Refinement Details for [{HC(CMeNAr)$_2$}GeH] (14).

Empirical formula	$C_{29}H_{42}GeN_2$
Formula weight	491.24
Temperature	100(2) K
Wavelength	1.54178 Å
Crystal system	Monoclinic
Space group	$P2_1/n$
Unit cell dimensions	a = 15.238(3) Å
	b = 18.201(4) Å β = 99.11(3)°
	c = 20.485(4) Å
Volume	5610(2) Å^3
Z	8
Density (calculated)	1.163 Mg/m^3
Absorption coefficient	1.593 mm^{-1}
F(000)	2096
Crystal size	0.10 x 0.05 x 0.02 mm^3
θ range for data collection	3.27 to 58.97°.
Index ranges	$-16 \le h \le 16$, $-20 \le k \le 19$, $-21 \le l \le 22$
Reflections collected	35990
Independent reflections	7983 (R_{int} = 0.0418)
Completeness to θ = 59.61°	99.0%
Refinement method	Full-matrix least-squares on F^2
Data / restraints / parameters	7983 / 111 / 629
Goodness-of-fit on F^2	1.085
Final R indices ($I > 2\sigma(I)$)	R1 = 0.0388, wR2 = 0.1021
R indices (all data)	R1 = 0.0406, wR2 = 0.1035
Largest difference peak and hole	1.474 and –0.476 e·Å^{-3}

Table CD9. Crystal Data and Structure Refinement Details for [{HC(CMeNAr)$_2$}SnH] (15).

Empirical formula	$C_{29}H_{42}N_2Sn$
Formula weight	537.34
Temperature	100(2) K
Wavelength	1.54178 Å
Crystal system	Monoclinic
Space group	*C*2/*c*
Unit cell dimensions	a = 25.209(5) Å
	b = 15.139(3) Å β = 94.92(3)°
	c = 14.682(3) Å
Volume	5583(2) Å^3
Z	8
Density (calculated)	1.279 Mg/m^3
Absorption coefficient	7.392 mm^{-1}
F(000)	2240
Crystal size	0.10 x 0.05 x 0.05 mm^3
θ range for data collection	3.41 to 58.90°.
Index ranges	$-28 \le h \le 27$, $-16 \le k \le 16$, $-16 \le l \le 16$
Reflections collected	22645
Independent reflections	4000 (R_{int} = 0.0315)
Completeness to θ = 59.61°	99.6%
Refinement method	Full-matrix least-squares on F^2
Data / restraints / parameters	4000 / 0 / 310
Goodness-of-fit on F^2	1.047
Final *R* indices ($I > 2\sigma(I)$)	*R*1 = 0.0216, *wR*2 = 0.0548
R indices (all data)	*R*1 = 0.0218, *wR*2 = 0.0547
Largest difference peak and hole	0.761 and –0.749 e·Å^{-3}

Table CD10. Crystal Data and Structure Refinement Details for [{HC(CMeNAr)$_2$}PbBr] (17).

Empirical formula	$C_{29}H_{41}BrPbN_2$	
Formula weight	704.74	
Temperature	100(2) K	
Wavelength	1.54178 Å	
Crystal system	Triclinic	
Space group	$P\bar{1}$	
Unit cell dimensions	a = 10.361(2) Å	α = 89.33(2)°
	b = 12.033(2) Å	β = 72.91(2)°
	c = 12.431(2) Å	γ = 70.56(2)°
Volume	1391(1) Å^3	
Z	2	
Density (calculated)	1.683 Mg/m^3	
Absorption coefficient	13.603 mm^{-1}	
F(000)	692	
Crystal size	0.05 x 0.05 x 0.03 mm^3	
θ range for data collection	3.74 to 58.75°.	
Index ranges	$-11 \le h \le 11$, $-12 \le k \le 13$, $-13 \le l \le 13$	
Reflections collected	13333	
Independent reflections	3852 (R_{int} = 0.0331)	
Completeness to θ = 59.61°	97.0%	
Refinement method	Full-matrix least-squares on F^2	
Data / restraints / parameters	3852 / 0 / 311	
Goodness-of-fit on F^2	1.063	
Final R indices ($I > 2\sigma(I)$)	R1 = 0.0173, wR2 = 0.0424	
R indices (all data)	R1 = 0.0175, wR2 = 0.0425	
Largest difference peak and hole	0.430 and –0.786 e·Å^{-3}	

Table CD11. Crystal Data and Structure Refinement Details for [{HC(Et$_2$NCH$_2$CH$_2$NCMe)$_2$}BiCl$_2$] (19).

Empirical formula	$C_{17}H_{35}BiCl_2N_4$
Formula weight	575.37
Temperature	100(2) K
Wavelength	1.54178 Å
Crystal system	Monoclinic
Space group	$P2_1/c$
Unit cell dimensions	a = 12.825(2) Å
	b = 11.585(2) Å β = 104.47(3)°
	c = 14.771(3) Å
Volume	2125(1) Å^3
Z	4
Density (calculated)	1.798 Mg/m^3
Absorption coefficient	18.639 mm^{-1}
F(000)	1128
Crystal size	0.10 x 0.10 x 0.05 mm^3
θ range for data collection	3.56 to 58.96°.
Index ranges	$-14 \le h \le 14$, $-12 \le k \le 11$, $-16 \le l \le 16$
Reflections collected	14026
Independent reflections	3015 (R_{int} = 0.0383)
Completeness to θ = 59.61°	98.8%
Refinement method	Full-matrix least-squares on F^2
Data / restraints / parameters	3015 / 0 / 226
Goodness-of-fit on F^2	1.073
Final R indices ($I > 2\sigma(I)$)	R1 = 0.0183, wR2 = 0.0422
R indices (all data)	R1 = 0.0188, wR2 = 0.0425
Largest difference peak and hole	0.541 and –0.929 e·Å^{-3}

7. Supporting Materials

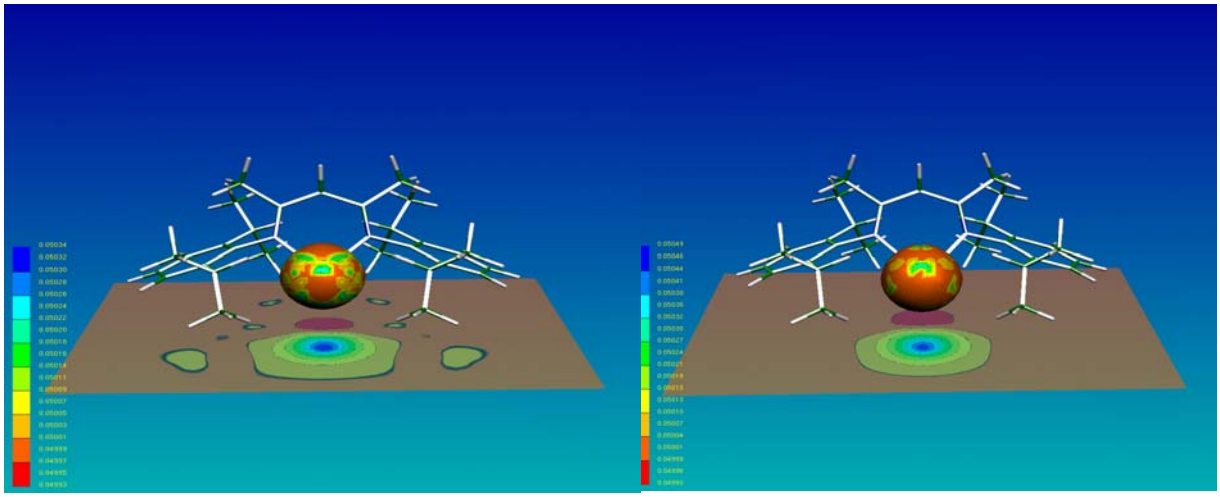

Figure S1. A 2D cross section in the metal hydrogen plane (bottom) and 3D representation (top) of the electron density (ED) in [{HC(CMeNAr)$_2$}GeH] (**14**) (left picture) and [{HC(CMeNAr)$_2$}SnH] (**15**; right picture). The colors at each point of the 2D images correspond to the density values given in the color bar on the left side of both pictures and range from dark blue (ED = 0.051) to dark red (ED = 0.049).

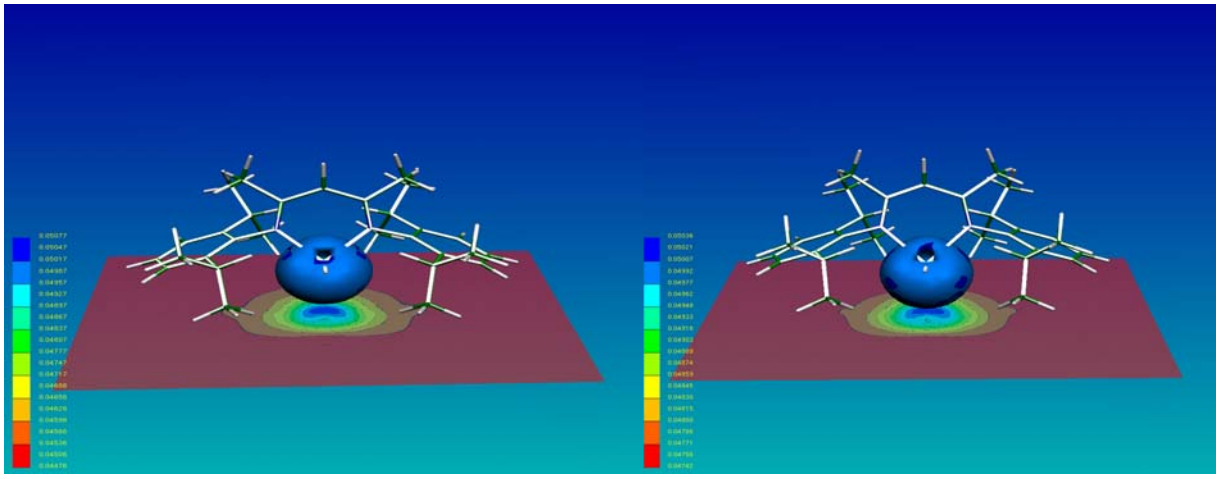

Figure S2. A 2D cross section of the lone pair in the metal hydrogen plane (bottom) and 3D representation (top) of the electron density (ED) in [{HC(CMeNAr)$_2$}GeH] (**14**) (left picture) and [{HC(CMeNAr)$_2$}SnH] (**15**; right picture). The colors at each point of the 2D images correspond to the density values given in the color bar on the left side of both pictures and range from dark blue (ED = 0.051) to dark red (ED = 0.044).

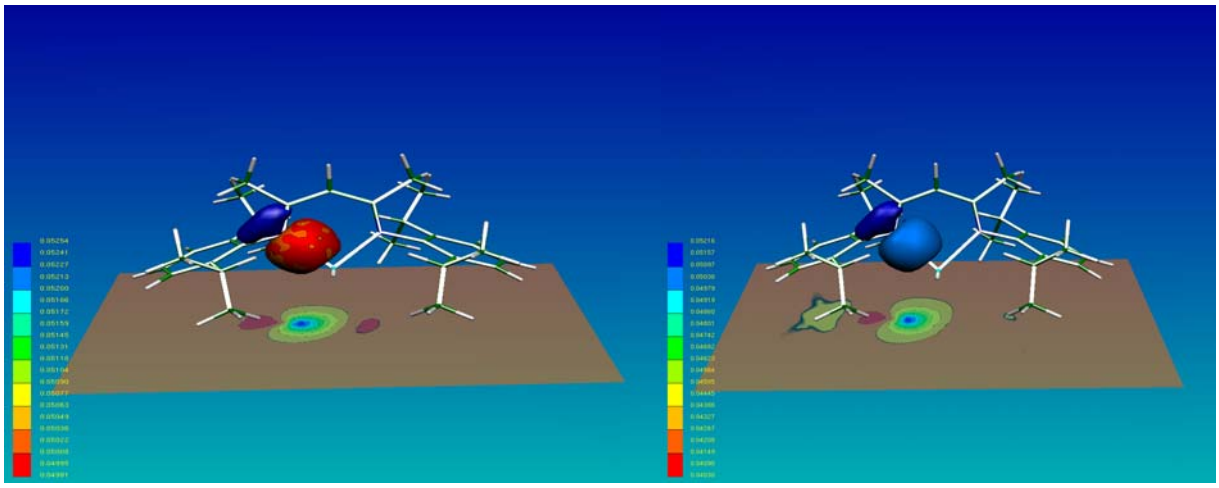

Figure S3. A 2D cross section of the lone pair delocalization in the metal nitrogen plane (bottom) and 3D representation (top) of the electron density (ED) in [{HC(CMeNAr)$_2$}GeH] (**14**) (left picture) and [{HC(CMeNAr)$_2$}SnH] (**15**; right picture). The colors at each point of the 2D images correspond to the density values given in the color bar on the left side of both pictures and range from dark blue (ED = 0.052) to dark red (ED = 0.040).

8. References

[1] N. Tokitoh, R. Okazaki, *Adv. Organomet. Chem.* **2001**, *47*, 121–166.

[2] A. Sekiguchi, M. Tsukamoto, M. Ichinohe, *Science* **1997**, *275*, 60–61.

[3] P. v. R. Schleyer, *Science* **1997**, *275*, 39–40.

[4] M. Ichinohe, M. Igarashi, K. Sanuki, A. Sekiguchi, *J. Am. Chem. Soc.* **2005**, *127*, 9978–9979.

[5] N. Tokitoh, Y. Arai, R. Okazaki, S. Nagase, *Science* **1997**, *277*, 78–80.

[6] T. Iwamoto, M. Tamura, C. Kabuto, M. Kira, *Science* **2000**, *290*, 504–506.

[7] W. E. Billups, M. M. Harley, *J. Am. Chem. Soc.* **1991**, *113*, 5084–5085.

[8] R. K. Saini, V. A. Litosh, A. D. Daniels, W. E. Billups, *Tetrahedron Lett.* **1999**, *40*, 6157–6158.

[9] K.-C. Kim, C. A. Reed, D. W. Elliott, L. J. Mueller, F. Tham, L. Lin, J. B. Lambert, *Science* **2002**, *297*, 825–827.

[10] P. Jutzi, A. Mix, B. Rummel, W. W. Schoeller, B. Neumann, H.-G. Stammler, *Science* **2004**, *305*, 849–851.

[11] G. Bertrand, *Science* **2004**, *305*, 783–785.

[12] A. Sekiguchi, R. Kinjo, M. Ichinohe, *Science* **2004**, *305*, 1755–1757.

[13] R. West, *Science* **2004**, *305*, 1724–1725.

[14] M. Weidenbruch, *Angew. Chem.* **2005**, *117*, 518–520; *Angew. Chem. Int. Ed.* **2005**, *44*, 514–516.

[15] P. P. Power, *Chem. Rev.* **1999**, *99*, 3463–3503.

[16] P. P. Power, *J. Chem. Soc. Dalton Trans.* **1998**, 2939–2951.

[17] P. P. Power, *Chem. Commun.* **2003**, 2091–2101.

[18] P. P. Power, in *Structure and Bonding*, Vol. 103 (Ed.: D. M. P. Mingos), Springer, Berlin, **2002**, pp. 57–84.

[19] L. Pu, B. Twamley, P. P. Power, *J. Am. Chem. Soc.* **2000**, *122*, 3524–3525.

[20] Y. Chen, M. Hartmann, M. Diedenhofen, G. Frenking, *Angew. Chem.* **2001**, *113*, 2107–2112; *Angew. Chem. Int. Ed.* **2001**, *40*, 2052–2055.

[21] P. P. Power, *Appl. Organometal. Chem.* **2005**, *19*, 488–493.

[22] C. Cui, M. M. Olmstead, J. C. Fettinger, G. H. Spikes, P. P. Power, *J. Am. Chem. Soc.* **2005**, *127* 17530–17541.

[23] Y. Sugiyama, T. Sasamori, Y. Hosoi, Y. Furukawa, N. Takagi, S. Nagase, N. Tokitoh, *J. Am. Chem. Soc.* **2006**, *128*, 1023–1031.

[24] G. H. Spikes, Y. Peng, J. C. Fettinger, J. Steiner, P P. Power, *Chem. Commun.* **2005**, 6041–6043.

[25] P. P. Power, *J. Organometal. Chem.* **2004**, *689*, 3904–3919.

[26] P. J. Davidson, M. F. Lappert, *J. Chem. Soc. Chem. Commun.* **1973**, 317.

[27] J. D. Cotton, C. S. Cundy, D. H. Harris, A. Hudson, M. F. Lappert, P. W. Lednor, *J. Chem. Soc. Chem. Commun.* **1974**, 651–652.

[28] D. E. Goldberg, P. B. Hitchcock, M. F. Lappert, K. M. Thomas, A. J. Thorne, T. Fjeldberg, A. Haaland, B. E. R. Schilling, *J. Chem. Soc. Dalton Trans.* **1986**, 2387–2394.

[29] L. Bourget-Merle, M. F. Lappert, J. R. Severn, *Chem. Rev.* **2002**, *102*, 3031–3065.

[30] S. S. Malhotra, M. C. Whiting, *J. Chem. Soc. Soc.* **1960**, 3812–3822.

[31] G. Scheibe, *Ber. Dtsch. Chem. Ges.* **1923**, *56*, 137–148.

[32] C. Cui, H. W. Roesky, H.-G. Schmidt, M. Noltemeyer, H. Hao, F. Cimpoesu, *Angew. Chem.* **2000**, *112*, 4444–4446; *Angew. Chem. Int. Ed.* **2000**, *39*, 4274–4276.

[33] Y. Peng, H. Fan, H. Zhu, H. W. Roesky, J. Magull, C. E. Hughes, *Angew. Chem.* **2004**, *116*, 3525–3527; *Angew. Chem. Int. Ed.* **2004**, *43*, 3443–3445.

[34] Y. Peng, H. Fan, V. Jancik, H. W. Roesky, R. Herbst-Irmer, *Angew. Chem.* **2004**, *116*, 6316–6318; *Angew. Chem. Int. Ed.* **2004**, *43*, 6190–6192.

[35] Z. Yang, X. Ma, R. B. Oswald, H. W. Roesky, H. Zhu, C. Schulzke, K. Starke, M. Baldus, H.-G. Schmidt, M. Noltemeyer, *Angew. Chem.* **2005**, *117*, 7234–7236; *Angew. Chem. Int. Ed.* **2005**, *44*, 7072–7074.

[36] H. W. Roesky, S. S. Kumar, *Chem. Commun.* **2005**, 4027–4038.

[37] G. Bai, Y. Peng, H. W. Roesky, J. Li, H.-G. Schmidt, M. Noltemeyer, *Angew. Chem.* **2003**, *115*, 1164–1167; *Angew. Chem. Int. Ed.* **2003**, *42*, 1132–1135.

[38] V. Jancik, L. W. Pineda, J. Pinkas, H. W. Roesky, D. Neculai, A. M. Neculai, R. Herbst-Irmer, *Angew. Chem.* **2004**, *116*, 2194–2197; *Angew. Chem. Int. Ed.* **2004**, *43*, 2142–2145.

[39] V. Jancik, L. W. Pineda, A. C. Stückl, H. W. Roesky, R. Herbst-Irmer, *Organometallics* **2005**, *25*, 1511–1515.

[40] V. Jancik, Y. Peng, H. W. Roesky, J. Li, D. Neculai, A. M. Neculai, R. Herbst-Irmer, *J. Am. Chem. Soc.* **2003**, *125*, 1452–1453.

[41] C. Cui, H. W. Roesky, H. Hao, H.-G. Schmidt, M. Noltemeyer, *Angew. Chem.* **2000**, *112*, 1885–1887; *Angew. Chem. Int. Ed.* **2000**, *39*, 1815–1817.

[42] D. Neculai, H. W. Roesky, A. M. Neculai, J. Magull, B. Walfort, D. Stalke, *Angew. Chem.* **2002**, *114*, 4470–4472; *Angew. Chem. Int. Ed.* **2002**, *41*, 4294–4296.

[43] A. F. Wells, *Structural Inorganic Chemistry*, Clarendon, Oxford, **1984**, pp. 627; 357.

[44] A. F. Holleman, E. Wiberg, *Lehrbuch der Anorganischen Chemie*, Walter de Gruyter, Berlin, **1995**, pp. 960, 102, 136, 1838.

[45] N. N. Greenwood, A. Earnshaw, *Chemistry of the Elements*, Butterworth-Heinemann, Oxford, **1997**, pp. 382–383; 60.

[46] J. Janssen, J. Magull, H. W. Roesky, *Angew. Chem*. **2002**, *114*, 1425–1427; *Angew. Chem. Int. Ed.* **2002**, *41*, 1365–1367.

[47] G. Bai, H. W. Roesky, J. Li, T. Labahn, F. Cimpoesu, J. Magull, *Organometallics* **2003**, *22*, 3034–3038.

[48] H. W. Roesky, M. G. Walawalkar, R. Murugavel, *Acc. Chem. Res*. **2001**, *34*, 201–211.

[49] M. Lesbre, P. Mazerolles, J. Satgé, *The Organic Compounds of Germanium*, John Wiley & Sons, London, **1971**, pp. 403; 259–265.

[50] J. Beckmann, K. Jurkschart, M. Schürmann, *Eur. J. Inorg. Chem*. **2000**, 939–941.

[51] Y. Zhang, F. Cervantes-Lee, K. H. Pannell, *Organometallics* **2003**, *22*, 510–515.

[52] P. Rivière, M. Rivière-Baudet, J. Satgé, in *Comprehensive Organometallic Chemistry*, Vol. 2 (Eds.: G. Wilkinson, F. G. A. Stone, E. W. Abel), Pergamon, Oxford, **1982**, pp. 405–503; 424–425.

[53] Y. Ding, H. W. Roesky, M. Noltemeyer, H.-G. Schmidt, *Organometallics* **2001**, *20*, 1190–1194.

[54] A. J. Arduengo, III, H. V. R. Dias, R. L. Harlow, M. Kline, *J. Am. Chem. Soc*. **1992**, *114*, 5530–5534.

[55] J. R. T. Johnson, I. Panas, *Chem. Phys*. **1999**, *249*, 273–303.

[56] H. Puff, S. Franken, W. Schuh, W. Schwab, *J. Organomet. Chem*. **1983**, *254*, 33–41.

[57] A. Fischer, K. Jacob, F. T. Edelmann, *Z. Anorg. Allg. Chem*. **2003**, *629*, 963–967.

[58] Y. Ding, H. Hao, H. W. Roesky, M. Noltemeyer, H.-G. Schmidt, *Organometallics* **2001**, *20*, 4806–4811.

[59] Y. Ding, Q. Ma, H. W. Roesky, R. Herbst-Irmer, I. Usón, M. Noltemeyer, H.-G. Schmidt, *Organometallics* **2002**, *21*, 5216–5220.

[60] M. Stender, A. D. Phillips, P. P. Power, *Inorg. Chem*. **2001**, *40*, 5314–5315.

[61] D. L. Reger, P. S. Coan, *Inorg. Chem*. **1996**, *35*, 258–260.

[62] J. McMurry, *Organic Chemistry*, Brooks-Cole Publishing Co., California **1992**, pp. 695–705.

[63] N. Tokitoh, T. Matsumoto, R. Okazaki, *Bull*. *Chem*. *Soc*. *Jpn*. **1999**, *72*, 1665–1684.

[64] T. Matsumoto, N. Tokitoh, R. Okazaki, *J*. *Am*. *Chem*. *Soc*. **1999**, *121*, 8811–8824.

[65] Y. Ding, Q. Ma, H. W. Roesky, I. Usón, M. Noltemeyer, H.-G. Schmidt, *Dalton Trans*. **2003**, 1094–1098.

[66] F. Duus, in *Comprehensive Organic Chemistry*, Vol. 3 (Eds.: D. Barton, W. D. Ollis), Pergamon, Oxford, **1979**, pp. 420–421.

[67] J. Hine, *Physical Organic Chemistry*, McGraw-Hill, **1962,** p. 238.

[68] A. Fischer, K. Jacob, F. T. Edelmann, *Z. Anorg. Allg. Chem*. **2003**, *629*, 963–967.

[69] M. Veith, S. Becker, V. Huch, *Angew*. *Chem*. **1989**, *101*, 1287–1289; *Angew*. *Chem*. *Int*. *Ed*. *Engl*. **1989**, *28*, 1237–1238.

[70] M. C. Kuchta, G. Parkin, *J*. *Chem*. *Soc*. *Chem*. *Commun*. **1994**, 1351–1352.

[71] M. Veith, A. Rammo, *Z. Anorg. Allg. Chem*. **1997**, *623*, 861–872.

[72] I. Saur, G. Rima, H. Gornitzka, K. Miqueu, J. Barrau, *Organometallics* **2003**, *22*, 1106–1109.

[73] Z. T. Cygan, J. W. Kampf, M. M. Banaszak Holl, *Organometallics* **2004**, *23*, 2370–2375.

[74] I. Saur, S. Garcia Alonso, J. Barrau, *Appl*. *Organometal*. *Chem*. **2005**, *19*, 418–428.

[75] O. Kühl, *Coord*. *Chem*. *Rev*. **2004**, *248*, 411–427.

[76] N. N. Zemlyanskii, I. V. Borisova, M. S. Nechaev, V. N. Khrustalev, V. V. Lunin, M. Y. Antipin, Y. U. Ustynyuk, *Russ*. *Chem*. *Bull*. *Int*. *Ed*. **2004**, *53*, 980–1006.

[77] M. Weidenbruch, *J*. *Organomet*. *Chem*. **2002**, *646*, 39–52.

[78] B. Gehrhus, M. F. Lappert, *J*. *Organomet*. *Chem*. **2001**, *617–618*, 209–223.

[79] M. Haaf, T. A. Schmedake, R. West, *Acc*. *Chem*. *Res*. **2000**, *33*, 704–714.

[80] N. Tokitoh, R. Okazaki, *Coord*. *Chem*. *Rev*. **2000**, *210*, 251–277.

[81] R. Okazaki, N. Tokitoh, *Acc*. *Chem*. *Res*. **2000**, *33*, 625–630.

[82] M. Weidenbruch, *Eur*. *J*. *Inorg*. *Chem*. **1999**, 373–381.

[83] J. Barrau, G. Rima, *Coord*. *Chem*. *Rev*. **1998**, *178–180*, 593–622.

[84] J. Barrau, G. Rima, T. El Amraoui, *J*. *Organomet*. *Chem*. **1998**, *570*, 163–174.

[85] H. V. R. Dias, Z. Wang, W. Jin, *Coord*. *Chem*. *Rev*. **1998**, *176*, 67–86.

[86] R. West, M. Denk, *Pure Appl*. *Chem*. **1996**, *68*, 785–788.

[87] W. P. Neumann, *Chem*. *Rev*. **1991**, *91*, 311–334.

[88] M. Haaf, A. Schmiedl, T. A. Schmedake, D. R. Powell, A. J. Millevolte, M. Denk, R. West, *J*. *Am*. *Chem*. *Soc*. **1998**, *120*, 12714–12719.

[89] F. S., Jr. Guziec, in *Organoselenium Chemistry*, (Ed.: D. Liotta), Wiley, New York, **1987**, pp. 215–273.

[90] F. S., Jr. Guziec, in *The Chemistry of Organic Selenium and Tellurium Compounds*, Vol. 2 (Ed.: S. Patai), Wiley, Chishester, **1987**, pp. 277–324.

[91] T. Murai, S. Kato, *Top*. *Curr*. *Chem*. **2000**, *208*, 177–199.

[92] S. Kato, O. Niyomura, *Top*. *Curr*. *Chem*. **2005**, *251*, 13–85.

[93] O. Niyomura, S. Kato, *Top*. *Curr*. *Chem*. **2005**, *251*, 1–12.

[94] T. Murai, *Top*. *Curr*. *Chem*. **2005**, *251*, 247–272.

[95] S. Fujiwara, N. Kambe, *Top*. *Curr*. *Chem*. **2005**, *251*, 87–140.

[96] T. Wirth, *Top*. *Curr*. *Chem*. **2000**, *208*, 1–5.

[97] C. W. Nogueira, G. Zeni, J. B. Rocha, *Chem. Rev.* **2004**, *104*, 6255–6285.

[98] H. Kageyama, T. Murai, T. Kanda, S. Kato, *J. Am. Chem. Soc.* **1994**, *116*, 2195–2196.

[99] S. Kato, Y. Kawahara, H. Kageyama, R. Yamada, O. Niyomura, T. Murai, T. Kanda, *Organometallics* **2002**, *21*, 2940–2943.

[100] G. Ossig, A. Meller, C. Brönneke O. Müller, M. Schäfer, R. Herbst-Irmer, *Organometallics* **1997**, *16*, 2116–2120.

[101] S. R. Foley, C. Bensimon, D. S. Richeson, *J. Am. Chem. Soc.* **1997**, *119*, 10359–10363.

[102] M. Kuchta, G. Parkin, *Coord. Chem. Rev.* **1998**, *176*, 323–372.

[103] For shortest and longest Ge–Se single bond see: (a) H. Ahari, A. Garcia, S. Kirkby, G. A. Ozin, D.Young, A. J. Lough, *J. Chem. Soc. Dalton Trans.* **1998**, 2023–2028. (b) H. H. Karsch, G. Baumgartner, S. Gamper, J. Lachmann, G. Müller, *Chem. Ber.* **1992**, *125*, 1333–1339.

[104] C. Lee, W. Yang, R. G. Parr, *Phys. Rev. B.* **1988**, *37*, 785–789.

[105] B. Miehlich, A. Savin, H. Stoll, H. Preuss, *Chem. Phys. Lett.* **1989**, *157*, 200–206.

[106] Gaussian 03, Revision C.02, M. J. Frisch, G. W. Trucks, H. B. Schlegel, G. E. Scuseria, M. A. Robb, J. R. Cheeseman, J. A. Montgomery, Jr., T. Vreven, K. N. Kudin, J. C. Burant, J. M. Millam, S. S. Iyengar, J. Tomasi, V. Barone, B. Mennucci, M. Cossi, G. Scalmani, N. Rega, G. A. Petersson, H. Nakatsuji, M. Hada, M. Ehara, K. Toyota, R. Fukuda, J. Hasegawa, M. Ishida, T. Nakajima, Y. Honda, O. Kitao, H. Nakai, M. Klene, X. Li, J. E. Knox, H. P. Hratchian, J. B. Cross, V. Bakken, C. Adamo, J. Jaramillo, R. Gomperts, R. E. Stratmann, O. Yazyev, A. J. Austin, R. Cammi, C. Pomelli, J. W. Ochterski, P. Y. Ayala, K. Morokuma, G. A. Voth, P. Salvador, J. J. Dannenberg, V. G. Zakrzewski, S. Dapprich, A. D. Daniels,

M. C. Strain, O. Farkas, D. K. Malick, A. D. Rabuck, K. Raghavachari, J. B. Foresman, J. V. Ortiz, Q. Cui, A. G. Baboul, S. Clifford, J. Cioslowski, B. B. Stefanov, G. Liu, A. Liashenko, P. Piskorz, I. Komaromi, R. L. Martin, D. J. Fox, T. Keith, M. A. Al-Laham, C. Y. Peng, A. Nanayakkara, M. Challacombe, P. M. W. Gill, B. Johnson, W. Chen, M. W. Wong, C. Gonzalez, J. A. Pople, Gaussian, Inc., Wallingford CT, **2004**.

[107] G. A. Petersson, M. A. Al-Laham, *J. Chem. Phys*. **1991**, *94*, 6081–6090.

[108] G. A. Petersson, A. Bennett, T. G. Tensfeldt, M. A. Al-Laham, W. A. Shirley, J. Mantzaris, *J*. *Chem*. *Phys*. **1988**, *89*, 2193–2218.

[109] M. D. Liptak, K. C. Cross, P. G. Seybold, S. Feldgus, G. Shields, C. *J*. *Am*. *Soc*. **2002**, *124*, 6421–6427.

[110] A. M. Magill, K. J. Cavell, B. F. Yates, *J*. *Am*. *Chem*. *Soc*. **2004**, *126*, 8717–8724.

[111] E. Cancès, B. Mennucci, J. Tomasi, *J*. *Chem*. *Phys*. **1997**, *107*, 3032–3041.

[112] J. Clayden, N. Greeves, P. Wothers, *Organic Chemistry*, 1st Ed.; Oxford: Oxford, U. K., **2004**, pp. 181–206.

[113] J. E. Carpenter, F. Weinhold, *J. Mol. Struct.* **1988**, *169*, 41–62.

[114] J. P. Foster, F. Weinhold, *J*. *Am*. *Chem*. *Soc*. **1980**, *102*, 7211–7218.

[115] A. E. Reed, F. Weinhold, *J*. *Chem*. *Phys*. **1985**, *83*, 1736–1740.

[116] A. E. Reed, L. A. Curtiss, F. Weinhold, *Chem*. *Rev*. **1988**, *88*, 899–926.

[117] F. Weinhold, C. Landis, *Valency and Bonding*, Cambridge University Press, Cambridge, **2005**, pp. 19–20; 94–96; 125–128; 184–188.

[118] C. Coperèt, M. Chabanas, R. P. Sait-Arroman, J.-M. Basset, *Angew*. *Chem*. **2003**, *105*, 164–191; *Angew*. *Chem*. *Int*. *Ed*. **2003**, *42*, 156–181.

[119] H. W. Roesky, I. Haiduc, N. S Hosmane, *Chem*. *Rev*. **2003**, *103*, 2579–2595.

[120] T. Carofiglio, C. Floriani, M. Rosi, A. Chiesi-Villa, C. Rizzoli, *Inorg. Chem.* **1991**, *30*, 3245–3246.

[121] M. S. Rau, C. M. Kretz, G. L. Geoffroy, A. L. Rheingold, B. S. Haggerty, *Organometallics* **1994**, *13*, 1624–1634.

[122] G. Erker, M. Albrecht, S. Werner, C. Krüger, *Z. Naturforsch.* **1990**, *45b*, 1205–1209.

[123] S. Bansal, Y. Singh, A. Singh, *Heteroat. Chem.* **2004**, 21–25.

[124] H. Li, M. Eddaoudi, J. Plévert, M. O'Keeffe, O. M. Yaghi, *J. Am. Chem. Soc.* **2000**, *122*, 12409–12410.

[125] P. Jutzi, S. Keitemeyer, B. Neumann, H.-G. Stammler, *Organometallics* **1999**, *18*, 4778–4784.

[126] B. Cetinkaya, I. Gümrükcü, M. F. Lappert, J. L. Atwood, R. D. Rogers, M. J. Zaworotko, *J. Am. Chem. Soc.* **1980**, *102*, 2088–2089.

[127] T. Fjeldberg, P. B. Hitchcock, M. F. Lappert, S. J. Smith, A. J. Thorne, *J. Chem. Soc. Chem. Commun.* **1985**, 939–941.

[128] E. Samuel, M. D. Rausch, *J. Am. Chem. Soc.* **1973**, *95*, 6263–6267.

[129] Y. Ding. H. W. Roesky, M. Noltemeyer, H.-G. Schmidt, *Organometallics* **2001**, *20*, 1190–1194.

[130] J. F. Clarke, M. G. B. Drew, *Acta Cryst.* **1974**, *B30*, 2267–2269.

[131] E. N. Jacobsen, M. K. Trost, R. G. Bergman, *J. Am. Chem. Soc.* **1986**, *108*, 8092–8094.

[132] B. Morosin, L. A. Harrah, *Acta Cryst.* **1981**, *B37*, 579–586.

[133] K. M. Mackay, B. K. Nicholson, in *Comprehensive Organometallic Chemistry*, Vol. 6 (Ed.: G. Wilkinson), Pergamon, Oxford, **1982**, pp. 1043–1114.

[134] W. Petz, *Chem. Rev.* **1986**, *86*, 1019–1047.

[135] H. Wagner, J. Baumgartner, C. Marschner, *Organometallics* **2005**, *24*, 4649–4653.

[136] M. S. Holt, W. L. Wilson, J. H. Nelson, *Chem. Rev.* **1989**, *89*, 11–49.

[137] A. C. Filippou, H. Rohde, G. Schnakenburg, *Angew. Chem.* **2004**, *116*, 2293–2297; *Angew. Chem. Int. Ed.* **2004**, *43*, 2243–2247.

[138] A. C. Filippou, P. Portius, A. I. Philippopoulos, H. Rohde, *Angew. Chem.* **2003**, *115*, 461–464; *Angew. Chem. Int. Ed.* **2003**, *42*, 445–447.

[139] A. C. Filippou, A. I. Philippopoulos, G. Schnakenburg, *Organometallics* **2003**, *22*, 3339–3341.

[140] M. Okazaki, H. Tobita, H. Ogino, *Dalton Trans.* **2003**, 493–506.

[141] R. D. Adams, B. Captain, W. Fu, *Inorg. Chem.* **2003**, *42*, 1328–1333.

[142] R. D. Adams, B. Captain, W. Fu, M. D. Smith, *Inorg. Chem.* **2002**, *41*, 5593–5601.

[143] A. C. Filippou, P. Portius, A. I. Philippopoulos, *Organometallics* **2002**, *21*, 653–661.

[144] A. C. Filippou, A. I. Philippopoulos, P. Portius, D. U. Neumann, *Angew. Chem.* **2000**, *112*, 2881–2884; *Angew. Chem. Int. Ed.* **2000**, *39*, 2778–2781.

[145] D. Agustin, G. Rima, H. Gornitzka, J. Barrau, *Eur. J. Inorg. Chem.* **2000**, 693–702.

[146] D. Agustin, G. Rima, H. Gornitzka, J. Barrau, *Inorg. Chem.* **2000**, *39*, 5492–5495.

[147] R. S. Simons, P. P. Power, *J. Am. Chem. Soc.* **1996**, *118*, 11966–11967.

[148] C. Bibal, S. Mazières, H. Gornitzka, C. Couret, *Organometallics* **2002**, *21*, 2940–2943.

[149] M. F. Lappert, R. S. Rowe, *Coord. Chem. Rev.* **1990**, *100*, 267–292.

[150] M. F. Lappert, P. P. Power, *J. Chem. Soc. Dalton Trans.* **1985**, 51–57.

[151] P. Jutzi, W. Steiner, *Chem. Ber.* **1976**, *109*, 3473–3479.

[152] P. C. Ford, *Acc. Chem. Res.* **1981**, *14*, 31–37.

[153] D. F. Shriver, P. W. Atkins, *Inorganic Chemistry*, 3rd Ed.; Oxford: Oxford, U. K., **1999**, pp. 544–549.

[154] I. Saur, G. Rima, K. Miqueu, H. Gornitzka, J. Barrau, *J. Organomet. Chem.* **2003**, *672*, 77–85.

[155] M. Veith, S. Becker, V. Huch, *Angew. Chem.* **1990**, *102*, 186–188; *Angew. Chem. Int. Ed. Engl.* **1990**, *29*, 216–218.

[156] P. B. Hitchcock, M. F. Lappert, S. A. Thomas, A. J. Thorne, *J. Organomet. Chem.* **1986**, *315*, 27–44.

[157] W. Gäde, E. Weiss, *J. Organomet. Chem.* **1981**, *213*, 451–460.

[158] D. Melzer, E. Weiss, *J. Organomet. Chem.* **1984**, *263*, 67–73.

[159] W.-P. Leung, C.-W. So, K.-W. Kan, H.-S. Chan, T. C. W. Mak, *Inorg. Chem.* **2005**, *44*, 7286–7288.

[160] D. Lei, M. J. Hampden-Smith, E. N. Duesler, J. C. Huffman, *Inorg. Chem.* **1990**, *29*, 795–798.

[161] H. D. Kaesz, R. B. Saillant, *Chem. Rev.* **1972**, *72*, 231–281.

[162] G. S. McGrady, G. Guilera, *Chem. Soc. Rev.* **2003**, *32*, 383–392.

[163] S. Aldridge, A. J. Downs, *Chem. Rev.* **2001**, *101*, 3305–3365.

[164] H.-J. Himmel, *Dalton. Trans.* **2003**, 3639–3649.

[165] H.-J. Himmel, *Z. Anorg. Allg. Chem.* **2005**, *631*, 1551–1564.

[166] N. W. Mitzel, *Angew. Chem.* **2003**, *115*, 3984–3986; *Angew. Chem. Int. Ed.* **2003**, *42*, 3856–3858.

[167] W. M. Mueller, J. P. Blackledge, G. G. Libowitz, *Metal Hydrides*, Academic Press, London, **1968**, pp. 1–21.

[168] F. Lefebvre, J.-M. Basset, *Main Group Met. Chem.* **2002**, *25*, 15–32.

[169] J. Zhao, A. S. Goldman, J. F. Hartwig, *Science* **2005**, *307*, 1080–1082.

[170] R. F. Service, *Science* **2004**, *305*, 958–961.

[171] J. A. Turner, *Science* **2004**, *305*, 972–974.

[172] W. Grochala, P. P. Edwards, *Chem. Rev.* **2004**, *104*, 1283–1315.

[173] F. Schüth, B. Bogdanović, M. Felderhoff, *Chem. Commun.* **2004**, 2249–2258.

[174] E. J. Kupchik, in *Organotin Compounds*, Vol. 1 (Ed.: A. K. Sawyer), Marcel Dekker, New York, **1971**, pp.7–72.

[175] A. G. Davies, P. J. Smith, in *Comprehensive Organometallic Chemistry*, Vol. 2 (Eds.: G. Wilkinson, F. G. A. Stone, E. W. Abel), Pergamon, Oxford, **1982**, pp. 584–585.

[176] V. I. Dodero, M. B. Faraoni, D. C. Gerbino, L. C. Koll, A. E. Zuñiga, T. N. Mitchell, J. Podestá, *Organometallics* **2005**, *24*, 1992–1995.

[177] D. S. Hays, G. C. Fu, *J. Org. Chem.* **1997**, *62*, 7070–7071.

[178] V. I. Dodero, L. C. Koll, M. B. Faraoni, T. N. Mitchell, J. Podestá, *J. Org. Chem.* **2003**, *68*, 10087–10091.

[179] V. I. Dodero, T. N. Mitchell, J. Podestá, *Organometallics* **2003**, *22*, 856–860.

[180] K. Sasaki, Y. Kondo, K. Maruoka, *Angew. Chem.* **2001**, *113*, 425–428; *Angew. Chem. Int. Ed.* **2001**, *42*, 411–414.

[181] B. E. Eichler, P. P. Power, *J. Am. Chem. Soc.* **2000**, *122*, 8785–8786.

[182] G. Trinquier, *J. Am. Chem. Soc.* **1990**, *112*, 2130–2137.

[183] R. A. Kovar, J. O. Callaway, *Inorg. Synth.* **1976**, *22*, 37–47.

[184] H. W. Roesky, *Aldrichimica Acta*, **2004**, *37*, 103–108.

[185] S. S. Kumar, H. W. Roesky, *Dalton. Trans.* **2004**, 3927–3737.

[186] Alternatively, compound **14** could also be prepared in good yield by the reaction of [{HC(CMeNAr)$_2$}GeOH] and $AlH_3 \cdot NMe_3$.

[187] A. F. Richards, A. D. Phillips, M. M. Olmstead, P. P. Power, *J. Am. Chem. Soc.* **2003**, *125*, 3204–3205.

[188] A. Castel, P. Rivière, J. Satgé, H. Y. Ko, *Organometallics* **1990**, *9*, 205–210.

[189] F. Riedmiller, G. L. Wegner, A. Jockisch, H. Schmidbaur, *Organometallics* **1999**, *18*, 4217–4324.

[190] P. Rivière, J. Satgé, *Bull. Soc. Chim. Fran.* **1967**, *11*, 4039–4046.

[191] G. H. Spikes, J. C. Fettinger, P. P. Power, *J. Am. Chem. Soc.* **2005**, *127*, 12232–12233.

[192] M. L. Maddox, N. Flitcroft, H. D. Kaesz, *J. Organometal. Chem.* **1965**, *4*, 50–56.

[193] G. Yamamoto, S. Ohta, M. M. Kaneko, K. Mouri, M. Ohkuma, R. Mikami, Y. Uchiyama, M. Minoura, *Bull. Chem. Soc. Jpn.* **2005**, *78*, 487–497.

[194] F. Schager, R. Goddard, K. Seevogel, K.-R. Pörschke, *Organometallics* **1998**, *17*, 1546–1551.

[195] M. N. Hansen, K. Niedenzu, J. Serwatowska, J. Serwatowski, K. R. Woodrum, *Inorg. Chem.* **1991**, *30*, 866–868.

[196] K. Balasubramanian, *J. Chem. Phys.* **1988**, *89*, 5731–5738.

[197] A. D. Becke, *J. Chem. Phys.* **1993**, *98*, 5648–5652.

[198] P. J. Hay, W. R. Wadt, *J. Chem. Phys.* **1985**, *82*, 270–283.

[199] W. R. Wadt, P. J. Hay, *J. Chem. Phys.* **1985**, *82*, 270–298.

[200] P. J. Hay, W. R. Wadt, *J. Chem. Phys.* **1985**, *82*, 299–310.

[201] K. S. Pitzer, *Acc. Chem. Res.* **1979**, *12*, 271–276.

[202] a) P. Pyykkö, J.-P. Desclaux, *Acc. Chem. Res.* **1979**, *12*, 276–281; b) P. Pyykkö, *Chem. Rev.* **1988**, *88*, 563–594.

[203] N. Kaltsoyannis, *J. Chem. Soc. Dalton. Trans.* **1996**, 1–11.

[204] S.-G. Wang, W. Liu, W. H. E. Schwarz, *J. Phys. Chem. A* **2002**, *106*, 795–803.

[205] M. Kaupp, P. v. R. Schleyer, *J. Am. Chem. Soc.* **1993**, *115*, 1061–1073.

[206] P. G. Harrison, in *Comprehensive Organometallic Chemistry*, Vol. 2 (Eds.: G. Wilkinson, F. G. A. Stone, E. W. Abel), Pergamon, Oxford, **1982**, pp. 670–673.

[207] C. Eaborn, K. Izod, P. B. Hitchcock, S. E. Sözerli, J. D. Smith, *J. Chem. Soc. Chem. Commun*. **1995**, 1829.

[208] C. Eaborn, P. B. Hitchcock, J. D. Smith, S. E. Sözerli, *Organometallics* **1997**, *16*, 5653–5658.

[209] W.-P. Leung, C.-W. So, Y.-S. Wu, H.-W. Li, T. C. W. Mak, *Eur. J. Inog. Chem.* **2005**, 513–521.

[210] S. Hino, M. Brynda, A. D. Phillips, P. P. Power, *Angew. Chem*. **2004**, *116*, 2709–2712; *Angew. Chem. Int. Ed*. **2004**, *43*, 2655–2658.

[211] A. Filippou, N. Weidemann, G. Schnakenburg, H. Rohde, A. I. Philippoulos, *Angew. Chem*. **2004**, *116*, 6674–6678; *Angew. Chem. Int. Ed*. **2004**, *43*, 6512–6516.

[212] S. Kamepalli, C. J. Carmalt, R. D. Culp, A. H. Cowley, N. C. Norman, *Inorg. Chem*. **1996**, *35*, 6179–6183.

[213] C. J. Carmalt, A. H. Cowley, R. D. Culp, R. A. Jones, S. Kamepalli, N. C. Norman, *Inorg. Chem*. **1997**, *36*, 2770–2776.

[214] N. J. Hardman, B. Twamley, P. P. Power, *Angew. Chem*. **2000**, *112*, 2884–2886; *Angew. Chem. Int. Ed*. **2000**, *39*, 2771–2773.

[215] L. Balázs, H. J. Breunig, *Coord. Chem. Rev*. **2004**, *248*, 603–621.

[216] H. J. Breunig, *Z. Anorg. Allg. Chem*. **2005**, *631*, 621–631.

[217] M. Stender, R. J. Wright, B. E. Eichler, J. Prust, M. M. Olmstead, H. W. Roesky, P. P. Power, *J. Chem. Soc. Dalton. Trans*. **2001**, 3465–3469.

[218] D. Neculai, H. W. Roesky, A. M. Neculai, J. Magull, H.-G. Schmidt, M. Noltemeyer, *J. Organometal. Chem*. **2002**, *643–644*, 47–52.

[219] C. P. Poole, H. A. Farach, *Relaxation in Magnetic Resonance*, Academic Press: New York, **1971**, p. 75.

[220] A. Sebald, R. K. Harris, *Organometallics* **1990**, *9*, 2096–2100.

[221] S. Hino, M. Olmstead, A. D. Phillips, R. J. Wright, P. P. Power, *Inorg. Chem*. **2004**, *43*, 7346–7352.

[222] L. Pu, B. Twamley, P. P. Power, *Organometallics* **2000**, *19*, 2874–2881.

[223] C. Stanciu, S. S. Hino, M. Stender, A. F. Richards, M. M. Olmstead, P. P. Power, *Inorg. Chem*. **2005**, *44*, 2774–2780.

[224] A. Murso, M. Straka, M. Kaupp, R. Bertermann, D. Stalke, *Organometallics* **2005**, *24*, 3576–3576.

[225] H. Althaus, H. J. Breunig, R. Rösler, E. Lork, *Organometallics* **1999**, *18*, 328–331.

[226] B. Twamley, C. D. Sofield, M. M. Olmstead, P. P. Power, *J. Am. Chem. Soc*. **1999**, *121*, 3357–3367.

[227] N. C. Norman, *Periodizität*: *Eingenschaften der Hauptgruppenelemente*, VCH: Weinheim, **1996**, p. 24.

[228] U. Wirringa, H. W. Roesky, M. Noltemeyer, H.-G. Schmidt, *Inorg. Chem*. **1994**, *33*, 4607–4608.

[229] W. Clegg, N. A. Compton, R. J. Errington, G. A. Fisher, M. E. Green, D. C. R. Hockless, N. C. Norman, *Inorg. Chem*. **1991**, *30*, 4680–4682.

[230] D. F. Shriver, M. A. Drezdon, *The manipulation of Air-Sensitive Compounds*, 2nd Ed.; McGraw-Hill, New York, USA, **1969**.

[231] "SHELXS-97, *Program for Structure Solution*": G. M. Sheldrick, *Acta Crytallogr*. *Sect. A* **1990**, *46*, 467–473.

[232] G. M. Sheldrick, SHELXL-97, *Program for Crystal Structure Refinement*, Universität Göttingen, Göttingen (Germany), **1997**.

[233] J. Meyer, *Ber.* **1913**, *46*, 3089–3091.

[234] B. Hübler-Blank, M. Witt, H. W. Roesky, *J. Chem. Educ.* **1993**, *70*, 408–409.

9. Abbreviations

δ	chemical shift
η	hapticity
λ	wavelength
μ	bridging
ν	frequency
$\tilde{\nu}$	wave number
aq	aqueous
Ar	aryl
av	average
br	broad
*t*Bu	*tert*-butyl
°C	Celsius degree
calcd	calculated
Cp	cyclopentadienyl
Cp*	pentamethylcyclopentadienyl
d	doublet, day(s)
dec	decomposition
DFT	density functional theory
EI	electron impact ionization
ELF	electron localization function
Et	ethyl
eV	electron volt
G	free energy
G°	standard free energy

ΔG°	standard free energy change
g	grams, gaseous
h	hour(s)
Hz	Hertz
*i*Pr	*iso*-propyl
IR	infrared
J	coupling constant
K	Kelvin
L	ligand
Ln	lanthanide
MAO	methylaluminoxane, "$(MeAlO)_n$"
M	metal
m	multiplet, medium
m/*z*	mass/charge
M.p.	melting point
M^+	molecular ion
Me	methyl
mes	mesityl
min	minute(s)
MS	mass spectrometry, mass spectra
NBO	natural bond orbital
NLMO	natural localized molecular orbitals
NMR	nuclear magnetic resonance
Ph	phenyl
ppm	parts per million
q	quartet

R	organic substituent, gas constant
RT	room temperature
s	singlet, strong
sept	septet
solv	solvation
t	triplet
T	absolute temperature in Kelvin
THF	tetrahydrofuran
TMS	tetramethylsilane
UV	ultraviolet
V	volume
w	weak
Z	nu

List of Publications

[1] **L**. **W**. **Pineda**, V. Jancik, H. W. Roesky, D. Neculai, A. M. Neculai, *"Preparation and Structure of the First Germanium(II) Hydroxide: The Congener of an Unknown Low-Valent Carbon Analogue"*, *Angew*. *Chem*. **2004**, *116*, 1443–1445; *Angew*. *Chem*. *Int*. *Ed*. **2004**, 43, 1419–1421.

[2] V. Jancik, **L**. **W**. **Pineda**, J. Pinkas, H. W. Roesky, D. Neculai, A. M. Neculai, R. Herbst-Irmer, *"Preparation of Monomeric [LAl(NH$_2$)$_2$]—A Main-Group Metal Diamide Contaning Two Terminal NH$_2$ Groups"*, *Angew*. *Chem*. **2004**, *116*, 2191–2197; *Angew*. *Chem*. *Int*. *Ed*. **2004**, 43, 2142–2145.

[3] **L**. **W**. **Pineda**, V. Jancik, H. W. Roesky, R. Herbst-Irmer, *"Germacarboxylic Acid: An Organic-Acid Analogue Based on a Heavier Group 14 Element"*, *Angew*. *Chem*. **2004**, *116*, 5650–5652; *Angew*. *Chem*. *Int*. *Ed*. **2004**, 43, 5534–5536.

[4] **L**. **W**. **Pineda**, V. Jancik, H. W. Roesky, R. Herbst-Irmer, *"OH Functionality of Germanium(II) Compounds for the Formation of Heterobimetallic Oxides"*, *Inorg*. *Chem*. **2005**, *44*, 3537–3540.

[5] V. Jancik, **L**. **W**. **Pineda**, A. C. Stückl, H. W. Roesky, R. Herbst-Irmer, *"Preparation of Monomeric LGa(NH$_2$)$_2$ and of LGa(OH)$_2$ in the Presence of a N-Heterocyclic Carbene as HCl Acceptor Organometallics"*, **2005**, *25*, 1511–1515.

[6] H. W. Roesky, V. Jancik, **L**. **W**. **Pineda**, H. Zhu, G. Bai, *"Beta-diketiminate Ligands for the Kinetic Stabilization of Unusual Compounds"*, Abstracts of Papers, 230th ACS National Meeting, Washington, DC, United States, Aug. 28–Sept. 1, **2005**.

[7] **L**. **W**. **Pineda**, V. Jancik, K. Starke, R. B. Oswald, H. W. Roesky, *"Stable Monomeric Germanium(II) and Tin(II) Compounds with Terminal Hydrides"*, *Angew*. *Chem*. **2006**, *118*, 2664–2667; *Angew*. *Chem*. *Int*. *Ed*. **2006**, 45, 2602–2605.

[8] **L**. **W**. **Pineda**, V. Jancik, R. B. Oswald, H. W. Roesky, *"Preparation of [{HC(CMeNAr)$_2$}Ge(Se)OH]: A Germanium Analogue of a Selenocarboxylic Acid (Ar = 2,6-iPr$_2$C$_6$H$_3$)"*, *Organometallics* **2006**, *25*, 2384–2387.

[9] **L**. **W**. **Pineda**, V. Jancik, J. F. Colunga-Valladares, H. W. Roesky, A. Hofmeister, J. Magull, *"Lewis Base Character of Hydroxygermylenes for the Preparation of Heterobimetallic [{HC(CMeNAr)$_2$}Ge(OH)M] Systems (Ar = 2,6-iPr$_2$C$_6$H$_3$; M = Fe, Mn)"*, *Organometallics* **2006**, *25*, 2381–2383.

About the Author

Leslie W. Pineda was born in David, Chiriquí, Panamá. He completed his basic school formation in 1989 at the David Institute. He then entered to the Autonomous University of Chiriquí in 1991, graduating with a Licentiate degree in chemistry in 1996. That same year and for a one year period, he accepted a job position at PanaCobre, Inc. as Senior Research Chemist and Metallurgist at the Cerro Colorado Copper Deposit in Chiriquí. In 1998, he moved to the University of Costa Rica, Costa Rica, where he was awarded an M.Sc. degree in chemistry in 2001, working on the synthesis and characterization of transition metal saccharinato complexes in oxidation state (II) with imidazole and pyrazole ligands. He returned to Panamá to work as chemist for a five months period in 2002 at the Panamá Research Institute of Agriculture (IDIAP), at the Gualaca Experimental Station, Chiriquí, before moving to Germany in the same year, to spend a six months German language course period at Goethe Institute, Göttingen. Since 2003, he has been working in his Ph.D. project on some aspects of the synthesis and characterization of heavier Group 14 and 15 elements in low oxidation states, at the University of Göttingen, Germany, in the research group of Prof. Dr. Herbert W. Roesky.